Available online at www.sciencedirect.com
ScienceDirect
Surface Science Reports 61 (2006) 383–428
surface science reports
www.elsevier.com/locate/surfrep

Clusters on soft matter surfaces

A.M. Bittner

Max-Plank-Institut für Festkörperforschung, Department of Nanoscale Science (Abt. Kern), Heisenbergstraße 1, 70569 Stuttgart, Germany

Accepted 27 March 2006

Abstract

Clusters built from metals, semiconductors and dielectric materials, whether they are bare or coated by ligand molecules, interact in many different ways with soft matter. The ensuing phenomena are of great relevance for technical problems such as metal/polymer interfaces, but also to fundamental questions such as controlled charging of single clusters. Clusters on soft matter may be employed for nanotechnology, when a collective physical property of an assembly of many clusters is aimed at. Most interesting is the fact that the interaction with a solid substrate that supports the soft layer can be suppressed. This means that the clusters are adsorbed, but preserved as entities, and hence their size-dependent physical properties are not affected by coupling to the solid substrate (e.g. optical excitation or electronic properties).

"Soft matter" is anything but a well-defined term, but thin layers and organic molecules assembled on solid substrates can exhibit excellent ordering and conformational stability, and a wide range of highly interesting and finely tunable chemical properties. The layers can be organic monolayers such as self-assembling monolayers, but also two-dimensional arrangements of proteins. The surfaces of polymers and organic crystals are very nicely comparable to such systems. In all cases, the surfaces may show conformational flexibility, but their composition and atomic arrangement (in each molecule) are well defined. Special cases are inert gas layers at low temperature, used for soft landing of clusters, again with the aim of preserving the clusters' properties.

Typically a cluster/soft matter system is prepared by vacuum deposition, adsorption from solution, or by electrochemical or chemical synthesis, all of which are considered here. For a proper description of the system, cluster/surface interactions can be treated macroscopically, inspired from colloid science, but also microscopically on the atomic level.

Contents

E-mail address: a.bittner@fkf.mpg.de.

0167-5729/$ - see front matter © 2006 Elsevier B.V. All rights reserved.
doi:10.1016/j.surfrep.2006.03.003

1. Introduction

The topic of this review is the marriage between cluster science, Surface Science, and soft matter. The concept of soft matter is as yet quite unusual in Surface Science [1], but there is a bright future. Metal films, including extremely narrow contact lines, are required as top electrodes in molecular electronics devices [2] — in other words on “soft” molecular, even monomolecular layers. Whether a gate dielectric of molecular dimensions [3] or an organic transistor [4] is aimed at, any progress in the metallization of soft matter is important, even on simplified model systems. Note that clusters are not directly relevant for this goal — however, any metal film will grow from nuclei, clusters: the rational design or control of nucleation of metal films on soft matter requires a much better understanding of the cluster/molecule interaction than achieved until now. In this respect, this review tries to give an overview over possibilities and already achieved goals.

Nanoobjects such as clusters exhibit physical properties that are different from those of the bulk material, such as highly non-ohmic electrical conductance (e.g. Coulomb blocking in gold clusters [5]), (dis)appearance of ferromagnetic coupling (e.g. for pivalate-$Mn_{12}O_{12}$ [6]), or changes in light absorption and emission (e.g. for luminescent Au_5 clusters [7]), or field enhancement (e.g. of the Raman effect [8]), and also changes in the electrochemical characteristics (e.g. stepwise charging of clusters [9]). As an example, the immobilization of metal nanoclusters can be envisaged as the first step towards nanoscale construction procedures. Clusters may either be building blocks, i.e. parts of a scaffold, or functional units, by virtue of some special property. This functionality can be catalytic, chemical binding, marking, but especially valuable are electrical conduction, optical properties, and magnetism. In view of such properties, we here consider not only metal but also semiconductor and dielectric materials (note that these terms correspond to the bulk properties, not to those of the cluster). An example for a nanoscale device is a layer of clusters on top of organic monolayers that are in turn immobilized on electrodes. A very small gap (2 nm) results, and in this way a molecule-sized switch was devised [10]. For such applications,

Acronyms

CVD	Chemical Vapor Deposition
ECSTM	ElectroChemical Scanning Tunneling Microscopy
ISS	Ion Scattering Spectroscopy
LB	Langmuir–Blodgett (molecular layers on solid substrates)
LBL	Layer-By-Layer (assembly of polyelectrolyte molecules)
SAM	Self-Assembling Monolayer (of molecules on solid substrates)
SEM	Scanning Electron Microscopy
SFG	Sum Frequency Generation (in molecules at interfaces, excited by mixing a visible and a tunable infrared laser beam)
SFM	Scanning Force Microscopy (also known as AFM)
STM	Scanning Tunneling Microscopy
TEM	Transmission Electron Microscopy
UPS	Ultraviolet Photoelectron Spectroscopy
XPS	X-ray Photoelectron Spectroscopy (also known as ESCA)
XRD	X-Ray Diffraction

one has to prevent the aggregation of the clusters, which would render them less or nonfunctional, because they can then take on bulk properties.

Many of the size effects on the nanoscale are due to the comparatively large surface area of small particles. Table 1 shows the relation between the numbers of atoms and the diameter of several gold clusters. Obviously, the surface atoms make up a large fraction of the small clusters. This and the physical properties mentioned above create a driving force to develop new and more complex nanostructures that are core products for scaling down computing, memory storage, and sensor devices. These possible application areas are linked with the field of "nanotechnology" (for the various definitions of this term see Schmid et al. [11]). An intriguing feature is that many, if not most attempts towards devices heavily rely on surfaces, mainly solid substrates. In other words, a 2D assembly of nanoobjects is the starting point towards further possible applications. This assembly can either be achieved by immobilization of prefabricated objects, or by synthesis of objects on the surface. Here, both strategies will be considered in detail.

In the course of the past decades, new instrumental developments, such as the scanning probe methods, allowed for synthesis and/or analysis on ever decreasing length scales. Surface Science and its analysis methods [1,12] played a key role. With the help of atom-by-atom assembly, nanoobjects can be created, usually on well-defined, atomically smooth surfaces. It is obvious that functional devices are more complex and thus call for a more elegant strategy, i.e. for parallel fabrication and/or bottom-up construction, such as in organic synthesis and biochemistry. In this way, chemistry becomes increasingly important for Surface Science, which was originally more physics-oriented.

Table 1
Diameter of gold clusters as a function of the number of atoms

Atoms	Surface atoms	Diameter (nm)
1	1	0.3
55	42	1.4
147	90	1.6
460	240	2.4
1 000	410	3.1
2 600	790	4.2
30 000	2200	9.5

1.1. Included topics and section overview

The review predominantly concerns clusters on top of soft matter layers, hence the clusters should not be located in the layers or even be in contact with the substrate surface. However, whenever appropriate, such cases will be mentioned for comparison. For example, the question of avoiding penetration of clusters through soft matter can be decisive for proper assembly of the system; or metal overlayers on soft matter surfaces — grown from clusters — are a very important technical and also scientific issue for "plastic electronics".

The definition of "clusters" in this review is very broad and comprises all types of inorganic nanoparticles up to tens of nanometers in size — which may also be referred to as colloids (Fig. 1). The lower limit is a cluster comprised of only two or three atoms; in some cases, even the interaction of single atoms with soft matter layers will be included for comparison. In terms of chemical species, metals, metal oxides, semiconductor materials and others are considered. In fact most clusters deposited or synthesized on soft matter surfaces are made up from metal and semiconductor nanoparticles. It should be noted that the inorganic chemical definition of a cluster is much narrower than the one employed here: metal–metal bonds must be present. In physics, the definition is less clear; usually an entity that contains a defined number of identical atoms is meant. The problem with this definition is that it excludes many of today's most investigated clusters, namely metal clusters with a certain size distribution (strictly speaking, these are impure chemical compounds), coated by organic ligands. Note that in the following, "metal", "semiconductor" and "dielectric" will be used for the atoms or compounds that show the relevant property when in bulk form.

The soft matter surface is most difficult to define [13] (we define "surface" as the interface of the soft matter with gases or liquids, while the soft matter–solid substrate interface is not termed "surface"). Soft matter can be thermodynamically either a liquid or a solid, but in either case a complex one, such that the liquid is extremely viscous or that the solid is not crystalline [13]. The term comprises for example colloidal gels, polymers, and liquid crystals — in any event, the conformation of the molecules is not fixed. Here it is further narrowed to organic materials, the most typical soft matter candidates. One can include also molecular crystals, in

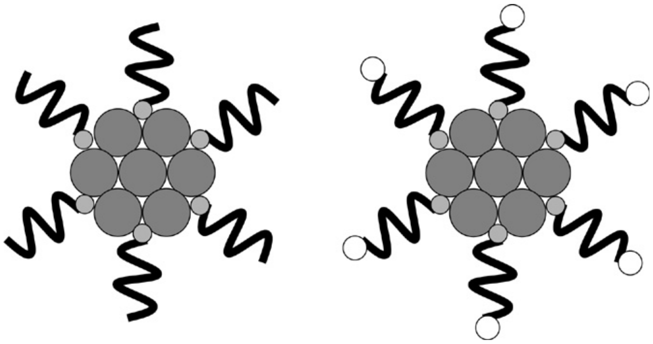

Fig. 1. Cartoon of two clusters. Left: capped by a ligand shell, head groups contact the cluster, tails point outwards. If the flexible chains (black) are alkyl or aryl groups, the cluster is hydrophobically coated. Right: tails with functional chemical groups (empty circles) for possible interactions or chemical reactions.

which the subunits are relatively loosely bound, resulting in mechanical properties that are different from those of simple solids. Quite often it turns out that soft matter is better defined, e.g. aligned or partially crystallized, in thin films (with a thickness below 100 nm). Thin films down to the molecular level (monomolecular films, or monolayers) can be comprised of ordered molecular assemblies. Classic examples are lipid bilayers on solid supports and thiol monolayers on metals. For such thin systems we require a ("hard matter") solid support, the substrate, which is required to be flat and chemically homogeneous, ideally a crystalline surface. Due to the amorphous nature of silica-based materials, glass and oxidized silicon wafers do not strictly fulfill these requirements, but are included.

Archetypical systems are self-assembling monolayers (SAMs) of thiols on gold surfaces [14,15] (mainly Au(111) which is not reconstructed in contact with the sulphur atoms) and of silanes on oxides or on hydroxylated surfaces. Thicker layers are especially well defined when they are transferred from amphiphilic molecules, spread on a liquid surface, to a solid substrate: Langmuir–Blodgett (LB) layers [12]. Thin polymer layers show much less order and much rougher surfaces than molecular layers, and this is especially true for bulk polymers above the glass transition temperature. However, several examples will be considered; in this way it is hoped that the communities working with thin polymer films and those working with molecular layers will benefit equally. Furthermore condensed rare gas layers — typically investigated in physics — are supposed to be "soft", first, because the atoms therein interact exclusively with van der Waals interactions, second, because the issue of placing clusters on top of and into such layers is quite nicely comparable with atom and cluster penetration into polymers and SAMs.

The article is organized as follows: Section 2 will give a systematic classification of the various types of soft matter surfaces considered. Section 3 will introduce several concepts in order to describe the interaction between clusters and soft matter surfaces. Section 4 is the main section, presenting all relevant experiments. The subsections are organized for various aspects: small clusters (4.1) are distinguished from metal, semiconductor and dielectric clusters (4.3–4.5). Since metal clusters are much more investigated than others, their synthesis is briefly reviewed (4.2). Special sections (4.6–4.8) focus on important soft matter systems and on the dominant physical properties, electronic structure and conductivity. In Section 5 the process that opposes the formation of a proper cluster/soft matter structure, penetration of soft matter by atoms and clusters, is investigated. Section 6 gives a short view of surfaces of biomolecules, which are not yet recognized as a topic on their own in Surface Science.

1.2. Related reviews

A large number of reviews on the topics of clusters and molecular layers is available. Some of them are related to the topics discussed here, and can be recommended for further information on special topics. Binns [16] and Meiwes-Broer [17] focused on cluster deposition from the gas phase to solid substrates, which can be seen as the best defined experimental design in the absence of soft matter. Data from such experiments often form the basis for interpretation of the data discussed here. Concerning the soft matter layers, SAMs are the best defined and in widespread use. Schreiber [15] gave an excellent overview (see also a smaller recent review [14]). Fendler reviewed self-assembling nanoscale materials [18], including sections on LBL and LB films. Sastry reviewed electrostatic assembly, especially LB films and evaporated lipids [19]. Some of the newer reviews on LB films are by Basu and Sanyal [20] (specialized on X-ray scattering), and a very concise and commendable introduction is the one by Norgaard and Bjornholm [21].

Daniel and Astruc presented a detailed survey on the main cluster types discussed throughout this work: gold nanoparticles [22]. Two of the few reviews that focus on the interaction of clusters (and atoms) with soft matter are the classic, but still very useful metal/SAM works by Jung and Czanderna [23] and by Herdt et al. [24]. Faupel et al. [25] gave an excellent overview over metal atoms and clusters in polymers. Sacher covered the metallization of polymers, especially fluoropolymers [26], while Tirrell and Parsonage focused on the properties of polymer surfaces [27].

Hostetler and Murray published a short report on colloids and SAMs [28] that concentrates on 2D and 3D assemblies of clusters. With a similar focus, Zhang et al. reviewed electrochemistry towards the single-molecule level [29], and Chen gave a chemical/electrochemical view of electron transfer [30]. All three reviews provide details on Coulomb blockade theory and experiments. More device-oriented is a short review by Vuillaume and Lenfant [31]. Other specialized publications present magnetism/structure relations for clusters [32], soft landing [33] and metallic properties of islands and films [34]. Further work is available on a special case of soft matter surfaces, organic crystals [35], and on SAMs for site-selective nucleation of materials [36]. Kasemo introduced biological Surface Science [37], and Niemeyer published a survey on biochemical nanoscale science [38].

2. Soft matter surfaces

The surfaces of bulk soft matter show a wide variety and great complexity. Only in some cases (e.g. molecular crystals or crystalline polymers) the surface is comparable to truncated bulk matter, and the crystalline order of the substrate results in phenomena such as epitaxial growth of adsorbate layers [39] or change of superlattice parameters for adsorbed molecules. On the other hand, the dynamics is usually much slower than that of liquids. The flexibility and the soft mechanical properties mean that atoms can fluctuate or move between some location inside the layer and a certain maximum extension. The simplest examples for this are polymer chains with their conformational instability [13], but the scenario is also valid for the nanoscale, e.g. the sub-nanometer movement (conformational changes, reversible *gauche* defects) of terminal alkyl groups in a thiol layer on gold [40], and for the surface of a molecular crystal [41].

2.1. Comparison with "hard matter" surfaces

Classic Surface Science is built on the principle that the surface structure of a given solid is the structure of a plane cut through a crystal of the solid. While reconstructions can change the local structure substantially, for example the arrangement of the top atom layer that is subject to strain, or the number and location of atomic steps, this principle is generally fulfilled [1]. When one considers the second (subsurface) atomic layer, the principle is very strict: usually only small atomic rearrangements compared to the bulk structure are found. With a few exceptions, soft matter surfaces cannot be analyzed in this way. The essence of the structure of soft matter is flexibility, and any interface to another substance, be it a gas or a solid, will structurally differ from the bulk. Moreover, the bulk is quite often not crystalline, and thus hard to characterize. The extreme example may be polymers above the glass transition temperature, which exhibit constant rearrangement of the surface by "reptation", i.e. movement of a polymer chain within the accessible voids between the neighboring chains [13]. In this way, changes of the surface chemistry are reversible: when the "surface" is modified by chemical reactions, in fact, certain parts of polymer chains exposed to the reaction medium are modified. The affected chains (or parts of chains) can then move back into the bulk, until very few or no modified chains remain in the surface — effectively a fresh, unmodified surface forms. The other extreme are small molecules that form ordered crystals, such as molecular crystals or molecular monolayers at low temperature; these materials are well comparable to solid surfaces, since they show negligible movement, at least normal to the surface.

For the combination of thin layers and solid substrates, thorough analyses are available for a range of systems; especially well investigated are alkanethiols on gold [14] and rare gas multilayers [42]. In general the soft matter–substrate interface may reconstruct when the soft matter molecules form (strong) chemical bonds, but the reconstruction cannot influence the properties of the soft matter surface: Even for small molecules, the thickness of a monolayer corresponds to at least two atomic distances in the substrate, which means that small atomic rearrangements or strain can relax very efficiently. In our examples, the rare gas atoms in the multilayers are mobile because they interact very weakly with the substrate and with each other; the alkyl chains in the thiols can easily change their conformation and thereby provide a layer of flexible spacers.

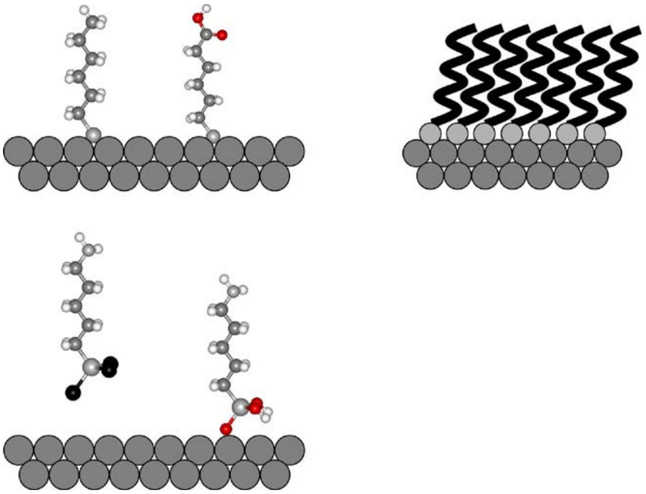

Fig. 2. Models for SAMs. Top: alkanethiol (left) and carboxylate-terminated alkanethiol (right). Top right: model of assembly; the head groups are light grey). Bottom: covalent attachment of a chlorosilane molecule to a hydroxylated surface. Chlorine (dark) at the trichlorosilyl head group (left) is substituted by hydroxyl (right).

2.2. Organic monolayers on flat substrates

When only a single layer of small, relatively rigid molecules adsorbs on a solid substrate, the substrate can exert at least indirect influence on the soft matter surface by slightly changing the molecular orientation in the layer. The influence is larger at low coverage, where molecules tend to adsorb with as many contact points as possible to maximize van der Waals interactions with the substrate (here and in the following van der Waals interactions are defined to exclude electrostatic interactions). This generally results in flat-lying structures, which are typical for vacuum studies. Adsorption from solutions, which usually provide many more molecules than required for building monolayers (or even thin films), or exposure to sufficient amounts of the adsorbing molecules, results in densely packed phases, often accompanied by a reorientation from a low- to a high-coverage phase. Now the noncovalent interactions between the molecules are maximized, and often only a single atomic contact to the substrate is preserved, with the so-called head group (Fig. 2).

2.2.1. Self-Assembling Monolayers (SAMs)

Self-Assembling Monolayers (SAMs) bind to the solid substrate covalent-like, i.e. they chemisorb (Fig. 2). The assembly is based on adsorption followed by surface diffusion and — if required — molecular reorientation. Widely used systems are thiols on gold substrates [14,15] and silanes on hydroxyl-terminated surfaces. Thiols R-SH adsorb in RS–Au fashion as thiolates. Their hydrocarbon (alkyl or aryl) backbones R orient parallel at a certain angle from the surface normal. A range of terminal groups can replace CH_3. These groups allow further covalent modification, but they can change the SAM conformation. In fact, the picture of nicely ordered thiol chains, and especially that of *all-trans* (zigzag) methylene chains $(CH_2)_n$ as in Fig. 2, collapses as soon as functional groups are present (usually in the ω position, i.e. terminal). Sum Frequency Generation (SFG), as opposed to simple InfraRed Reflection Absorption Spectroscopy (IRRAS), is an ideal method to prove this, because of its inherent surface sensitivity and strict selection rules. All SFG resonances stem from non-centrosymmetric vibrations in adsorbed molecules, while the *all-trans* conformation is practically centrosymmetric.

The following example is typical for soft matter surfaces: two methylene stretching vibrations at 2855 cm^{-1} and 2925 cm^{-1} are observed in infrared and also in SFG spectra of ω-carboxylic acid hexadecanethiol (or mercaptohexadecanoic acid), $HS\text{-}(CH_2)_{15}\text{-}COOH$, on Au(111). The SAM exhibits *gauche* defects, i.e. not all methylene groups are in the *all-trans* (zigzag) conformation [43]. The positive shift of the C–H vibrational frequencies (as compared to *all-trans* methylene chains) points towards substantial disorder. This disorder is especially pronounced in deprotonated phases with low thiol coverage, in which each molecule has sufficient space to reorient without interacting with its neighbor. The orientation can then be reversibly switched by application of an electrochemical potential, which results in attractive or repulsive interaction between substrate and the COO^- group [44]. Nevertheless, the ellipsometric thickness of 1.8 to 2.1 nm at high coverage is well comparable with that of alkanethiols of similar length, hence the SAM is dense. It appears that intermolecular hydrogen bonds (and most likely also adsorption of water) are energetically so much favored that defects build up in the C_{15} chains in order to allow for as many hydrogen bonds as possible. The occurrence of the methylene peaks in SFG is a direct proof for disorder. The peak intensities are larger than those of methyl peaks from alkanethiols, so one can infer *gauche* defects (rotations of C–C bonds) in the methylene chain. Since this and similar SAMs are often employed to bind nanoobjects and also biomolecules, one should be aware of their surprising flexibility. On the other hand, the advantage is surely that the reactivity of the terminal group is not much impeded by neighboring molecules. Indeed, further functionalization is easily achieved.

A special family of SAMs deserves mentioning since it is intensively used: dithiols (HS–R–SH) possess two "sticky" groups to attach to gold substrates or to metals. One tries to organize a SAM in such a way that one of the groups points away from the surface and is thus available for coordination/linking to clusters. Fig. 1 (right) depicts a bifunctional molecule on a cluster that could be a dithiol (dark and light circles would both symbolize sulphur atoms). Replacing the carboxylate with a thiol group in Fig. 2 shows the desired orientation on the substrate.

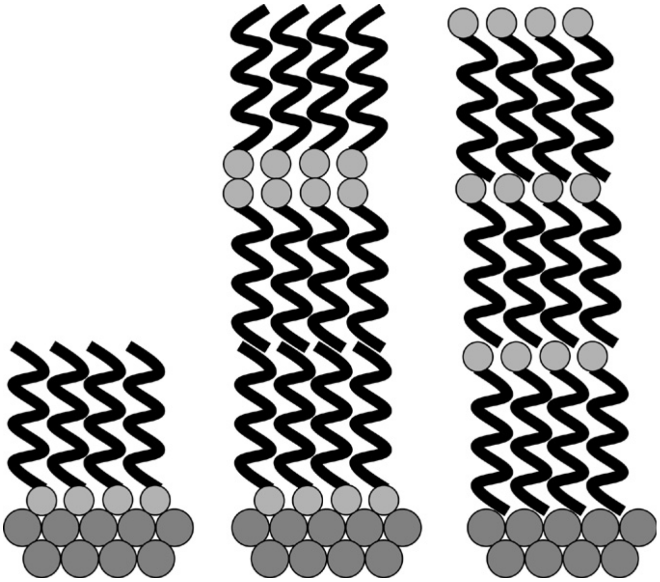

Fig. 3. Model for typical LB film structures. From left to right: monolayer on hydrophilic substrate (Z-type), Y-type layer on hydrophilic substrate, X-type layer on hydrophobic substrate.

2.2.2. Langmuir–Blodgett (LB) layers

The best and longest known organic layers are Langmuir–Blodgett (LB) films from amphiphilic molecules, usually long alkane chains with a polar head group. LB films have been a research topic for many decades. To synthesize LB films, amphiphilic molecules are spread on the surface of a liquid so-called "subphase" (mainly aqueous) in a Langmuir (or Pockels) trough and compressed with a film balance until a densely packed monolayer, the so-called "solid phase", is obtained. This can be transferred to a solid substrate, either by horizontal contact (Langmuir–Schaefer technique), or by immersion of the substrate, followed by emersion at controlled speed. Usually the nonpolar head group of the amphiphile adsorbs on a hydrophobic substrate, forming a monolayer. Vice versa, a method to obtain a hydrophobic substrate from a hydrophilic one is to coat it with a monolayer LB film (Fig. 3). Repeated immersion can result in well-controlled multilayers, based on tail-to-tail bilayer formation as for a cell membrane. The layers often show excellent vertical and lateral ordering, hence X-ray studies such as specular reflectivity (for the vertical structure) and even grazing incidence diffraction (for the lateral ordering) can give valuable information [20,21].

The transfer to the solid support can be very well controlled by (repeated) immersion under adjusted surface pressures [12]. Mono, tri- and multilayers with typical orientations form (Fig. 3). Their structure is determined by a non-covalent interaction of either the head group with a hydrophilic surface, or the tail with a hydrophobic surface, combined with strong intermolecular forces. The latter cause self-assembly to an ordered molecular film, without much influence from the substrate [18,20]. Hence many researchers tend to mention the substrate only as an experimental detail. In analogy to biological membranes (e.g. lipid membranes), the films can be impermeable for aqueous solutions since the molecular packing can become very dense. All this would allow addressing LB layers as "SAMs", but this term is not usually employed. Functional groups can be present in or on LB layers: a popular example is Cd arachidate (eicosanate, $C_{19}H_{39}COO^-$) that can, depending on substrate chemistry, expose its carboxylate groups, similar to the thiol discussed in Section 2.2.1.

2.2.3. Protein layers

Compared to the systems discussed above, very few good examples for protein monolayers are known. Layer-like more or less flat structures are well known in biology, the best example being cell membranes (lipid double layers), which can be compared to Langmuir films (see Section 2.2.2). Such structures can extend over macroscopic distances, as required for a membrane, but they have as yet not found widespread use as support for clusters. On solid supports, the best analogues are LB layers as discussed above. However, some membranes are made up entirely from proteins and form well-defined monolayers on solid supports. Concerning the handling, bacterial outer membrane proteins of so-called S layers [45–49] are especially valuable for the construction of stable sheets due to their chemical, thermal and mechanical resilience. The membrane has a highly complex chemistry and topography that allows binding or synthesizing clusters.

Note that protein assembly tasks require, with current technology, very often a supporting flat substrate and careful control of this surface's chemistry. In this context one has to note that multiple interactions between large molecules (biomolecules >1 kDa) and flat surfaces are still not well studied on the atomic scale (with respect to which group in which conformation and chemical state interacts with the surface) [37]. We note that this 2D problem is related to the more general problem of crystallizing proteins (in 2D or 3D). Since biochemistry offers many tools for molecular assembly, there are virtually infinite possibilities to create new structures, so that this and similar questions will be of great interest. In fact the combination of biology with chemistry and nanoscale physics is increasingly searched for [38,50,51], for example with the aim of constructing nanodevices from small molecules. Again, surface assembly will likely play a crucial role.

2.3. Surfaces of bulk soft matter

The nature of polymers gives them a special place as substrates [27]. First, the units that make up a bulk polymer, long molecular chains, are far less defined than for example molecules in a molecular crystal. This concerns mainly their length and hence mass, and in many cases also their configuration, i.e. the sequence of chemical groups. Their conformation is only on short length scales well defined — in other words, their persistence length is in the molecular range; systems with either a linear structure or with a superstructure such as the helical DNA show much higher persistence. Note that only very few polymers form true crystals. However, chain–chain interactions can in many systems induce crystalline order by chain alignment on small scales, so-called semicrystalline order. Since most polymer chains are very flexible, the "random coil model" applies, and hence the amorphous parts of the bulk phase consist of intertwined chains. In contrast to most other materials, a considerable unoccupied "free" volume exists between the chains; the free volume fraction often exceeds 10%. Consequently, polymers exhibit viscous flow with a relatively high viscosity.

All these properties influence directly the surface of a polymer. This means that for the large majority of polymers we deal with an amorphous surface. The free volume confers a surprising mobility to the chains, especially those at the surface. This mobility can be "frozen" — in fact, polymers show a glass transition in the bulk. This transition is defined by kinetic parameters such as a huge increase of the viscosity. A similar transition has to be expected at the surface. In this case, the molecular structure of the polymer plays an even larger role than in the bulk, and hence the nature of the surface glass transition, its detection and its significance for the surface properties are under intense scrutiny.

"Bulk soft matter" means that no solid substrate is required to support the structure. Except for very stable systems such as lipid bilayers, this implies a certain minimum thickness of the order of 10 nm (for example free-standing polymer films used in TEM grids). In most cases the polymer can be cast or even produced from monomers on a rigid and flat support. This has implications for the surface topography: soft matter on solid substrates will follow the substrate topography and can thus be prepared nearly as flat as the substrate, e.g. with spin coating, typically with only a few nanometers height differences on μm^2 areas. Chip technology has even stricter requirements (cm^2 areas), which cannot always be met by bulk soft matter. A typical problem is the segregation of a polymer mixture, which can induce roughness. Roughness in turn means a more complex surface (comparable to steps, kinks and impurities on a crystalline surface); moreover analysis methods face difficulties in measurement (scanning probe technologies that cannot tolerate samples with steep surface slopes) and evaluation (data may have to be fitted to a topography model).

We note that the experimental methods in classic Surface Science are quite often not compatible with the nonconducting polymer samples. For this reason, but also due to the (often) inherently amorphous and dynamical structure, polymer surfaces are better known in engineering and applications than for fundamental investigations. However, some methods, especially ion scattering, are of great value since they can probe films at various well-defined depths [25,27,52]. The importance of the surface dynamics shows up in relevant research topics such as molecular diffusion, viscosity and the glass transition that will be discussed in the following.

2.3.1. Polymers and polyelectrolytes

One of the most important parameters for a polymer surface (and indeed its bulk) is the glass transition temperature T_g. Similar to the surface melting temperature of a solid, T_g can differ by a few K at the surface. Below T_g, one can envisage the structure as frozen. While some polymers are crystalline, and many show nanoscale crystallites, most are not, hence no order can be expected. The chemical nature of polymer

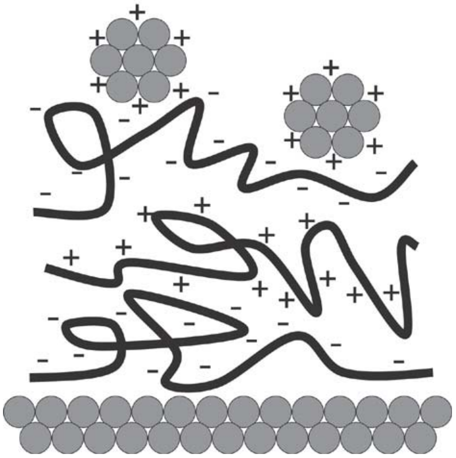

Fig. 4. Model for LBL assembly of polyelectrolytes with multiple opposite charges; on top adsorbed clusters with positively charged surfaces that interact electrostatically with the negatively charged polymer that makes up the top layer.

surfaces is thus known in greater detail than the structure. However, above T_g the surface can be addressed as a liquid, and thus fluctuations play a huge role. For detailed Surface Science analyses, polymers should be held above T_g during the surface formation in order to have a chance to organize. Optimal use of this principle has been made with polyelectrolytes: these molecules contain ionized groups, usually either COO^- or NH_3^+ (or other protonated amines), and they are applied in a solution together with counterions such as K^+ or Cl^-. Polyelectrolytes considered here have a flexible structure and can adsorb more or less elongated. The counterions can be replaced by sequential adsorption of the oppositely charged polyelectrolyte, again more or less elongated. In this way quite well defined layers of oppositely charged molecules can be constructed (Fig. 4). Due to the flexibility, intermixing is always possible, but is not of major concern. This Layer-By-Layer (LBL) technique has found widespread application [53]. The surface of the topmost layer is sufficiently flat to allow for many methods of Surface Science probes. Note that the top layer determines the chemical properties: the counterions are mobile and can now be exchanged with charged adsorbents. This process is the basis for very simple layerwise assembly of charged objects, and the foundation of all applications of the LBL method.

2.3.2. *Organic crystals*

Organic crystals [35] are the most important material class for organic transistors, which are discussed in connection with applications like mechanically flexible microelectronics. The formation of clusters on top of an organic crystal is not a topic of intensive research. However, since the crystals have to be contacted electrically, the metal/crystal interface is of great importance [31]. To this end, the formation and growth of metal overlayers (contacts) is investigated. The issues are often of rather technical nature, and although the formation of clusters accompanies all relevant contacting methods, relatively little is known about it. Certainly an exciting new field is currently developing. Two examples that focus on fundamental questions are a study on thin film deposition of metallic layers below and on top of organic light-emitting diode material, where ion beam deposition was found to result in especially smooth layers [4], and diindenoperylene layers, which crystallize very nicely and form well-defined interfaces with metals [54]. Related systems with less order are liquid crystals, whose surfaces, in contrast to their interfaces with rigid substrates, are rarely investigated.

2.4. *Biomolecule surfaces*

It is not common to interpret the outer atoms of a biological structure as a surface, and indeed a “Surface Science of biomolecules” does not exist, in contrast to the field of “Biological Surface Science” that concerns the interface between solid substrates and biomolecules [37]. Note that many immobilization strategies for biomolecules on solid surfaces are known, but that they are only rarely specific down to the atomic level, as known from organic chemistry. Here, for a better comparison, but especially due to the close analogy to soft matter surfaces, we call those atoms that are responsible for interaction with the surrounding medium a “surface”. This surface will usually not only be soft, as required for all types of protein interactions and especially for natural or artificial nanomechanical machines and switches, but it will also be highly curved, and of course it will be chemically very heterogeneous. Hence spatial selectivity down to the atomic level is even harder to obtain; it was shown for gold clusters that bind selectively to the cystein groups on an icosahedral plant virus capsid [55]. Other promising systems are two-dimensional layers such as the bacterial S layers (see Section 2.2.3). One task of a “Surface Science of biomolecules” could be to identify surface groups that favor the formation of covalent links. This in turn is related to problems that are tackled with molecular modeling and other calculation methods, especially electrostatics; in other words the distribution of charges and dipoles on a biomolecular surface [56,57]. Certainly the presence and dynamics of water on biomolecules is crucial [58], and probably one can develop ties to the well-developed electrochemical Surface Science.

A special role of biomolecules and their surfaces is that of a template: nanostructures can be synthesized in or at biomolecules, with the aim of attaining the biomolecule’s shape. While organic soft matter may show surface segregation on the nanoscale, such as for block copolymers, biomolecules can provide many more and more complex shapes. For example, upon cluster growth a bio-(in)organic “nanocomposite” is formed, in which the biomolecule determines the spatial arrangement (distribution) of the clusters synthesized at the biological surface(s). We note that spheres can act as molds for spherical clusters; in nature ferritin is an example, while plant virus systems were used for artificial cluster synthesis [59–61]. Clusters can align or coalesce at 1D structures such as rods (“wires”) and tubes; again plant and bacterial viruses are most important [62, 63]. This may be of relevance for connections between nanostructures and the macroscopic world, e.g. electrical contacts (maybe also as antennae for electromagnetic waves).

Table 2
Comparison of condensation energies of metals (as approximate bond energies) and bond energies in molecules [26,231]

Atom(s)	Condensation or bond energy (kJ mol^{-1})	Condensation or bond energy (eV)
Ag	290	3.0
Al	330	3.4
Au	355	3.7
Cr	395	4.1
Cu	335	3.5
Fe	415	4.3
Ni	425	4.4
Pd	395	4.1
Pt	530	5.5
Ti	470	4.9
C–H	410	4.3
C–C	350	3.6
C–O	385	4.0
C = O	750	7.8
C–N	305	3.2
N–H	390	4.0

A more sophisticated concept was demonstrated for DNA: a carbon nanotube was biochemically coupled to an ss-DNA/nucleoprotein filament that was bound to a specific location on a long dsDNA; metallization produced a nanoscale field effect transistor [64].

2.5. Rare gas layers at low temperature

Solidified rare gases are ideal examples for van der Waals crystals due to the very low interatomic interaction energies. Rare gases (and similarly unreactive gases like N_2) adsorb readily at low temperatures. They can form well defined (sub)monolayers and multilayers on crystalline substrates such as graphite or metals. Such layers are valuable tools for surface physics research, since the surface and also the interatomic bonding are based mainly on van der Waals interactions. In fact, rare gas layer experiments had considerable influence on the development of Surface Science. Multilayer growth in vacuum obviously requires temperatures below the bulk sublimation temperature. The bond in the multilayers is weak: the condensation energies are in the kJ mol^{-1} (tens of meV) range, and thus are only a fraction of those of metals (Table 2). This predominance of weak interactions suggests calling rare gas layers “soft”. Certainly this is true in the narrow temperature range of the bulk liquids (at high pressure), but also the atoms in the solid crystal can easily be displaced. This ability was shown to be ideally suited for “soft landing”: an adsorption of clusters without structural change in the clusters requires a soft cushion to dissipate the impact energy [65]. At the same time, the unreactive nature of the layers protects the clusters from any chemical reactions.

3. Cluster/soft matter interactions

“Cluster” is, in the framework of this review, an extremely broad definition, ranging from atomic dimers to large nanoparticles with tens of nanometers diameters. The synthesis of clusters is as diverse as their sizes and properties. Adsorption of atoms from the gas phase is as common as wet chemical synthesis based on reduction of a metal salt, or on reactions of cations with anions. Growing clusters and layers on flat solid substrates is a well-investigated process for solid–gas and solid–liquid surfaces. Usually, adatoms diffuse and collide until they form a nucleus of a certain critical size, often only a few atoms [66,67]. A very interesting question, especially for nanoscale science, is whether this is also possible on organic surfaces. Mechanistic details such as surface diffusion on and penetration into the organic layer, but also growth modes are not known. For example, layerwise growth (in epitaxial fashion) usually requires a good match of interatomic distances between deposited compound and substrate (e.g. the Frank–van der Merwe growth mode), and the opposite is true for cluster growth (Volmer–Weber mode). Since substrate rearrangements are much more facile on soft layers — conformational changes are easily possible — it is hard to estimate whether clusters or layers or even metal/organic compounds can form.

An important concept is that clusters can carry organic molecules, in analogy to inorganic chemistry called “ligands”, which form a dense shell around the cluster, quite like a SAM (Fig. 1). The shells usually stem from a solution synthesis process, but quite often one can substitute the shell by other molecules. Typical molecules are based on thiols RSH, phosphines R_3P and amphiphiles (molecules with a nonpolar chain R and a polar head group, such as carboxylic acids RCOOH).

3.1. Macroscopic description; colloid science

Estimates for pure van der Waals binding between a metallic cluster and an organic surface can be based on the Hamaker constant A, as defined by the interaction energy [68]

$$W = -\frac{Ar}{6D} \qquad (1)$$

where r is the radius of the cluster and D the closest cluster–surface distance. The value for gold on polystyrene is 1.7×10^{-19} J (1.1 eV or 102 kJ mol^{-1}), which is clearly above the 6.5×10^{-20} J (0.4 eV or 39 kJ mol^{-1}) for polystyrene on polystyrene [69]. This means on the one hand that the polymer chains have a reduced mobility when they encounter a cluster (in the bulk or on the surface); on the other hand, a metal cluster has higher adsorption energy than an organic cluster or molecule (note that this is only valid when entropic effects play no role). An interesting and usually ignored effect is that the interfacial energy causes strain in embedded (and also adsorbed) clusters. Akamatsu and Deki [70] measured the change of the lattice constant of gold clusters in a polymer with selected area electron diffraction. This thermodynamic effect, observed for large clusters, remains to be related to other local bond length changes, e.g. the change of the Au–Au distance when the Au atoms are in contact with sulphur from adsorbed thiols.

The scenario changes whenever electrostatic interactions are invoked, and the typical question of dispersion stability [71] is now posed for particle–surface interactions. Considering only a single functional group, they are stronger than van der Waals interactions, and thus dominate the binding between a polar functional group on the cluster and a polar functional group on the surface. Obviously, the polarities of the charges or dipoles have to result in attractive forces. However, one should be aware that van der Waals interactions could easily dominate the binding since they are working between nonpolar and also polar groups, and they involve the complete cluster — they can easily add up to larger binding energies than electrostatic interactions. Note that for separations above several nanometers, Casimir forces also have to be taken into account [13].

At the solid/liquid interface the interaction is more complex [18]. First, a coagulation or coalescence, which is energetically favored (Table 2), has to be suppressed. To this end, clusters have to be stabilized either electrostatically or sterically. The first stabilization is more common since surface charges on the clusters are often present from the synthesis. In this case, counterions in the solution (the electrolyte) form an electrical double layer whose extension depends on the concentration and charge of all other ions in the electrolyte. This means that the pH value and the presence of salts can finely tune the cluster–cluster interactions. The DLVO theory gives a more detailed description [13,68,71]. The second possibility of stabilization is an uncharged polymer on the cluster surface; both stabilization mechanisms are combined when charged polyelectrolytes are present on the cluster, which is quite common. Note that the stabilization is not attained by electrostatic repulsion; rather entropic and osmotic effects for the solvation of the polymer chains are caused by reorganization of the solvent structure and by the relatively high concentration of the chains close to the particle, respectively. Similar arguments apply for the uncharged thiol or phosphine molecules on metal and semiconductor clusters (synthesized in solution).

For the charged clusters, the usual concept is electrostatic binding to a surface with countercharges. The effect is strongest for ionized groups such as COO^- and NH_3^+. Since the charge depends on protonation equilibria, the pH value controls the amount of charges:

$$RCOOH \leftrightarrow RCOO^- + H^+ \tag{2}$$

$$RNH_2 + H^+ \leftrightarrow RNH_3^+. \tag{3}$$

($RCOOH$ and RNH_2 designate molecules bound to the cluster or the surface). One can employ quarternary amines, such as $RN(CH_3)_3^+$, to circumvent the problem. In this case, only Eq. (2) applies; the pH should be as high as possible, and indeed at low pH values no binding occurs. However, high pH values mean that ions (OH^-) have to be added, which will change the ionic strength, and might induce cluster aggregation. A good example is the adsorption of positively charged (quarternary amine-coated) gold nanorods on a carboxylate-terminated SAM [72], where an optimal pH value of 6.5 was found, rather than higher values. Shyue et al. tried to mimic a cluster with negative charges by ZrO_2 particles. When these are attached to an SFM tip, detailed investigations of the electrostatic double layers on various amine SAMs become possible. Again, attractive interactions with quarternary amines require relatively high pH values (here to deprotonate the ZrO_2 surface). However, primary amines RNH_2 show a complex behavior — repulsion–attraction inversion, depending on the tip–SAM distance — because they form a Stern-type (inverted) double layer [73].

Until now, the thermodynamic interpretation was in the focus. Of course one also has to invoke kinetics whenever the adsorption process is not sufficiently fast. While standard procedures involve monitoring the cluster coverage after various contact times between clusters and soft matter surface, the results are not usually interpreted in terms of kinetic schemes. One of the few examples is the multilayer adsorption of metal clusters with negatively charged ligands on positively charged or thiol-terminated silane SAMs: Park et al. [74] found that monolayers with 16 nm clusters build up faster than with very large clusters (>40 nm), while the large clusters quickly form multilayers. The kinetics scheme involves adsorption and desorption rates for the first and for the second layer.

3.2. Description on the atomic level; chemistry

For deposition processes on surfaces, one can distinguish between adsorption and reactive deposition; reactive means that either two (or more) precursors react at the surface (mineralization, electroless deposition, chemical vapor deposition), or that a single precursor reacts *with* the surface. A special case of the latter is electrodeposition [75] where the surface reactant is an electron [40,76,77].

Furthermore one has to consider other cases where the substrate surface is covered by a layer, which can provide protection (e.g. SiO_2 on Si against oxygen) as well as function (e.g. organic monolayers with a terminal group). A more important function can be that deposited clusters preserve their characteristics; in other words, coupling to the underlying substrate is suppressed. This is usually achieved quite naturally: the cohesive energy between two metal atoms, or the lattice energy of an ion in an ionic lattice, is much higher than the interaction between a metal atom or ion and organic matter (Table 2). This means that there will always be the tendency of metals to coalesce or to fuse with a metallic substrate, and a similar argument applies to other inorganic clusters. Obviously, these thermodynamic arguments can become invalid in the case of slow kinetics.

A very versatile layer system is provided by self-assembling monolayers (SAMs). They consist of more or less densely packed molecules adsorbed on a solid substrate. A head group provides strong interaction such as electrostatic or covalent binding to the substrate. For simplified systems like small gold clusters in contact with short alkanethiols, quantum chemical calculations can detail the type of binding. It certainly entails expansion (weakening) of the gold lattice next to the sulphur atom, and charge transfer [78]. In many cases a simple model is assumed: the head group chemisorbs to the substrate surface, a straight backbone is pointing roughly in the direction of the surface normal, and functional end groups form the exterior SAM surface. All three assumptions can be wrong, and many (electro)chemical and physical properties of a SAM are heavily influenced by defects [40,76,77,79,80]. Hence, the presence and nature of defects will determine whether or not a SAM is suitable for cluster immobilization. While defects that allow a penetration of the SAM will strongly influence the electrochemical behavior [76], more subtle changes are found in the molecular conformation. The energies involved are of the order of several kJ mol^{-1} (tens of meV), so the mere contact with electrolytes and electrochemical reactions can produce these conformations [76,77,81]. Non-functionalized alkanethiol SAMs can change their conformation upon contact with electrolytes [82] and upon change of the electrochemical potential [76,77,81,83]. Even in the absence of electrochemical potentials it is known that functionalized thiol SAMs can respond to their chemical environment by assuming different conformational structures [79]. A good example is an alkoxy-terminated SAM that was shown to be ordered in air, but disordered in D_2O and CCl_4 due to solvent penetration [84].

Surprisingly, the presence of an organic layer on a metal can be exploited in electrodeposition to create nanoislands [76]. Since the rate is in this case determined by penetration through the layer to the soft matter–substrate interface, the kinetics can easily be tuned by the molecules' size or by temperature (see Fig. 5). Note that the islands are in contact with the metal substrate, so several size-dependent properties (e.g. optical [85,86]) cannot develop. The driving force is certainly the high metal–metal interaction energy (Table 2). Purely thermodynamically, the energy should suffice to break chemical bonds in the SAM, which is however not required since transient defects in the SAM allow for a relatively fast penetration. Amine-terminated surfaces are very interesting because, on the one hand, they can bind noble metal cations as complexes, and on the other hand they are subject to protonation/deprotonation equilibria (Eq. (3)). In contrast to metal ion–organic ligand binding, the properties of metal cations on organic layers are not well known and cannot simply be extrapolated from available data. Certainly the most valuable information for metal ion–soft matter interactions comes from analogies to metal ion–ligand interactions. The relevant information is found in inorganic chemistry textbooks [87].

Related to this is a major question we will encounter again and again, namely how metal structures can be deposited onto soft matter layers without penetration. A good example is electroless deposition of cobalt onto an aminothiol SAM with palladium islands (see Section 4.3.1.1). A combination of in situ STM, in situ SFG and ex situ XPS was employed for surface analysis [88]. The complex formation between Pd(II) and the terminus of the molecular layer is kinetically much favored over penetration; moreover, in the absence of (negative) polarization, the thermodynamic driving force for forming palladium/gold is reduced. The interaction between amine terminus and Pd(0) islands appears to be relatively weak (the islands can be moved by STM). A simple explanation of this phenomenon is not possible, but the bond strengths N–Pd(0) < N–Pd(II), P–Pd(0) < P–Pd(II) follow the usual trends in complex chemistry (hard and soft bases and acids) [87].

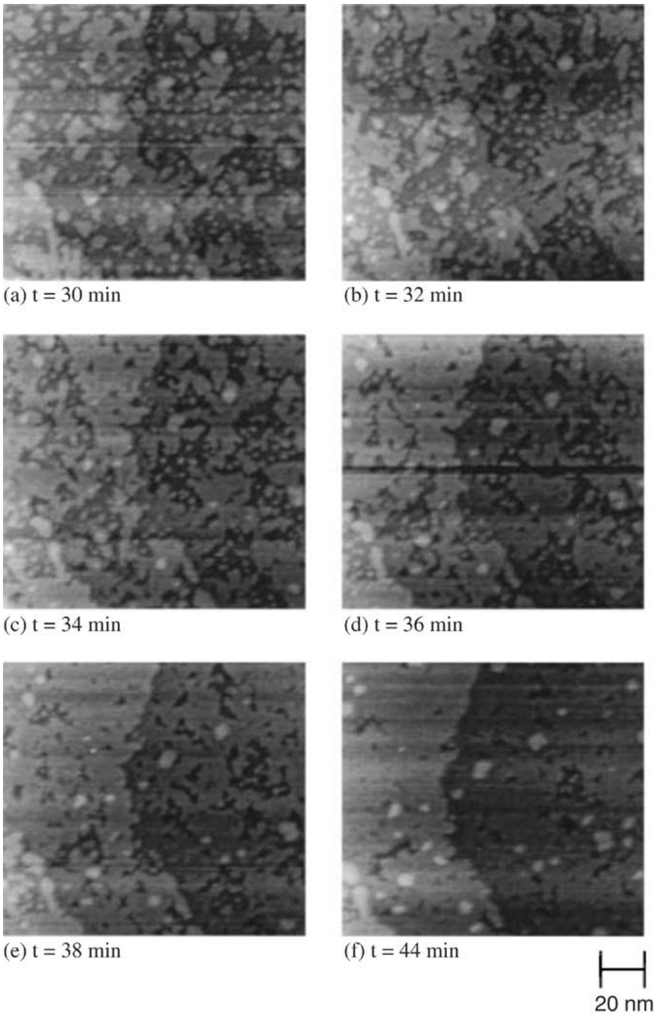

Fig. 5. In situ STM image sequence of Cu layer-by-layer growth on $C_{18}H_{37}SH$-covered Au(111) at 345 K. A constant potential of −50 mV versus Cu/Cu^{2+} was applied at $t = 0$. Islands grow and coalesce (a)–(d) to form an almost complete layer underneath the SAM (e) and (f) with some islands of the following layer. A substrate step divides the image into a bright area (left) and a darker one (right), that is, an upper and a lower terrace. Electrolyte: 50 mM H_2SO_4 + 1 mM $CuSO_4$ in a 2:1 mixture of $HOCH_2CH_2OH$ and H_2O [40].

3.3. Experimental methods

The analytical methods employed in Surface Science are for a large part described in physics and chemistry textbooks and in many reviews, in some cases also specifically for soft matter surfaces [12,27]. Here the focus will be on the most important methods for cluster and soft matter analysis (see also the acronym list). First, we have to note that most methods require electrons traversing a certain distance, so vacuum, usually ultrahigh vacuum, is used. The other extreme, solid/liquid interfaces, and thus also soft layers on substrates in contact with liquids, can be probed by electrochemical or optical techniques.

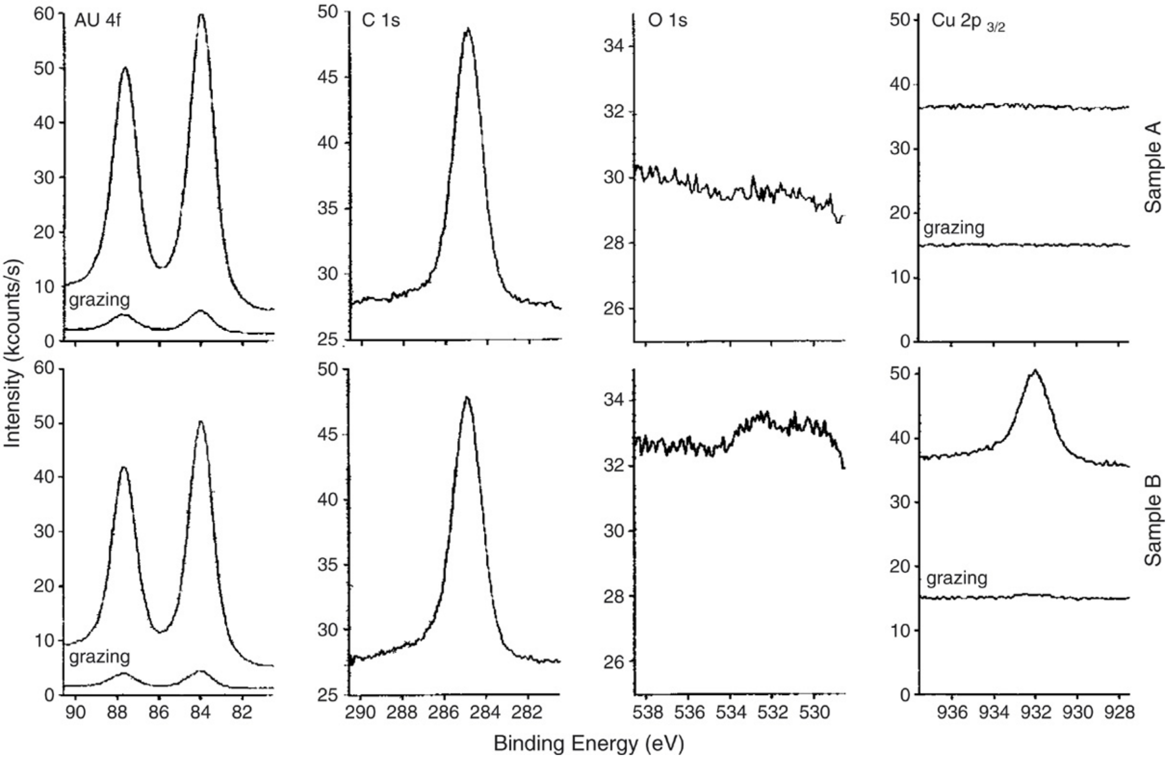

Fig. 6. Normal emission XPS before (sample A) and after (sample B) Cu electrodeposition on an alkanethiol SAM on Au. For Cu grazing emission is also shown (lower traces): the photoelectrons leave the surface at a low angle, thus enhancing sensitivity for the topmost surface atoms; Cu is not on top. The peaks correspond to the expected elements; despite a transfer through air, very little oxygen is present [76].

Ion Scattering Spectroscopy (ISS) is a very powerful technique, when the exact vertical location of clusters is searched for. An ion beam with energies in the keV range is directed to the surface, and the scattered ions are analyzed with respect to their energy, which yields the chemical information. When the erosion rate of the sample is calibrated, the duration of the analysis translates directly into depth information. An example is the analysis of nickel penetration into a SAM [89]. We note that Medium Energy Ion Scattering (MEIS) and Rutherford BackScattering (RBS) are related methods working at much higher energies (MeV range). The better-known Secondary Ion Mass Spectroscopy (SIMS) has the advantage of detecting molecular fragments, but is not very well suited for cluster detection.

The classic chemical surface analysis is obtained with XPS (ESCA). In passing we note that it is possible to compute the thickness of a (chemically homogeneous) soft matter layer from XPS intensities with the help of the inelastic mean free path of the electrons; however, the method is not very exact, especially for soft matter [90]. In contrast, for distinguishing the topmost atomic layers from the others (clusters on top of or below organic matter), spectra taken at various take-off angles are helpful. A high take-off angle (measured from the surface normal) means that the photoelectrons have to travel through up to several nanometers of material. Only the topmost atoms at the surface (and a few atomic layers below) can emit electrons directly to the detector, and in this way give enhanced selectivity to an analysis of the sample/vacuum interface (Fig. 6). Alternatively, XPS can be combined with depth profiling with an ion beam: now the signal can be interpreted as being solely from the topmost (exposed) surface layer, and very clear results can be obtained [91].

In most cases the soft layer is not or very little conductive. Thus the layer, but also the clusters, cannot dissipate the charge that builds up during emission of the photoelectrons. This leads to unwanted gradual positive shifts of the same order of magnitude (1 eV) expected for chemical shifts, which are caused by neighboring atoms. When the shift is negative, as found for more or less metallic clusters on top of a SAM [92, 93], one can invoke other factors like chemical interaction or increasing metallicity. When it is positive, one may try to neutralize the sample with a low energy electron beam or “cloud”. Controlled surface charging (CSC) uses the beam without complete neutralization to create potential gradients on the surface; from XPS data one can now calculate depths [94].

One of the best diffractive methods is specular X-Ray Diffraction (XRD). Not only can it be used in air or for solid/liquid interfaces, from the data one can also calculate vertical density profiles, for example for the location of metal clusters. Of the imaging methods, SFM deserves special credit for its high resolution and very general applicability. Moreover, one can also record local forces or local elastic properties. Optical (UV–vis) spectroscopy is a straightforward method to detect metal clusters. In a refinement, Akamatsu and Deki used Maxwell–Garnett theory to show how shifts in the optical absorption of metal clusters depend on the fraction of the volume they occupy. The effective dielectric constant of the system soft matter/metal changes such that increasing metal content leads to a redshift that can be quantified [91].

4. Clusters on soft matter surfaces

4.1. Small stoichiometrically defined clusters

The best-known clusters with exact stoichiometry are bare metal clusters. The very smallest of these are produced in the gas phase. Their deposition will be discussed in connection with soft landing (Section 5.2), since this method appears to be the only possibility for the deposition of such clusters without any change of their geometry. When ligands are present, or when the clusters are larger, the situation becomes more favorable, and one can achieve a nondestructive deposition. The cluster material can vary from metals to carbon, and the ligands are chosen accordingly.

Let us first discuss typical transition metal clusters. Due to the metal–metal bonds the electron density at the metal nuclei has to be very high (low oxidation states), and thus compatible ligands — capable of donor-back donation bonds — such as CN^- or CO are chosen. The clusters are fixed to organic monolayers with a donor end group that can exchange a ligand on the cluster, hence a more or less covalent bond is obtained. For example, Ru_3 and Os_3 carbonyls can bind to a cyano-terminated silane SAM on fused quartz [95]. IR spectra prove that the cyano groups replace step by step the CO groups, even up to the point that the cluster breaks into single-centered complexes. A closely related system uses a gold substrate on which a thiol-terminated silane adsorbs. The thiol group likely binds to the gold surface, while the silane parts form a presumably amorphous siloxane network by hydrolysis of the methoxy groups. This yields a stripe-like molecular superstructure, on which an osmium carbonyl with an acetonitrile ligand is bound. The latter is known to react with silanol groups. XPS shows that this process does not influence the thiol, hinting at a defined bond with the gold. However, with STM clusters were found whose size points towards coalescence of the Os_3 units. Hence the expected reaction did not take place or was slower than diffusion on the silane layer. But also clusters with relatively "hard" ligands (oxygen- and nitrogen-based) qualify: a triruthenium cluster with a disulphide-terminated ligand was bound to gold. The resulting SAM can then be assumed to be terminated by the cluster. The reduction of one center from Ru(III) to Ru(II) was followed electrochemically by voltammetry [96]. In another case, the electrooxidation of one Ru(II) center eliminated a CO ligand and allowed binding of the Ru_3 complex, detected by voltammetry [97]. Analogously, a trinickel cluster with a disulphide ligand was bound to gold and characterized by IR, ellipsometry, and voltammetry [98,99].

A larger cluster system that recently attracted much attention is the $Mn_{12}O_{12}L_{16}$ structure. With ligands L such as acetate, the system contains neutral molecules, each of which exhibits magnetism. A major goal is to assemble these single molecular magnets in such a way that they form dense layers without too much intermolecular interaction. Hence a soft layer might well be the best solution. Attachment to a carboxylate-terminated SAM on gold can yield well-defined films [100]; multilayers can be fabricated with polyelectrolytes replacing the SAM [101]. Alternatively, one may first exchange one or more ligands with a thiol-terminated carboxylic acid, followed by adsorption on gold. For a related system with pivalate ligands ($(CH_3)_3CCOO^-$) the assembly was confirmed by XPS and STM: the sulphur atoms show no signal and hence should be located at the gold surface. The superstructure of the clusters is not very regular, but dense [6]. This is in fact surprising since the formation of dense structures requires surface diffusion, which in turn should not operate when strong bonds are formed. So one may assume that the clusters first diffuse until they are in close contact with their neighbors, and thereafter react with the monolayer terminus. Other polyoxometallates can be obtained in well-defined stoichiometry, too; Liu et al. provide detailed preparation and analysis methods [102]. For example, $SiMo_{11}VO_{40}^{5-}$ can be organized in mono- and multilayers, the spacers being a polycation. The material can be deposited and also analyzed electrochemically [103].

One of the largest defined metal systems is the Au_{55} cluster, classically with phosphine and chloro ligands. Thiol-terminated layers can bind such clusters by reaction with the gold core. In fact the clusters are irregularly distributed on surfaces. One demonstration system was a wafer with a silane SAM that was locally changed into a "double" silane SAM with thiol termini. SFM data show that the clusters are about 50% larger than expected, certainly a consequence of mechanical interactions with the double silane layer [104]. Similarly, GaAs with an oxide layer can be modified with a thiol-terminated SAM, and the Au_{55} compound can bind. The measured SFM height was attributed to the combined thickness of SAM and Au_{55} compound [105]. Another soft layer was constructed by spin coating a dendrimer with 96 terminal thiol functions on silicon wafers, again allowing for immobilization [106]. For this system, treatment with CH_2Cl_2 vapor — a good solvent for the cluster compound — induces mobility, resulting in growth of nanoscale hexagonal crystallites. The clusters and the crystallites are partially embedded in the dendrimer layer. The growth mechanism is thought to be based on the slow loss of the ligand shell of Au_{55} by interaction with the thiol groups, while the cluster diffuses on and in the dendrimer layer during this process.

Multilayers of Au_{55} with phosphine and chloro ligands can be assembled with dithiol linkers, starting from a GaAs substrate with a thiosilane layer. Such cluster multilayers show hopping conductivity with a quasi-1D current path, as determined from temperature-dependent current–voltage curves [107]. This is also known for layers of much larger gold clusters connected by dithiols [108]. An improvement is a double layer of two silanes, of which the top one is modified locally with an SFM tip [109], followed by thiol formation. In this way, very narrow stripes of Au_{55} can form by adsorption on top of these thiol groups. The width of the lines reaches the single cluster size [110]. Au_{55} can also be coated with sulphonate-bearing ligands. These negatively charged clusters can adsorb from aqueous solution

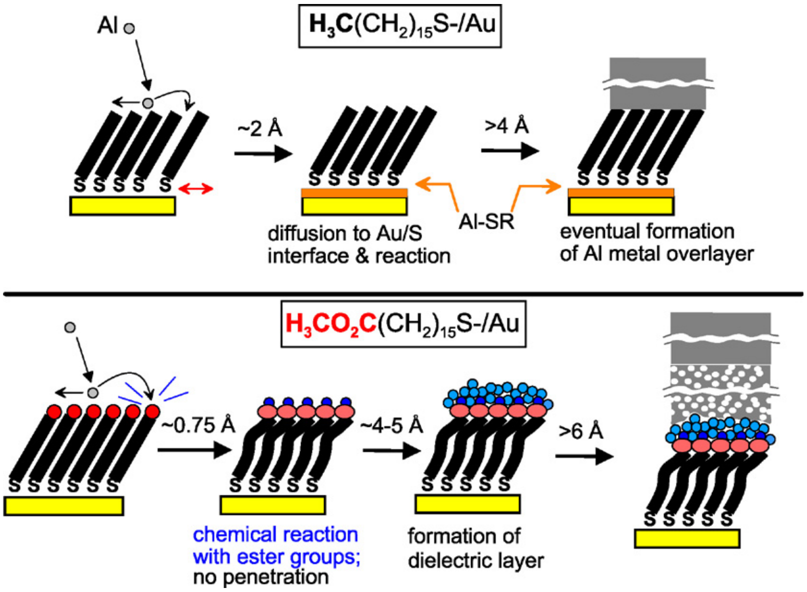

Fig. 7. Cartoon illustration of important features of the Al interaction mechanisms with the methyl- and methyl ester-terminated SAMS. The top figure shows that, for the methyl-terminated SAM, the first ∼0.2 nm of deposited Al diffuse directly to the S/Au interface to form a smooth interlayer, while after ∼0.4 nm a metallic overlayer at the SAM/vacuum interface forms. The bottom figure illustrates that, for the methyl ester-terminated SAM, the Al atoms react preferentially with the ester groups and do not diffuse to the S/Au interface. The first ∼0.075 nm of Al are shown as forming a specific 1:1 reaction product with the terminal ester groups. After ∼0.4 nm, metallic Al begins to nucleate in the form of discrete clusters, whereas at much larger thicknesses the Al forms a uniform metallic overlayer [294].

on protonated polyethyleneimine on mica and form dense layers. The distances between the clusters, as determined by SFM, correspond to the cluster diameter, 2.4 nm [111].

Larger gold clusters show less reliable stoichiometry. The Au_{101} system is still well accessible, and can be transferred with the Langmuir–Blodgett technique to graphite surfaces. It is, however, required that the neutral clusters form a mixed Langmuir layer with (partially N-alkylated, hence positively charged) poly(4-vinylpyridine). The layer exhibits good order, and Coulomb blocking (see 4.8.1) was measured with STM [112]. C_{60} as another well-defined systems has been deposited on so-called "striped" thiol phases on gold. The stripes feature rows that are supposed to contain S atoms, on which C_{60} is thought to nucleate into bimolecular chains [113]. However, why C_{60} should have a preference for sulphur over the nearly flat-lying alkyl chains, remains unclear.

4.2. Synthesis of metal clusters on soft layers

4.2.1. Metal clusters and atoms in the gas phase

Evaporation of a metal is one of the simplest and most used techniques to form clusters in vacuum systems. Usually, atoms form during evaporation, but one can also apply special methods to induce coalescence already in the gas phase to build clusters, mainly by adding inert gas [16]. There are many alternatives for cluster production, e.g. sputtering or laser ablation, which are not discussed in detail here. The advantage of these synthesis methods is that the clusters, as long as they are handled in vacuum, do not require further stabilization by ligands, hence their chemistry is very simple, and physical properties are more easily interpreted [17]. Another huge advantage of working in vacuum is that the clusters can be ionized, accelerated and filtered by electrical and magnetic fields, and in analogy to mass spectroscopy an exact size selection becomes possible [16,17].

For an interaction of the produced clusters with soft layers, the substrate has to be placed in the vacuum system. The question is now how to adsorb the clusters. When one wants to preserve the stable configuration of the atoms, the clusters have to be soft-landed, i.e. their kinetic energy should be minimized. For charged clusters, this can be achieved by electric fields, but for the general case of neutral clusters, one can employ soft landing on rare gas layers (see Section 5.2). While this special method is mainly focused on investigating the clusters, the interaction or landing on molecular layers leads to the main topics of this review (Sections 4.3–4.8).

Note that evaporation methods are less useful for the synthesis of binary clusters, as required for typical semiconductor clusters: evaporation of a mixture does not necessarily result in a mixed compound, especially not when single atoms impinge on a surface. Interesting alternatives are chemical vapor deposition of metal clusters (see Section 4.2.2) and synthetic (as opposed to mass spectrometry analytical) electron spray ionization of nanoobjects [114]. Another important point is that atoms can be easily obtained in the gas phase, and one can proceed to form clusters on the surface, rather than in the gas phase. The issues of impinging on a surface and ensuing coalescence to clusters (see Fig. 7, top part) will be discussed throughout Section 4. Here we note that on surfaces the coalescence itself is very hard to avoid, except at temperatures where surface diffusion is very slow [115].

4.2.2. Chemical vapor deposition (CVD)

As will be discussed in connection with penetration (Section 5.1) and soft landing (Section 5.2), low temperatures are favorable for on-top synthesis of clusters. CVD can be

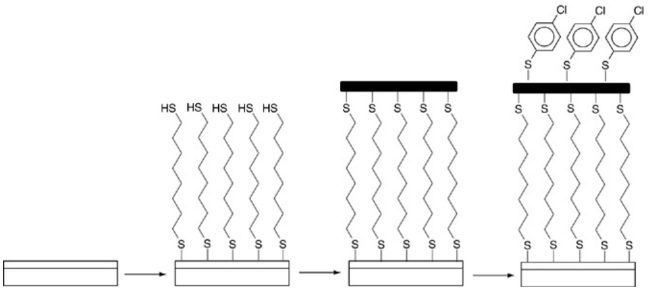

Fig. 8. Architecture after CVD of Au on top of a dithiol. The dithiol was assembled on a silver substrate, followed by CVD of Au (rectangle), and self-assembly of Cl–C_6H_4–SH on the Au layer [117].

successful whenever the temperature can be kept relatively low, usually around 70 °C, which is well below typical glass transition temperatures of many soft layers. An additional advantage of CVD is that conformal coating becomes possible. The process is based on the decomposition of evaporated precursors in the vicinity or on the sample. The decomposition products have to be volatile except for the material to be deposited. The Mittler group has investigated a range of materials in this respect, usually with organometallic molecules as precursors. Gold clusters of about 12 nm diameter were produced on dithiols on a silver substrate. The silver substrate facilitated XPS detection of the gold cluster growth. In this way, and by comparison with typical penetration systems such as alkanethiols, the on-top structure was proven. The method can easily be extended to microcontact-printed patterns [116]. Moreover, comparison to organometallic reactions allows elucidating metallization mechanisms: for example, Au–CH_3 groups react with terminal thiols to give an Au–S bond, obviously a nucleus for further metallization. Two distinct phases of metallization point to nucleation and growth in well-separated steps. The resulting clusters can be used to again bind thiols, as evidenced by mass spectroscopy [117] (Fig. 8). Quite similarly, palladium can be grown on a dithiol, but in this case the first step could be shown to result in binding of unreduced Pd(II) with an allyl ligand. Again, comparison with similar reactions in solution was of great help. To overcome the "passivation" by Pd(II), a hydroxyl-terminated SAM was first treated with trimethylamine alane, forming stable Al–O bonds, but leaving some very reactive Al–H groups. These groups are able to reduce palladium to the zero-valent state [118]. Semaltianos et al. [119] report CVD from a copper organic complex on a thiol silane. The silane is irradiated with UV light, and presumably reacts to a sulphonate, which has a high affinity to Cu(I) in the complex. The nucleation of copper islands was followed by SEM.

4.2.3. Adsorption from solution and binding

The physics behind the process has been discussed in Section 3.1. Clearly, "binding" refers to a strong adsorption — a chemisorption — that might also include the formation of a covalent bond. The preferred and simplest method is to employ electrostatic binding; this is especially favored by the fact that many clusters are synthesized with charged ligand shells. Unfortunately, even powerful theories like DLVO do not always allow predicting experiments; hence, to find the proper conditions requires a trial and error procedure. Certainly the safest way to bind a cluster strongly is by covalent bonds. This requires an appropriate functionalization. Best known and experimentally quite simple is the formation of an amide link between an amine R_1NH_2 and an acid R_2COOH:

$$R_1NH_2 + R_2COOH \rightarrow R1\text{–}NH\text{–}CO\text{–}R_2 + H_2O \quad (4)$$

The amine can be located on the surface, and the acid on the cluster, or vice versa. It is obvious that all these considerations become very complex on chemically (and topographically) inhomogeneous surfaces as encountered on biomolecules (Section 6). Another mechanism would be comparable to complex formation, i.e. the metal ions or atoms in the cluster would interact directly with potential ligands that are immobilized in the surface. The archetypical system is a gold cluster (either pure or with weakly bound ligands that can easily be substituted) that reacts with a thiol-covered surface. The latter is mostly fabricated by adsorbing a dithiol on a gold substrate (see 4.3.1), which leaves one thiol group per molecule exposed and ready to bind the gold cluster.

When only nonpolar interactions are present (no permanent dipoles, no charges) on both cluster and surface, the bonding would be of purely van der Waals type and thus weak for small clusters that contain only a few atoms (and a nonpolar ligand shell). However, when the solvent is not optimally suited to the solid/liquid interfaces, there is a tendency to interact more strongly (driven by the entropy of the solvent), comparable to the so-called hydrophobic effect for (bio)polymers. On the nanoscale, this translates into formation of bilayers where the nonpolar groups on the cluster interact with those on the soft layer surface and maybe even interdigitate, as will be discussed in the following.

4.2.4. Hydrophobic assembly

While all systems discussed up to now were bound by covalent bonds (including hydrogen bonds) or electrostatic interactions (dipolar or monopolar), it should also be possible to organize clusters exclusively with van der Waals interactions (induced dipoles only). At least for the adsorption process, the hydrophobic effect would be of importance (see Section 3.1). This is expected for clusters with a dense nonpolar coating, adsorbed on hydrophobic soft layers. For small clusters, the interactions are weak (see Eq. (1)), especially when one restricts the view to one pair of chemical groups (one group on the cluster, one on the surface); one could even expect diffusion of the cluster on the surface. We should however note that a multitude of such interactions (even the cluster atoms that are not in contact with the surface contribute substantially) [13,68] can amount to the same bond strength as a covalent bond. As an estimate one can take the van der Waals interaction modeled with the Hamaker constant, Eq. (1), and apply it with typical parameters ($A = 10^{-19}$ J, $D = 0.3$ nm) to Table 1: We obtain 47 kJ mol^{-1} (0.49 eV) for an Au_{55} cluster, and 320 kJ mol^{-1} (3.3 eV) for a 9.5 nm Au cluster.

Experimental evidence for such systems is scarce. Osman et al. [120] show a Coulomb staircase (see Section 4.8.1) detected by STM on alkanethiol-covered gold clusters adsorbed on alkanethiol/gold. The clusters formed a dense layer, but still a large STM bias voltage and small currents (i.e. little interaction with the otherwise mobile clusters) were required. These data suggest very weak interactions that should be associated with physisorption. In contrast, interdigitation of alkyl chains on the substrate and alkyl chains on the gold cluster would involve intermediate strength van der Waals interactions (certainly amounting to a higher binding strength than a single covalent bond) since not one, but many chains are in close contact. Peng et al. [121] explain the adhesion in this way for their system, gold clusters coated with alkyl SAMs, adsorbed on an alkyl SAM on a gold substrate (each SAM molecule bears the unusual mercaptothiophene head group). SFM indeed shows that the surface diffusion is slow or non-existing. Aslam et al. [122,123] assume the same effect for a closely related system; they prove the adsorption by measuring the mass uptake. An application for global conductivity measurements was expected. However, the use of silver paste to contact large areas can easily lead to mistakes (conductive pathways) when the layer is only a few nanometers thick (see also Section 4.8.1).

In several other systems it is not obvious whether a monolayer with a polar terminal group interacts with the clusters since the clusters are passivated by ligands. It is possible that the terminal group attaches directly to the cluster core: for this, several chains of the monolayer are not only required to interdigitate with the ligands to some extent, but actually to reach completely through the ligand shell in order to contact the cluster core. If this were to occur, the resulting bonds would be quite stable. On the other hand, interdigitation is only possible when not a few, but nearly all SAM molecules in proximity to the cluster take part in the binding, so the functional termini of the molecules should interact strongly with the cluster surface. A good example is provided by CdS clusters with an AOT (dioctyl sulphosuccinate) shell on hexanedithiol: the clusters remain attached to the SAM, presumably by Cd–S bonds, when rinsed with heptane, which is a good solvent for the clusters [124–126]. The clusters are not mobile, but easily shifted by an STM tip [125,126]. The fact that immobilization is possible, but that the clusters can be moved by moderate forces, indicate that interdigitation is the main attachment mechanism.

In conclusion, the ease of preparation and the simplicity of hydrophobic assembly — given that the system in question assembles in the way it is supposed to — would be of great interest especially for local transport measurements. Conclusive tests are still required; they are very likely hampered by preparation problems and by a tendency to cluster coalescence.

4.2.5. Electrochemical synthesis

Various methods to produce clusters in electrolyte might be called "electrochemical" in a broad sense. Here galvanic deposition is referred to, i.e. electron transfer from the substrate to some dissolved compound, mainly a metal cation. In the simplest case a metal cluster is formed by reduction of the cations to the zero-valent state, followed by coalescence of the atoms.

For thiol films, the method invariably entails penetration. Cavalleri et al. showed that copper deposition onto alkanethiols on gold can be induced under various conditions of electrochemical potential and temperature, always resulting in the thermodynamically favored penetration, i.e. Cu–Au contact [40,76]. The Kolb group investigated various structures in greater detail, and added more insights. Recently, the group presented a 4-pyridylthiol SAM that was shown to induce on-top electrodeposition [127]. To this end, first Pd(II) was adsorbed and bound to the pyridine ring. A subsequent negative potential scan was shown to result in palladium islands. The 2-pyridyl system did not show adsorption, which can be attributed to the nitrogen being in close proximity, if not in contact with the gold substrate. Proof for the location of the clusters was attained with angle-resolved XPS [128]. It is interesting that the palladium islands can act as nucleation centers for further deposition — obviously, the electron transfer through the SAM is sufficiently fast, as had been deduced also for the penetrating systems [76]. Stolarczyk et al. [129] deposited Au(III) on a thiol SAM with azo groups. In this case, islands form even without polarization, while negative scans produce a relatively rough structure (large clusters, but no islands). Hence here it is not clear whether or not penetration plays a role. This is typical also for most other attempts to deposit clusters electrochemically on top of SAMs.

It is relatively simple, but not very easily controllable, to produce ionic layer-by-layer assemblies and reduce them. In this way one can expect to form clusters sandwiched in the layers. For example, one can adsorb porphyrine cations alternately with AuCl_4^-, and electrochemical reduction creates gold clusters in mono- and multilayers [130]. Semiconductor materials might qualify, too, and one attempt to synthesize them electrochemically is based on tellurium cluster deposition on cyclodextrin layers [131]. The reduction of HTeO_2^+ is relatively complex, but nanoscale islands are produced. A comparison to pure alkanethiol showed that the cyclodextrin is indeed important for successful anchoring. However, conclusive proof for an on-top topography is still lacking.

Another method with a huge potential is electroless deposition, an autocatalytic redox process in which metal ions are chemically reduced to metal at a surface in the absence of any external current source [66]. In contrast to electrodeposition, no conductive surface is required, and protruding features do not build up electric field gradients that favor deposition at such features — even deep cavities can be plated quite uniformly. The through-hole plating of copper for printed circuit boards is a technical example. The electroless process requires that a cation of the metal to be deposited is reduced by receiving electrons from the surface of a metal substrate or from the surface of the catalysts used to initiate the deposition. The reductant in turn delivers electrons to this surface and is thereby oxidized. Hence simple electroless deposition baths consists of (complexed) metal ions and reductant, buffered usually at $\mathrm{pH} > 7$. An example is the Tollens reaction mixture, $\mathrm{Ag(NH_3)}_2^+$ with glucose. The redox process generally takes place only on catalytically active metal surfaces: noncatalytic surfaces first have to be activated with an appropriate catalyst before the metal deposition can start [132,133,66,88]. It can be shown that even very small clusters (subnanometer, difficult to resolve in electron microscopes) can act as catalysts. Such clusters can also be placed in and on biomolecules [61,62,134]. The big advantage of the method is that no contacting of the sample is required, which would be especially difficult for small objects. The metal surface growing on such clusters has of course to be catalytically active to insure a continuing plating process. Indeed this constitutes the difference to simple metal ion binding and reduction to clusters. Note that the plating process can also be used as an indirect detection method for the presence of noble metal clusters [135,136].

4.3. Metal clusters on SAMs

4.3.1. Thiol SAMs

Thiols employed for monolayer formation have alkyl or aryl tails and a head group that is a thiol or reacts to a thiol (disulphide, thiol ester) (Figs. 2 and 7). The head group binds to the substrate, which is very often gold, mainly due to the ease of preparation and the stability in air. However, many other metals qualify, too, and form a strong bond to thiols (the hydrogen likely desorbs). The bond itself is covalent and may best be compared to mono- or trihapto thiol complexes with transition metal cations. An important difference to covalently bound silanes is that the sulphur is quite mobile on the gold substrate (it is also possible that actually the sulphur moves together with one or more gold atoms bound to it, hence a thiol-gold compound moves on gold). This surface diffusion can, on the one hand, open up transient channels in the monolayer, while on the other hand, during the self-assembly it is likely the prerequisite to obtain densely spaced molecules. Probably the biggest advantage over other SAMs is that multilayer formation is strongly suppressed, since further physisorbed layers are easily rinsed off with a solvent.

To obtain clusters on top of thiol SAMs, penetration has to be prevented. This can be achieved at low temperatures, based on Tarlov's work [92], but simpler and much more applicable is the use of functional groups on the tail of the thiols. One has to be aware that these groups may also interact with the gold substrate, albeit much weaker; for example amine groups have quite a high affinity for gold, and even carboxylate can bind. Note that one can alternatively functionalize clusters with thiol-containing ligands, e.g. dithiols, and bind them on pure metal substrates [137]. Only in the direct vicinity of the cluster may the resulting structure be compared to that of pure clusters bound to SAMs, so the binding to bare substrates is not in the scope of this review.

One of the motivations to bind clusters on thiol SAMs is the fabrication of ultrathin model devices for nanoelectronics. The main task is to bind a single molecule (or a one molecule thick layer) without conductive defects to two electrodes with low contact resistance. Exactly this problem makes penetration studies (Section 5.1) highly relevant for future applications. The Grunze and Zharnikov groups tried successfully to irradiate a SAM with low-energy electrons to obtain chemical crosslinking between the molecular backbones (Fig. 9). The abstraction of H from aromatic rings induces C–C bonds between rings in neighboring molecules. A very long system (terphenyl) forms standing-up structures due to its stiff aryl backbone, even when head and tail groups are thiols. X-ray absorption measurements proved that the molecular orientation is not changed, which may have been suspected, and ISS depth profiles showed that only the crosslinked SAM is not penetrated by evaporated nickel [89]. Obviously the growth of such layers can be supposed to be based upon nucleation of islands or clusters. This was shown by STM of gold evaporated on top of a carboxylate-terminated SAM, supported by electron energy loss spectra of the SAM vibrations: coalescing clusters are formed [138]. When the atom dose is kept very low, it is possible to characterize the binding of single atoms. Whelan et al. [139] showed with XPS that copper atoms bind in a surprising monodentate fashion to carboxylate SAMs, while it is well known that carboxylate adsorbs bidentate on copper surfaces. This should remind us that the reactivity of single metal atoms, in contrast to that of solvated ions, can neither be compared with well-established inorganic solution chemistry, nor with the reactivity of extended surfaces of the same metal.

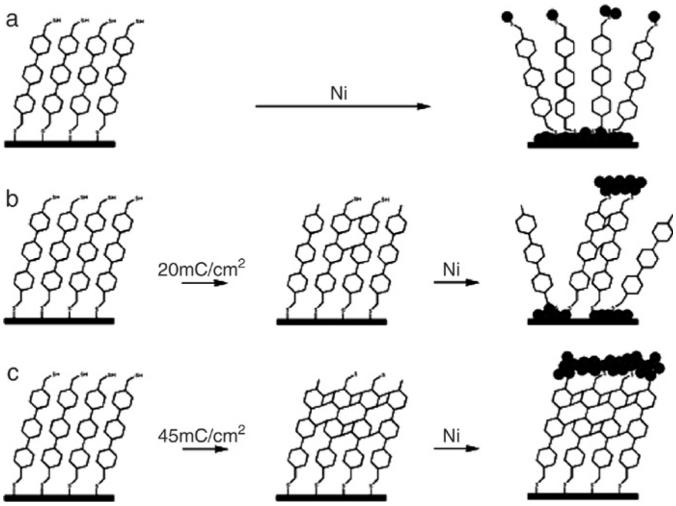

Fig. 9. Effect of electron irradiation and Ni evaporation in the case of pristine (a) and cross-linked ((b), (c)) aromatic SAMs on Au. The irradiation doses were 20 mC/cm^2 (b) and 45 mC/cm^2 (c) [89].

When a diluted dithiol/monothiol SAM is prepared, the density of clusters increases with the dithiol content. Note that such systems are sometimes favored over pure dithiol SAMs since a dithiol is surrounded by the nearly ideally oriented monothiol SAM molecules, and in this way unwanted binding with both sulphur atoms (resulting in flat-lying structures or even "loops") is suppressed. Sakotsubo et al. [140] interpreted STM data on such a system (evaporated gold atoms) as ballistic and diffusional growth. "Ballistic" means that only those atoms that strike an immobilized gold atom can attach and form a cluster, while all others penetrate the surrounding monothiol SAM; the diffusional growth refers to surface diffusion on top of the SAM. In other words, most atoms are lost due to penetration while diffusing on the SAM. A typical example for a cluster/SAM system is a study by

Stolarczyk et al., who showed with STM and voltammetry that gold clusters (with OH-terminated thiol ligands) bind on a dithiol SAM; presumably the dithiol substitutes several ligands on the cluster [141]. For this, the dithiol has to penetrate or interdigitate the ligand layer on the cluster (see also Section 4.2.4).

A special type of cluster is a nanorod: Its size can be seen as an intermediate stage between clusters and layers. Even such large objects can adsorb on top of SAMs, as shown for a carboxylate termination and 400 nm long gold rods. The assembly is dominated by electrostatics, since the rods are coated by a quarternary amine (positively charged), and indeed the expected pH dependence (low affinity at low pH when carboxylate is protonated [73], see Section 3.1) was found [72].

4.3.1.1. Synthesis of metal clusters on thiol SAMs. Adsorption of metal cations, followed by their reduction, or electroless deposition are methods that can create metal overlayers in solution. The reductant can be built into a SAM: a hydroquinone-containing SAM can reduce Ag^+ to silver clusters [142]. Electroless deposition [66,132] is an especially valuable tool, since it is easy to apply and can avoid penetration caused by electrochemical polarization or high temperatures [76]. In the following, we will focus on a specific example that highlights the principles: islands of palladium and Co/Pd can be obtained when palladium complexes in aqueous solution are bound to an amine-terminated (amide-containing) thiol SAM. The reduced palladium forms small islands, which are mobile when probed with STM in solution. Cobalt can then grow by electroless deposition, again in island shape. XPS at two take-off angles proved that the palladium islands reside on top [88].

A more detailed view at the energies involved can explain these observations, and similar considerations can be extended to many other systems: the Pd^{2+}–N binding energy can be calculated from thermodynamic data [143] to be 145 kJ mol^{-1} (the Pd^{2+}–Cl binding energy was estimated to be 200 kJ mol^{-1}). Pd(0)–N complexes cannot be found in the literature. The reason can be explained by the ligand-field theory. The electron configuration of Pd(0) is d^{10} and shows very unfavorable energetics compared to the Pd^{2+} configuration, which is d^8 (the stabilization of $-24.56D_{q0}$ with a ligand-field stabilization energy $D_{q0} > 14$ kJ mol^{-1} [87] is larger than a typical chemical bond energy). Therefore the Pd(0)–N bond must be much weaker than the Pd^{2+}–N bond, and thus the Pd(0) species can diffuse on the surface. Calculating, on the other hand, the Pd–Pd bond energy in bulk metal, one finds 375 kJ mol^{-1} for a macroscopic palladium solid [143] (see also Table 2). Calculations with an effective medium code estimated the bond energy for a palladium atom in a Pd(111) island containing 16 atoms to be 290 kJ mol^{-1}. In both cases (microscopic and macroscopic) the Pd–Pd bond energy is twice as high as the Pd^{2+}–N binding energy. This favorable situation allows the formation of stable palladium clusters. First, Pd(II) is reduced by the reductant to palladium atoms. During the reduction, the strength of the Pd–N bond is lowered and palladium atoms can diffuse. Nucleation and growth of the palladium atoms result in stable clusters. By STM, palladium clusters on this surface were found to be islands of presumably monatomic height, another hint at diffusion of single palladium atoms. It is very difficult to quantify their mobility — movement by the STM tip hints at a rather weak bond, that is neither a covalent bond, nor a complex is present. This is exactly what was predicted by the aforementioned theoretical considerations. Surprisingly, such islands are also catalytically active, and cobalt can be grown from an electroless deposition bath (Fig. 10). As expected for all electroless depositions, the influence of oxygen is pronounced; only in its absence can larger islands (more than 3 atomic layers) form [88].

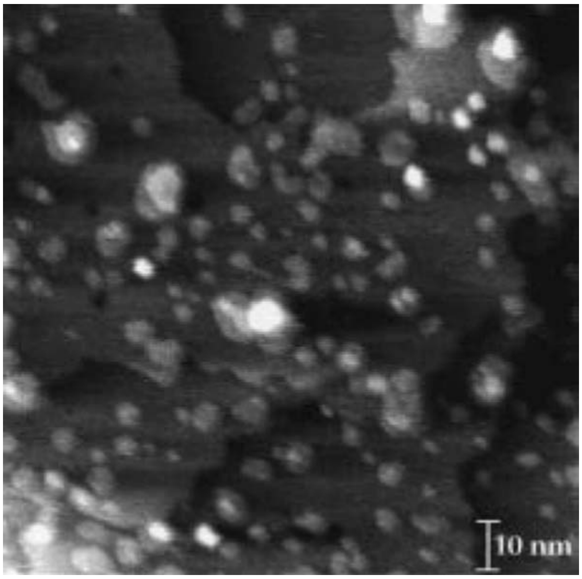

Fig. 10. In situ STM image of Co islands, grown by electroless deposition on a Pd^{2+}-activated amine-terminated thiol SAM on Au. Bath: 10 mM Co^{2+} + 50 mM $(CH_3)_2NHBH_3$ in H_2O. The brightest islands (e.g. in the upper right corner) contain two and three Co layers [88].

4.3.1.2. Adsorption of metal clusters on thiol SAMs. Most studies investigate the adsorption of prefabricated gold or silver clusters from solution. A standard wet chemical fabrication route involves citrate (and chloride), hence very often the clusters carry a negative charge. The electrostatic attraction to positively charged SAMs (most often terminated by protonated amines) is so strong that adsorption barriers are overcome easily (see Section 3.1). A typical example is the immobilization of citrate-stabilized gold clusters on amine-terminated thiols [144]. As expected, deprotonation of the amine binds fewer clusters (in a very similar system) [145]. For other systems, the optimal pH value (see Section 3.1) is around 8 since carboxylates on the cluster are deprotonated, and the surface amines are at least partially protonated. For example, silver clusters with carboxylate-terminated ligands probably carry a relatively high negative charge density compared to citrate ligands [146]. Since most clusters produced by wet chemical means carry surface functionalities, adsorption on functionalized thiols, e.g. with an amine group, can be used to obtain Surface-Enhanced Raman Scattering (SERS) of the thiol, based on the optical properties of the cluster [147]. In contrast, unenhanced Raman spectra of monolayers are extremely difficult to obtain. Note that the adsorption should be much stronger than physisorption, which is often assumed to operate.

More complex systems can involve multiply functionalized SAMs. The simplest example is a ligand-covered Au cluster on a dithiol layer, where the dithiol is supposed to contact the Au, e.g. by displacing the ligand. For thiol ligands, the mobility of a cluster with about 145 Au atoms is still quite high on bare, but not on dithiolated gold [148]. Another example is the binding of gold clusters on a dithiol SAM that contains ferrocenyl groups. Cyclic voltammetry in electrolyte reveals the well-known redox behavior, and STM can visualize the clusters. The adsorption of the 2.6 nm clusters does not influence the redox properties much [149]. In contrast, clusters on top of vertically oriented molecular conductors (molecular wires) can be used as local contacts (Section 4.8.1). When a dense coverage by clusters is intended, the Langmuir–Schaefer technique can be helpful: clusters with a nonpolar coating are spread on water in a Langmuir trough, compressed, and contacted with a horizontally placed substrate. The substrate can again be coated with a dithiol SAM, which may react with the clusters by displacing the coating. STM showed in some cases displacement of clusters, so thiol links did not always form. However, the coverage was close to optimal, and much better than obtainable by adsorption [150]. The evaporation of metal atoms on alkanethiol SAMs usually results in penetration. However, at low temperatures even the highly reactive sodium and potassium atoms can coalesce to clusters, whose optical absorption and second harmonic generation signals are typical for alkali metal clusters. Even air exposure does not result in complete oxidation of sodium, certainly due to (partial) penetration at ambient conditions [151].

The most refined schemes of immobilizing clusters do not rely on electrostatics (as discussed above), but employ chemically specific links. Apart from standard reactions, the whole spectrum of organic chemistry can be employed. For example, ketone groups on the ligand shell of a gold cluster can react with a mixed thiol SAM that is partially terminated by aminoxy (–O–NH_2) groups. In this way a very high density of 5.5 nm gold clusters (hexagonal packing) can be achieved on top of the SAM [152]. A disulphide SAM with terminal hydroxamate groups can bind Zr^{4+}, but leave further coordination sites on the Zr^{4+} open. Gold clusters, coated with the same SAM, bind selectively to the immobilized Zr^{4+}. Such a coordination chemical approach is certainly very versatile. It is quite simple to create a SAM multilayer system by consecutive adsorption of Zr^{4+} and a hexahydroxamate spacer — this strategy can also be used to obtain cluster multilayers. Optical spectra, SFM, contact angle measurements and the lack of conductivity of a spacer multilayer with a single cluster layer proved the functionality. Cross-sectional TEM shows the exact placing of the clusters above the soft matter–substrate interface [153] (Fig. 11). Even higher specificity is obtained by molecular recognition with hydrogen bridges. So-called Hamilton-type receptors (a structure based on amides and pyridine rings) can form multiple hydrogen bonds with barbituric acid (cyclic amide). For this, 5 nm gold clusters were coated with thiols with a barbituric acid terminus. They bound with high specificity to Hamilton-type receptors that had been synthesized on top of a thiol SAM. 3–4 receptors are involved in binding a single cluster [154].

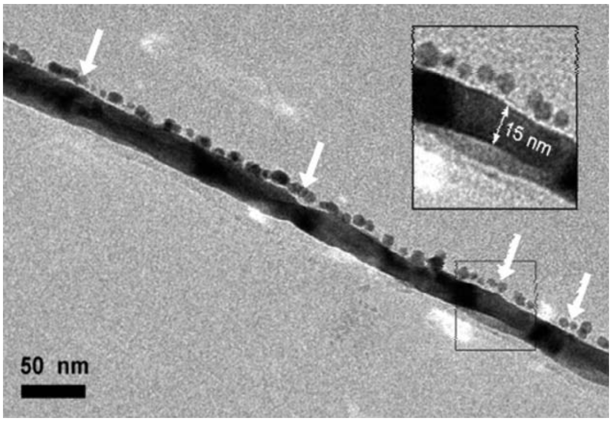

Fig. 11. Cross-sectional TEM image of a cluster monolayer bound on a coordinated organic multilayer. Inset: enlarged section showing the true thickness of the evaporated gold film (15 nm). White arrows indicate regions where a 3–4 nm spacing between the clusters and the gold substrate is observed [153].

Finally, the adsorption of clusters can also be directed into (usually microscale) patterns. For example, clusters on dithiol SAMs can aggregate into large structures that might be used as electrical contacts for the SAM [155]. Alternatively, adsorption of clusters on carboxylate-terminated patterned SAMs arranges the cluster aggregates in the desired pattern [156].

4.3.2. Silane SAMs

Silanes employed for film formation have alkyl tails and head groups with a mono-, di- and tri-substituted silicon atom, the substitution being chloro, methoxy or ethoxy (Fig. 2). In this way, covalent bonds with a wide variety of hydroxyl- or oxide-terminated surfaces become possible. Although hydrogen bridges can form, and although a substantial fraction of the molecules form intermolecular hydrogen bridges (or even Si–O–Si linkages), the most important binding mechanism is a covalent Si–O–surface bond. Hence the layers are very stable under many conditions. The tail can carry further functional groups, although in some cases they have to be protected during assembly (or created afterwards), since they are incompatible with the head groups (for example COOH). A relatively new development is the local production of COOH groups by tip-induced electrooxidation of vinyl groups, resulting in <10 nm wide COOH patterns [109]. A general problem is that monolayers are not as easily prepared as with thiols — the covalent linkage that probably hinders lateral diffusion is only one reason; more important is the facile formation of hydrolyzed aggregates that can reach tens of nanometers diameter and bind to surfaces quite strongly. Glass and oxidized silicon wafers are the most popular substrate systems.

Due to the large variability and stability, silanes are probably the most attractive thin films for technical applications.

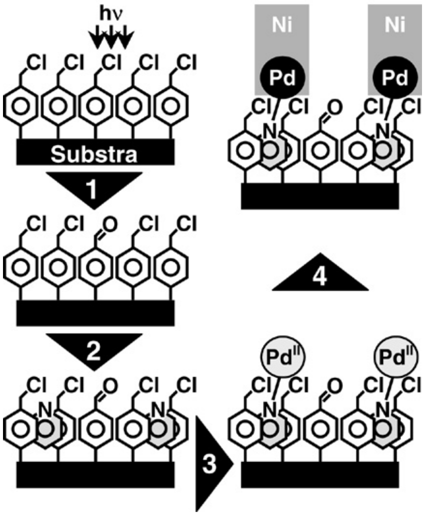

Fig. 12. Electroless patterning of metal overlayers via nanocavities in an aromatic SAM. Step 1: irradiation (through a mask to define a pattern) and reaction with water. Step 2: insertion of pyridine into the intact layer. Step 3: binding of Pd^{2+}. Step 4: electroless deposition of Ni [161].

Consequently they are discussed as barrier layer material for chip technology. For the production of layers, i.e. submicron or even larger electrodes on top of a silane layer, a recent example is instructive: Halik et al. made use of the fact that disorder in the topmost part of silane SAMs can effectively eliminate pinhole and other defects. To this end, a phenoxy-terminated silane was employed, which was able to tolerate evaporated gold contacts without penetration on areas as large as 30 000 μm^2. This translates into a high electrical breakdown voltage, which allows using the SAM as ultrathin gate dielectric in a low-voltage organic transistor [3]. In some cases layers of tens of nanometers of copper can be evaporated on silanes without interfering with the highly sensitive doping of an underlying silicon substrate with a thin oxide layer. When the SAM contains a thiol function, copper adheres even stronger than on the oxide. In this way, capacitors for the MOS technology can be produced, at the same time a proof for the large penetration barrier of the silanes [157]. Carboxylate and amine groups act in a similar way [158], and even a pyridyl group appears to be sufficient to substantially enhance the interaction with copper [159]. However, the effect may also be based on aromatic groups on flexible linkers as shown for a related system [3]. Obviously, the metal film forms by coalescence of clusters and islands. This process was followed by SFM and SEM; an even simpler and effective analysis method is UV absorption since the clusters and islands exhibit a plasmon band that is absent for a continuous film [160].

An excellent alternative to vacuum methods is adsorption of noble metal cations that can be reduced to the zero-valent state and coalesce to clusters, which in turn catalyze electroless deposition of metals. The Dressick group has developed a number of viable techniques that might be of high relevance for applications. To this end, silanes should contain groups that can be photochemically altered to allow optical or UV lithography. For example, aromatic trichlorosilanes can react with substrates, while their functional groups such as chloromethyl can bind Pd(II) complexes. The groups can be photochemically oxidized to oxygen-containing groups that do not bind Pd(II) (Fig. 12). Reduction and immersion in an electroless metallization bath create micropatterns of metal, e.g. nickel, with sharp boundaries on top of the silane layer [161].

As became already obvious, the first stages of producing metal films on silanes are connected to the growth of small islands, in other words clusters. Alternatively, clusters can be adsorbed from solution, and once again the terminal functionalization of the silane is of crucial importance. A few examples can illustrate this point: 5 nm gold clusters with carboxylate ligands bind well to amine-terminated silane SAMs, forming the core of a metal–insulator–semiconductor transistor [162]. Gold clusters of around 13 nm diameter can adsorb on thiol groups and be analyzed by SEM. Kinetic analysis gives a sticking coefficient of about 1, which means that thiol groups rapidly displace the originally employed citrate on the gold clusters (sometimes Cl^- is quoted). At an early stage the adsorption is controlled by diffusion in the solution, hence the coverage is proportional to the square root of the adsorption time. Later on effects of interparticle repulsion on the surface appear to slow down the rate. However, since the clusters are negatively charged, the kinetics should depend on surface charging, which was shown for a (conductive) SnO_2 substrate modified with an aminosilane [163]. It should be noted that longer immersion times (with interparticle interactions on the surface) for a nearly identical system can be fitted to Michaelis–Menten kinetics (for gold and also silver clusters of 16 nm diameter). This kinetic scheme, known from enzymatic reactions, here connects the fast immobilization to the slow multilayer formation [74].

A single gold cluster can be used as nucleation center for molecules, as demonstrated by linking Cu(II) hexacyanoferrate multilayers to the clusters [164]. Molecules attached to the gold clusters can be analyzed conveniently by Surface-Enhanced Raman Scattering (SERS), as shown for 12 nm gold clusters (note that SERS from flat gold surfaces gives practically no signal) [8]. Gold clusters can also be arranged in multilayers solely by a thiol-bearing silane: the silane adsorbs with its thiol head on the gold, while its tail reacts with another silane (condensation), again exposing a thiol head that can adsorb the following layer of gold clusters [165]. It can be expected that many other clusters show similar behavior; however, the gold systems are much easier to synthesize and exhibit no oxidation and few contamination problems. As an example for more sensitive clusters, Bae et al. [166] synthesized carboxylic acid-capped cobalt clusters that were partially coated with bromoalkanoic acid. The linkage to aminosilanized oxidized Si substrates was demonstrated: the primary amine reacts with the bromine, HBr is eliminated, and a covalent secondary amine link is formed. Microcontact printing of alkyl silanes, filling of the bare oxide surface with aminosilane, and again linking the clusters yields microscale patterns. This and similar schemes are in widespread use (however, mainly without silane or other soft layers).

4.3.3. Other SAMs

The dominance of thiol SAMs on gold (and other metals), and of silane SAMs on hydroxylated substrates, results from long-term experience, ease of use, and reliability. However, the disadvantages of the layers (discussed in Sections 4.3.1 and 4.3.2) are well known, and furthermore new systems with exciting properties may easily be overlooked (or never be tested). In this respect, several chemical groups that can be used as ligands for small metal clusters, e.g. isonitriles, have found applications for forming SAMs on metal substrates. Carboxylic acids are well known alternatives to silanes on oxides. For example, a carboxylate thiol can bind on Al_2O_3 by exposing its thiol moiety to the solution, thus allowing to bind silver clusters [167]. In all these cases, the concept of a SAM is of course the same as for thiols or silanes.

A more complex system that might be compared to thin polymer or polyelectrolyte films is a dendrimer layer. Dendrimers are highly branched, nearly spherically shaped molecules, often with multiple chemical groups. G4OH dendrimers of generation 4, with amine, amide and hydroxyl functional groups have been used as templates for the direct synthesis of metal clusters such as copper, platinum and palladium within the dendrimer [168]. Due to the fixed number of binding sites, thus-prepared metal clusters show narrow size distributions and keep their catalytic activities. These clusters are not supposed to be in contact with the substrate and thus worth mentioning; however, a proof was not given. They can be used to induce local metal plating in an elegant way [136] (Fig. 13). It is surprisingly simple to form sub(monolayers) of amine-terminated dendrimers on oxide surfaces [135], and the monolayers are quite flat. Bar et al. [90] showed that such films can be employed to adsorb gold and silver clusters: the dendrimers were pure tertiary amines with 64 primary amine end groups and formed a layer of roughly 2 nm thickness, which was determined by XPS of the original and sputter-removed film (considering the electron mean free path in organic matter). Certainly the partial protonation of the amine plays a role in binding the citrate-stabilized clusters. The clusters can in turn be used to adsorb organic molecules, of which surface-enhanced Raman scattering is easily measurable, despite the small coverage.

Thiol SAMs have been so successful in binding gold clusters that virtually any substrate is being functionalized with thiol groups. For substrate surfaces with very low reactivity, this poses additional challenges. Graphite can be modified with diazonium reagents under cathodic polarization. Attached thiol groups are not affected and can be used to immobilize gold clusters [169]. In analogy to gold substrates, dithiols appear to react with graphene sheets or defects therein, hence also with carbon nanotubes. The thiol groups can again be employed to immobilize gold clusters [170]. When the nanotube is first oxidized and exhibits carboxylate functions, more standard immobilization routes can be followed successfully [171]. In such cases of "grafted" or covalently linked molecules, it is usually not clear whether a SAM forms or whether molecules attach randomly at certain surface points. The drastic reaction conditions, e.g. formation or breaking of C–C bonds, should not allow for mobility of the grafted molecules on the substrate — in this way, self-assembly should not be able to operate. This does of course not mean that the resulting layers are not useful — whenever the grafting density is sufficiently high, one can address the molecules as a "layer", and their terminal group will now determine the substrate chemistry.

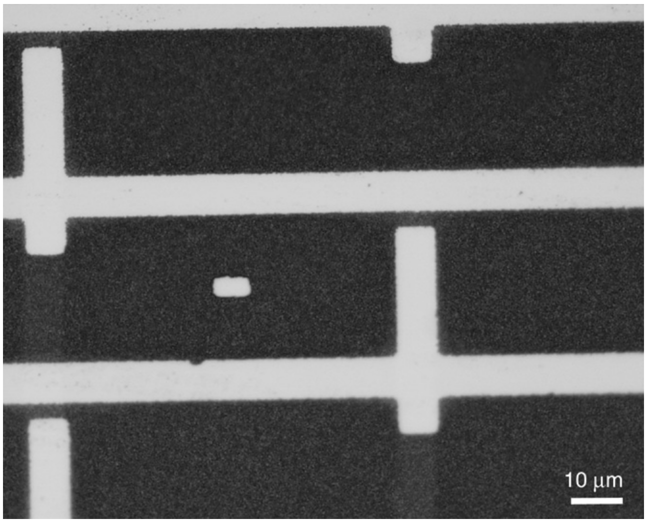

Fig. 13. Optical micrograph of Cu (dark) on thiol-passivated Au (bright). The bright areas were covered with an alkanethiol by microcontact printing, after which the (now) dark areas were backfilled with a dendrimer with amine and disulphide groups. The sample was then subjected to Cu electroless deposition [136].

4.4. Semiconductor clusters on soft layers

The synthesis and the assembly of semiconductor clusters are one of the most intensely studied fields in nanoscale science. The reason is primarily that a large number of applications is foreseen and in part already demonstrated in prototype devices. Mainly the optical properties form the basis for this, especially photo- and electroluminescence. These properties are attractive because the emission energy increases with decreasing particle diameter — this quantum confinement effect of the energy levels is one of the best examples that physical properties on the nanoscale differ from those on the macroscale. In fact, the emission can shift >1 eV, corresponding to more than 100 nm in the visible range. At the same time, the bandwidth can be narrower than for conventional fluorescent dyes. The fact that most particles are stabilized by ligand shells is of great advantage since the organic molecules making up the shell can be easily modified or exchanged to modified molecules. In this way a very broad chemical and even biochemical tunability of the clusters is attained, with a large range of possible applications. One of the best-researched materials is CdS. The photoluminescence (PL) can be shifted to the blue range, which is not easily accessible with other systems. However, band gap PL is aimed at, in other words, energy levels and traps between valence and conduction band should not be available, but can often not be avoided [172].

Immobilization of the clusters allows studying the immobilization itself, which is indispensable for device architecture and even biological applications (e.g. binding to antibodies). Moreover, the clusters can be separated without further chance to coalesce. On the other hand, the presence of a solid surface changes the physical properties, and metal substrates allow charge dissipation in electrochemical and also in photoelectron experiments. This task is not simple: when the soft matter layer is too thin, the cluster will couple to the substrate; when it is too thick, the charge cannot be dissipated any more, which is of course true also for metal clusters [94].

A classic synthesis is based on inverse micelles of surfactants such as AOT (Aerosol OT, bis-(2-ethylhexyl) sulphosuccinate) in nonpolar solvents, which can be sequentially loaded with Cd^{2+} and S^{2-} salts. Colvin et al. [124] showed how such particles can bind to dithiol monolayers on gold and to thiol-terminated fatty acids on (oxidized) aluminum. The exposed thiol group is supposed to bind to Cd^{2+} in CdS, and the resulting submonolayer is quite stable. While it is clear that thiol groups can easily displace AOT, and that in this way multilayers can be constructed [173], a direct proof of covalent links between dithiol and CdS is nearly impossible — in fact, interdigitation of the dithiol chain and the AOT shell could also provide the required attachment (see Section 4.2.4). XPS proved the presence of the elements, and UPS clarified that the electronic properties are different from those of bulk CdS. Ogawa et al. employed the same system to obtain tunneling spectra with an STM. For this, they had to adjust the STM conditions since the clusters were still mobile in interaction with STM tips. Current (and differential admittance) gave a conductance gap of 3.5 eV, thus >1 eV above that of bulk CdS [125].

A common problem is the conformational ordering of the dithiol monolayer. First, dithiols can oxidize to disulphides in solution or during assembly and in this way build up bi- or multilayers. Second, the dithiol has the possibility to adsorb with both thiol moieties in contact with gold — this is likely not as a loop, but flat lying. Third, many, if not all, substituted thiols tend to exhibit conformational disorder. Infrared spectroscopy and XPS at various take-off angles can help to elucidate the conformation. For example, methylene C–H stretches shift from the *all-trans* standard 2848 cm^{-1} (symmetric) and 2918 cm^{-1} (asymmetric) several cm^{-1} up, as found for dithiols and carbonyl-containing thiols on gold [79, 174].

Tsuruoka et al. showed another way: one can first replace the ligand shell (here AOT by a mixture of alkanethiols and hydroxyalkanethiols), and thereafter bind the ligands covalently to reactive groups on a surface. The employed diisocyanate has probably disadvantages like a dithiol; nevertheless, the formed carbamate group assures covalent and thus strong immobilization [175]. Like dithiols, multilayers can be formed with simple procedures. Multilayers are even simpler to produce with the layer-by-layer (LBL) technique: consecutive adsorption of polycations and polyanions is followed by adsorption of e.g. CdTe particles, passivated by alkane thiols with various end groups. In contrast to this electrostatic procedure, one can also produce covalent (amide) linkages to a substrate [176]. The variability of the LBL was shown by production of complex polyelectrolyte/gold cluster layers. In this way, one can tune the distance between adjacent CdTe layers and observe fluorescence transfer over several nanometers [177]. One of the layers can be replaced by a micron-sized polymer sphere, on which the clusters adsorb [178]. For an even more complex architecture, LBL allows sequential adsorption of clusters with varying diameter, so that excitation transfer can be directed [179].

Other strategies are based on SAMs with reactive amine groups. Citrate-capped particles are negatively charged and thus bind easily to protonated amine-terminated surfaces. This principle was used to bind CdSe and CdSe/CdS to an aminosilane on an oxidized silicon wafer surface. However, the particles also formed features of unexpected height that were linked to the presence of bi- and trilayers [180]. P-aminothiophenol can form a SAM on gold, but also be used to replace the usual AOT ligand on CdS clusters. Both amine functionalities can be oxidatively coupled by applying cyclic electrochemical potential sweeps. In this way, the course of the immobilization can be followed by measuring the current response, as for the synthesis of polyaniline. The presence of CdS provides for some doping of the resulting dianiline structure, so that the electrochemical parameters change slightly. Quartz microbalance measurements were used to obtain a particle density of 9×10^{11} cm^{-2} [181].

4.4.1. Synthesis of semiconductor clusters on soft layers

An obvious simplification would be the synthesis of the cluster directly on the monolayer. For example, Pb^{2+} can bind to the carboxylate terminus of a thiol layer on gold. The presumed electrostatic binding may also be complex formation, but the reaction with H_2S produces PbS clusters that can be detected by STM. To facilitate TEM analyses, a sharp gold tip was prepared in the same way as the flat surface, hence a PbS cluster could be imaged at the tip apex [174]. A similar layer can be used to immobilize TiO_2 clusters: Rizza et al. conducted one of the most careful studies on semiconductor/SAM systems. First, they analyzed the infrared spectra of an alkyl and of the carboxylate-terminated thiol SAM before and after cluster deposition (from solution). The conformation — *all-trans*, hence a zigzag- stretched methylene chain — remained identical, but only on the carboxylate TiO_2 actually adsorbed, as found by XPS at various take-off angles. The coverage was determined from ion scattering to be 2×10^{15} cm^{-2} titanium atoms. When TiO_2 clusters were first reacted with the same carboxylate thiol, they adsorb in a similar fashion, but with lower coverage and much less order in the methylene chains, as evidenced by infrared peak shifts [182]. However, whether unmodified clusters should be immobilized on a SAM, or modified clusters on the hard surface, cannot be answered generally. Indeed the first method appears more attractive to obtain a good characterization since the SAM can be subjected to a thorough investigation. But — other than in this study — a SAM and especially a polymer film can easily change when clusters adsorb. The second method is preferable, when the clusters carry already a ligand shell, which is either modified or which might be modified with ease.

The method of cluster synthesis on soft layers, as opposed to adsorption of preformed clusters, is not yet well developed; obtaining a good size distribution is apparently a major problem. One approach is the microscale template technique that can be employed for CdS cluster growth on a SAM. First, an alkanethiol/carboxylate thiol SAM is patterned on gold, and Cd^{2+} is bound selectively to the carboxylate termini. Treatment with S^{2-} leads to cluster growth only on the hydrophilic part, where cube-shape nanocrystals form. Here the size of each pattern substructure (10 μm square) determines the amount of Cd^{2+} bound, and the volume of the droplets on the pattern determine how much S^{2-} is offered. The nucleation on the well-dispersed immobilized Cd^{2+} favors the growth of nanocrystals over the growth of one large microcrystal. The nanocrystals can be removed by sonication; hence the attachment is probably based on hydrogen bonds to the carboxylate [183]. From all these results, it is obvious that semiconductor particles can not only adsorb, but also absorb into thicker molecular films. The Sastry group has published a range of relevant results; again, electrostatic interactions between ligand shells and functional groups play a big role, for example between carboxylate-terminated shells and long chain amines [184]. Similar to the synthesis of CdS on carboxylate groups in SAMs, CdS particles can also be synthesized in fatty acid films [185] and in amphiphilic AOT films [186], or TiO_2 in long chain amines [187].

4.4.2. *Electrochemistry of semiconductor clusters*

Electrochemical synthesis of clusters on soft layers is very rarely attempted, probably because the charge transfer through a soft layer is seen as a problem. In fact, the problem lies elsewhere: when the layer is sufficiently thin, electrons can be transferred, and reductions become possible (see Section 4.2.5); but now penetration becomes a serious issue. Since the interaction between a solid substrate and a semiconductor cluster can be estimated to be much weaker than between metal and metal, such a synthesis should be feasible whenever the product can attach to chemical groups on the layer. The reduction of Te(IV) to Te(0) on a mixed alkanethiol/cyclodextrin thiol SAM was followed with in situ STM, and indeed the growth of clusters was observed. However, the clusters have an island-like shape, and they grow at underpotential conditions, both suggesting an interaction with the underlying gold. Another interpretation would be that the clusters are located on the cyclodextrin thiols [131]. CVD is an alternative, and Winter et al. showed how to adsorb a GaN precursor by CVD on OH-terminated thiols [188]. Note that a III/V example was employed: clusters of these materials cannot easily be formed in aqueous and even organic solvents.

The photoelectrochemistry of cluster/soft matter systems is very different from the respective bulk systems: electrons and holes do not move in the band bending or space charge region, since the clusters are too small to contain such a region. Rather the presence or absence of levels for the applied potential is decisive [126]. Such levels can be provided by the cluster, defects in the cluster, or by redox-active additives in the electrolyte. CdS clusters immobilized on SAMs on metals are often contacted with triethylamine-containing electrolytes. The amine can scavenge holes and thus prolong the cathodic current flow [124,125,173,181]. Without photons, the clusters can be electrochemically oxidized and reduced. The oxidation should result in S(IV) and S(VI), species that can be found on air-exposed thiols. The reduction product is not as obvious. Under illumination (obviously with UV energies above the band gap), electron–hole pairs form in and at the clusters. At positive potentials, the amine in the electrolyte can scavenge the holes; at negative potentials, surface states can trap the produced electrons. A participation of the soft layer in electron transport is likely; for a redox-active SAM (aniline linkers), the dependence of the photocurrent on the redox potential was demonstrated [181]. Note that the photocurrent may be only a fraction of the electrochemical current; hence the electrochemical behavior has to be investigated in the dark and under illumination. Nakanishi et al. found a photocurrent that was much larger than the dark current [173]. PbS shows a similar photoelectrochemical behavior: the system can be built by adsorbing AOT-covered PbS clusters on hexanedithiol on gold. Dark currents are due to PbS oxidation and reduction (to Pb). Photocurrents in the presence of hole, and also electron scavengers were determined. Again, the presence of surface states below the conduction band aids the process, but the nature of the scavenger directs the behavior [126].

4.5. *Dielectric clusters on soft layers*

Dielectric nanoparticles are in widespread use, and many nanoparticles on and in bulk polymers are not only investigated in research, but also applied. Mineral dyes, paint, and cosmetic products can all contain submicroscopic dielectric particles. However, “truly” nanoscale particles (say <50 nm) are not (yet) used very often in connection with soft matter surfaces. Understanding of such systems is hampered by problems of obtaining structurally and chemically defined systems: only very rarely dielectric particles can be synthesized without size distribution and with proper stoichiometry. In this respect, dielectric nanoparticles are still not as popular as their semiconductor or metal counterparts, and indeed they often do not show strong nanoscale effects other than the usual high ratio surface/bulk atoms. A notable exception is the magnetic behavior of dielectric clusters [189].

Some of the quite well defined, albeit not ordered, substrate systems are evaporated layers of lipids on solid supports. Binding of metal cations can occur at functional groups, and subsequent cluster synthesis is achieved by treatment with solutions or exposure to gases. For example, Ba^{2+} binds to a 25 nm thick stearic acid film, and CrO_4^{2-} solution creates $BaCrO_4$ clusters of >10 nm size embedded in the film [190]. Sastry et al. reviewed their own and other activities [19]. Other methods aim at creating films on top of soft layers. For example, a pattern of alkanethiols and functionalized thiols on gold allows droplets of dissolved salts to assemble on the functionalized hydrophilic parts. Upon drying, crystallites form. Depending on the pattern size, the crystallites can be as small as 50 nm [156,191]. TiO_2 films can be grown on

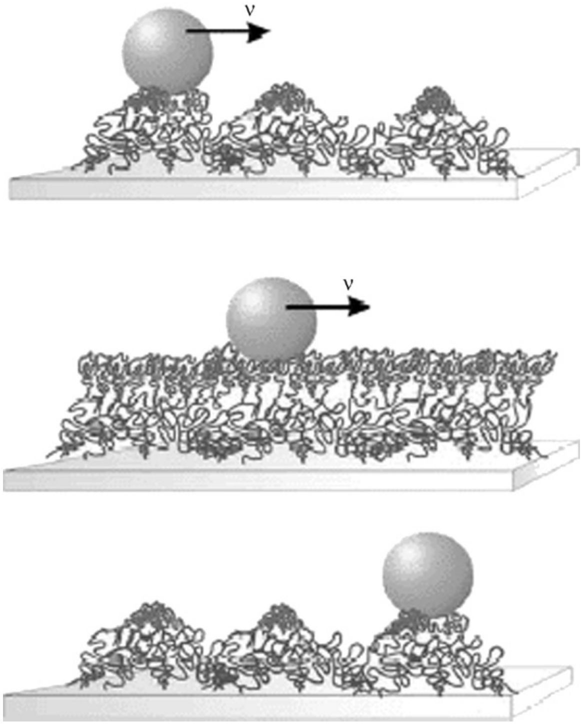

Fig. 14. Scheme of a polymer brush during topography switching, accompanied by changes in the interfacial energy. The “arms” of the brush grasp the cluster and move it along its surface [196].

silane SAMs [192]. Gao and Koumoto have reviewed this field [36] with a special focus on bio(inspired) mineralization. The principal idea is that highly complex mineral structures can form (or self-organize) in biological systems — detailed knowledge about the underlying processes should allow us to transfer many mineralization reactions to chemical laboratories to create a broad range of materials with great ease.

More complex systems employ prefabricated clusters such as ferritin, a huge self-assembling protein cage filled by iron oxides. Ferritin carries charged surface groups and can thus bind to amine- as well as carboxylate-terminated thiol SAMs on a gold substrate. SFM and voltammetry in electrolytes prove the immobilization [193]. Good alternatives to SAMs are polyelectrolyte layers. SFM of Fe_3O_4 clusters on polyelectrolyte layers shows that the clusters are better dispersed in the presence of the layers [194]. Easily available are silica nanoparticles. Masuda et al. demonstrated how to modify their surface to create COOH termini, and how to bind the 15 nm particles to silane monolayers on oxidized Si wafers. The layers were terminated and patterned with OH groups by UV irradiation. The immobilization is obviously strong, but whether hydrogen bridges or covalent bonds (ester formation) prevail, is not quite clear [195]. Santer and Rühe adsorbed silica spheres of 50 nm diameter on special mixed and diblock brushes (Fig. 14); we will discuss their results in detail in Section 4.7.2 [196].

4.6. *Clusters on and in Langmuir–Blodgett layers*

From Section 2.2.2 it is obvious that LB layers are attractive due to their controlled and simple synthesis. However, due to the type of assembly (Fig. 3), the terminal group cannot be modified as easily as for thiol monolayers, and not many chemical reactions can be applied to an LB layer. However, the head group and the tail length can be varied to some extent, and this turns out to be sufficient for changing many important parameters. To bind or synthesize clusters, one has an additional feature that is nearly impossible in SAMs: some structures allow addressing head groups that are located not on, but inside, the LB layer (e.g. in Y-type layers).

One of the best-characterized layers is formed from cadmium arachidate. This motivated the synthesis of II/VI semiconductors (CdS, CdSe, PbS, ZnO) in LB layers [18–20]. The material forms as nanoscale clusters that reside close to the metal ion sites. This is very likely due to the atomically flat arrangement of the cations, which does not allow a 3D phase to grow. On the other hand, the amphiphilic molecules can form a ligand shell on the cluster, similar to common cluster synthesis methods in solution. Several examples will be discussed below. The other important class of clusters comprises metals: a metal can be evaporated, a sol of metal clusters can adsorb, or metal ions can adsorb and be reduced to the zero-valent state. Norgaard and Bjornholm [21] discuss LB layers of metal clusters as the basis for a new type of molecular electronics. It is indeed possible to construct networks of densely spaced (compressed) cluster monolayers and to probe them electrically. In addition, simple masking strategies allow placing metal and semiconductor particles side-by-side [19].

Let us first investigate metal clusters on and in LB films in some detail. Very few publications discuss stoichiometric clusters; one example is the transfer of Au_{55} (coated with nonpolar molecules) onto hydrophilic substrates. These samples can easily be analyzed by STM and SFM, which both reveal the dense packing. Albeit the layers are not at all classic LB systems, they show at least some local order [197]. Mixing with polymeric amphiphiles appears to improve the order: Burghard et al. assembled Au_{55} with its phosphine ligands on silicon wafers. The dense packing was attributed to high lateral mobility on the liquid surface [198]. Alkanethiol-covered gold clusters with 8.3 nm diameter show a good ordering on hydrophobic Si(H) [199]. Cobalt clusters with a nonpolar coating can be transferred on hydrophobic alkylated silicon or on a siloxane stamp. In this way, microcontact printing of densely packed clusters and cobalt lines is feasible [200]; electroless deposition onto a printed pattern is a good alternative [135]. However, in all these cases the clusters are not supposed to reside on top of an organic (soft) layer, except for their own ligand shell.

In contrast, metal clusters formed by evaporation on LB layers might remain on top of the layer. For example, X-ray reflectivity shows that silver forms islands on top of LB films on hydrophobic Si(H) substrates [201]. Less well defined clusters are obtained by reducing metal salts in the subphase (i.e. in the liquid support for the Langmuir layer), again resulting in floating clusters attached to the head groups, used for building up LB multilayers [19]. An example is the production of gold clusters by reduction of $AuCl_4^-$ at a long-chain amine film. The clusters attach to the amine groups and can be transferred to solid substrates (including TEM substrates) [202]. Norgaard and Bjornholm present in their review some examples how this principle can be applied for the fabrication of conductive networks of clusters. The ligand shell of these particles is likely in direct contact with the substrate, hence again this is not an example for assembly on soft layers; however, similar systems with soft layers might turn out to be superior, and the goal, the production of self-assembling electronic nanocircuits, is of great importance [21]. One can also coat the metal cluster layer with another LB layer, and evaporate a contact on top. When the substrate is oxide-covered silicon, a metal–insulator–semiconductor structure forms, in whose insulating layers (LB layer and SiO_2) some capacitive elements are incorporated, namely the gold clusters. Such designs may be the basis for nanoscale charge storage devices [203].

We now focus on strategies starting with the standard system of cadmium arachidate [18,20]. For the cluster synthesis, the respective LB films are simply exposed to H_2S, and the changes are followed by various methods. By repeating the synthesis, one can hope to create defined multilayers of clusters. In fatty acid LB films, the first step is the substitution of the proton in the COOH group at not too low pH values (above 6) [204]. The nucleation and growth mechanism, e.g. for PbS, is based on the relatively fast formation of many seeds and on the high local concentration of Pb ions. One can assume the presence of PbS molecules to explain the following growth; certainly the spacing between two molecular layers in the LB film plays a role in limiting the cluster diameter [205]. Similar arguments are valid for CdS; the fact that mixtures of Cd^{2+} and Hg^{2+} do not give mixed or core-shell particles [204] may again point towards a strongly localized reaction without long-range diffusion. Konopny et al. studied the structural changes in Cd and Pb behenate ($C_{21}H_{43}COO^-$) multilayer films during H_2S treatment with XRD and TEM [206]. The initial high order is lowered, COOH groups form from the employed acid salt, and the layer spacing increases. It is suggested that blocks of the layer shift upwards whenever CdS (or PbS) forms. Moreover, Konopny et al. found that the addition of thiocarboxylic acid stabilizes the LB films to a large extent, presumably by increasing the bond strength between cluster and layer. It is still not common to employ sum frequency generation (SFG) to answer questions concerning the structure of molecules at interfaces. Holman et al. [207] showed how the surface specific signals and the resonance features on gold substrates, combined with deuterated LB layers, can result in detailed information on the C–H vibrations of each layer. A Y-type assembly was confirmed for Cd arachidate on alkanethiol/gold substrates, and the conformational changes of the arachidate backbones were followed after reaction with H_2S. The small number of *gauche* defects in the alkyl conformation may point towards more changes in the vertical direction, as discussed above.

It is, however, very hard to determine the exact vertical location of the clusters. New instrumental developments such as controlled surface charging (CSC) in XPS may open up new ways towards this goal: a neutralizing electron beam of low energy (4.2 eV) is employed to create potential gradients on a nonconductive surface; the shift in the XPS signals due to charging can now be translated into depth information. Combined with SFM and Kelvin probe measurements, clusters in direct contact with the substrate can easily be distinguished from those on top of a bilayer (the latter charge up easily since they are not well coupled to the substrate) [94].

Clusters can be introduced instead of synthesized in LB layers, as shown for CdTe capped with nonpolar molecules in behenic acid layers. The presence of the clusters changes the mechanical properties and introduces new phases on solid substrates, much dependent on the substrate and hence on the LB layer sequence [208]. The LB and the thiol SAM techniques can also be combined: LB films of CdS can be prepared on a dithiol-containing subphase, resulting in interlinking. Transfer to a dithiol SAM on a gold substrate should place the clusters at a distance from the substrate and result in a dense layer, as shown by SFM. Anodic photocurrents were determined in electrolyte [209].

Localized measurements of electrical properties become possible when a metal tip is coated with the LB layers, followed by exposure to H_2S. Now a few clusters are embedded in the layer close to the metal tip. When used as STM on conductive surfaces, the embedded clusters exhibit Coulomb staircases (stepwise charging, see Section 4.8.1) [210,211].

Several metal oxide clusters show permanent magnetic moments and can thus be addressed as “molecular magnets”. The LB method is an especially mild method to transfer $Mn_{12}O_{12}L_{16}$ clusters (with the ligands L acetate and benzoate) to a surface — first because the clusters reside inside the LB “sandwich” between two layers, apparently connected to the polar head groups, and second because the adsorption to the solid is straightforward and not damaging. An additional advantage was that hundreds of layers could be prepared, which was very useful for adding up the small magnetic moments of one layer of clusters to a nicely measurable signal [212]. Iron oxide nanocrystals are not molecular and thus less defined, but can be inserted from the subphase into stearic acid LB layers. After transfer to graphite, densely packed clusters can be imaged by STM. Magnetic interactions distort the structure from the expected hexagonal (densest) packing [213]. Magnetic $CoFe_2O_4$ nanocrystals with oleic acid ligands can be assembled by the LB technique without further amphiphiles [214].

4.7. *Clusters on polymers*

Polymer interfaces [27] with all types of materials are of very high technical significance and widespread use, and the concept of polymer surfaces as discussed in Section 2.3 can be applied. An increasingly important issue is the construction of polymer/metal interfaces. On the micro- and macroscale, polymers can be coated with metal layers for decoration purposes or to make the surface conductive or reflective. On the nanoscale, the first stages of the relevant technical processes are investigated. For example, the creation of adsorption sites at the polymer surface, and nucleation and growth of metal clusters make up the first stages of polymer metallization. A simple and important application is to use silver clusters as antibacterial units [215]. In microchip technology, high-temperature polymers, especially polyimides, can replace ceramics as insulation layers between metal structures. A good example is pyromellitic dianhydride-oxydianiline (PMDA-ODA) [25]. Microelectronics also requires photoresists, and polymers are the prime choice for the visible, UV and X-ray range, which is now being investigated [216]. In recent years, the construction of conductive polymer layers and — further on — of transistors, required polymer/metal contacts. For small transistors, including "chemical" field effect transistors (CHEMFETs), once again the nanoscale is asked for; but even for larger systems, excellent knowledge of the interaction of polymer surfaces with metals is required. Depending on the fabrication process, the metal can be in the form of atoms or clusters in the gas phase, or in the form of ions and complexes in solution.

Thin layers or even "monolayers" of polymer chains are, on the one hand, quite easy to produce for a range of polymers, while, on the other hand their structural characterization is very hard due to the amorphous and fluctuating nature. Fig. 15 shows that X-ray diffraction can give the vertical positions of adsorbed gold clusters on a polymer and at the same time measure the layer thickness. Keeping in mind the issues addressed above, polymer chains are of very high interest for nanotechnology, and consequently the interaction of such layers with clusters will be the main issue of this section.

In the following, Section 4.7.1 will detail some studies of clusters on and in polyelectrolyte layers. Section 4.7.2 will deal with thin films, while the penetration into films and bulk polymers is not in the focus of this review, but presented in the special section 5.1. The review by Faupel et al. [25] is recommended for further details, especially on embedding (Section 4.7.2.1).

4.7.1. *Clusters in and on polyelectrolytes; layer-by-layer (LBL) assembly*

Polymer films are often prepared in the form of "thin" layers — spin coating can easily give access to thicknesses below 1 µm. However, these films can mainly be addressed as bulk phases (see the preceding section), and only when the thickness is well below 100 nm, the vertical length scale approaches the polymer chain length, and new properties can be expected. When the interactions with the substrate surface are strong (ionic and dipole forces), relatively well-defined flat layers can be built. The "layer-by-layer (LBL) assembly" of polymers is the prime example: alternating layers of positively and negatively charged polymer chains (polyelectrolytes since they are ionized) can be assembled from solutions, and the respective counterions are replaced by each new layer (Fig. 7). One can replace one of the layers by charged clusters, e.g. in order to embed negatively charged CdTe (with COO^- groups) [177, 217], or polyacrylate-covered platinum clusters [218] between positively charged polyamines. Obviously, colloid chemistry is the way to understanding the syntheses, and in fact the ionic strength of the solutions determines the diameter of the ligand shell on the clusters and thus the surface coverage. LBL assembly is certainly one of the most promising ways towards applications, and this is reflected in the elegant way from metal clusters to metal patterns by electroless deposition: a carboxylate thiol is contact printed on gold, and LBL multilayers are constructed on the patterned areas. Adsorbed functionalized latex particles can be coated with a palladium catalyst, on which electroless deposition of nickel proceeds again with high local selectivity [219]. A similar process is possible on conventional polyelectrolyte layers [220]. Although the lateral organization of the LBL-assembled polymers is not as good as that of SAMs, the good vertical organization and the control over their chemical behavior are often searched for: a 3.5 nm thin bilayer of polyethyleneimine/polyacrylic acid is sufficient to prevent the penetration of evaporated copper layers into an underlying silicon wafer [221].

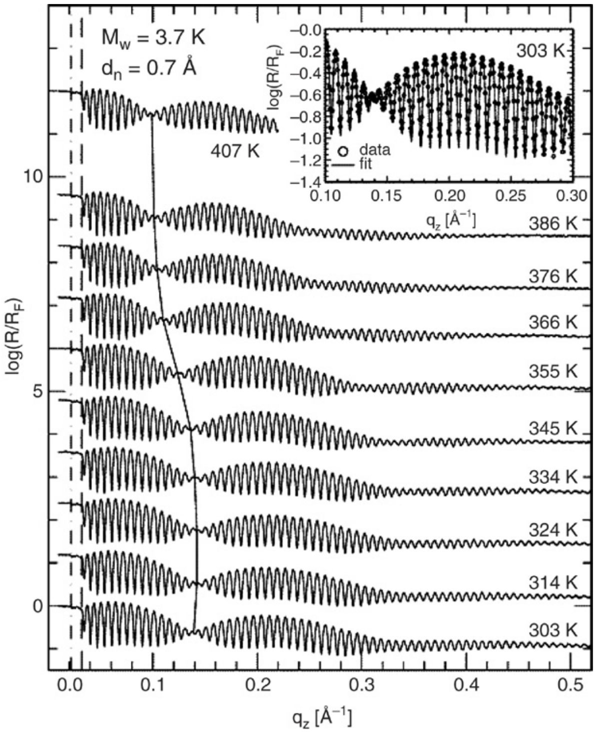

Fig. 15. X-ray reflectivity data of a polystyrene film sample with nominal gold layer thickness of 0.07 nm (made up from clusters), shifted with respect to the temperature differences. X-ray energy: 10.5 keV (λ = 1.181 Å). The dash-dotted line at $q_z = 0.0216$ Å^{-1} represents the critical angle of the polystyrene, and the dashed line at $q_z = 0.0318$ Å^{-1} that of the silicon substrate. The line connecting the nodes is a guide to the eye, which demonstrates the onset of changes in the near surface part of the sample. The inset shows a detailed presentation of the data measured at 303 K and the corresponding best fit [69].

The number of the anionic/cationic adsorption cycles determines the thickness of the films. In this way, controlled multilayers of clusters can be built. The number of immobilized cluster layers influences also the electrochemical response when electroactive groups are present on the clusters [222]. As mentioned above, X-ray diffraction can measure the location of the cluster and the polymer layer thickness, similar to the beat-like pattern in Fig. 15 [69]. However, single layers can be produced, too. For example, Au_{55} clusters with a sulphonate ligand shell adsorb readily on polyethyleneimine (PEI) in densely packed structures [111]. One can expect that the presence of the protonated amine groups reduces the otherwise strong cluster–cluster repulsion. C_{60}, too, can be immobilized on PEI [223]. Whether the proposed amine addition at C=C bonds in C_{60} is the reason for the adhesion was not clarified. Unfortunately, structural characterization of the nominal polyelectrolyte monolayers is not straightforward. This is also true for supposedly very thin layers/monolayers of PAH and PDDA, polyallylamine hydrochloride and poly(diallyldimethylammonium). Apparently, the completely ionized PDDA causes binding of single platinum clusters to give a densely covered surface [218], while PAH induces coalescence of the clusters. SFM studies may suggest that PAH "wraps around" the clusters [222], different from PDDA [218].

A more thorough characterization is possible when a copolymer of acrylamide and vinylpyridine is employed: it is first assembled at the water/air interface, where pressure–area isotherms allow for improved characterization including coverage of the pyridyl groups, followed by transfer to a solid surface (Langmuir–Blodgett method). Gold clusters can now bind, obviously to the pyridyl groups [224]. If a similar system is cast onto submicrometer patterns, a few polymer chains curl up by dewetting in the middle of a pattern. When metal clusters are bound to the polymer, these clusters can be positioned with sub-30 nm accuracy [225]. The vertical control exerted by polyelectrolyte LBL is even much better: for example, CdTe clusters can be assembled in layers on latex particles [178]; the assembly of 15 nm gold clusters (citrate-coated) can be finely tuned with multiple bilayers of sulphonate- and amine-functionalized polymers. Not only can a layer of clusters be placed with good accuracy, but also multilayers of clusters can be separated by well defined distances, as shown by X-ray reflectivity measurements. The first layer on top of the clusters is supposed to fill in the voids between the clusters. Since the spacer layer thickness corresponds nearly to the cluster diameter, induced dipole interactions between the cluster layers are eliminated, which is detected by optical spectra [53].

4.7.2. *Clusters on thin polymer films*

One should keep in mind that polyelectrolytes are not the only possibility to build up thin films. Conventional neutral polymers can be cast in thin films that are of great technical and scientific relevance. If the thickness is in the nanometer range, clusters can penetrate and reach the underlying substrate. But when the temperature of the polymer is low, especially below the surface glass transition temperature, and when atoms impinge at a relatively high rate, cluster growth on the surface is likely. It is even unavoidable when reactive metals are used, even though the metal atoms tend to bond to the polymer chains (which they encounter with much higher probability than another metal atom). The fact that islands or clusters form means that even a reactive metal requires many collisions with a chemical group to finally form a bond to a polymer. When it finally meets another metal atom, island or cluster formation is likely to be immediate. Continued exposure can result in impenetrable layers on the polymer (chromium and titanium). Such cluster layers or metal films are the starting point for further metallization.

Inoue et al. produced nylon films less than 20 nm thick with embedded gold clusters (see Section 4.7.2.1 for details). The usual subsurface location is now very close to the aluminum substrate, without approaching it. It is surprisingly simple to cover the structure with another aluminum film. Now a thin nylon film with embedded gold clusters is sandwiched between two aluminum electrodes, allowing for electrical measurements (Fig. 16). Low leakage currents mean that no metallic conduction channels have formed. Current–voltage curves exhibit Coulomb staircase features characteristic of single-electron tunneling (see Section 4.8.1), apparently due to one single path between the aluminum electrodes [226]. The clusters can also be synthesized, rather than adsorbed, on the polymer. Akamatsu and Deki show how a heat treatment induces rapid diffusion into the bulk, while the material stays at the surface when it is not heated [91] (Fig. 17). Charbonnier et al. describe how polymer surfaces can be modified by e.g. plasma treatment, followed by adsorbing noble metal complexes. Contacting such surfaces with an electroless deposition bath will reduce the complexes, and clusters form. These clusters are very good nucleation centers for electroless deposition — the general procedure can be used for the metallization of plastics [227]. The initial situation can be modeled by adsorption of gold clusters onto a dithiol, and their coalescence upon heating, shown after sequential coating with dithiols and gold clusters on a silane-covered polymer [228], may be similar to coalescence by growth.

More complex structures are polymer brushes. They can be grafted on H-terminated Si, and be terminated with viologen groups. Their redox chemistry was used to reduce noble metal cations to metal clusters [229]. Similarly, polyaniline can coat silane layers on glass and reduce the metal cations. Well-dispersed clusters are supposed to form in the polymer layer, and again electroless deposition can easily be initiated on these clusters [230]. Only very few reports focus on better-defined diameters of the clusters. In fact, electroless deposition depends very much on the shape and size of the initiating clusters: hence studies of this process are called for, also with the aim of designing and applying electroless deposition on the nanometer scale. For gas phase deposition, as a rule of thumb, reactive (non-noble) metals such as chromium and titanium tend to accumulate on a polymer surface, while less reactive (noble) ones such as copper, silver and gold tend to penetrate and diffuse into the bulk. One would expect that reactive metals form bonds to heteroatoms such as O and N, which is indeed verified by the observation of new compounds at the polymer surface [25,231]. It should also be possible that certain metals can form metal–C bonds.

One of the many methods for polymer surface modification relies on creating nucleation sites with ion beams. Such a surface, similar to the surface obtained after predosing reactive metals, can trap noble metal clusters [232]. The sticking/condensation coefficients of atoms (probabilities of adsorption vs. desorption) depend heavily on the chemical nature of the polymer — the coefficient approaches unity for

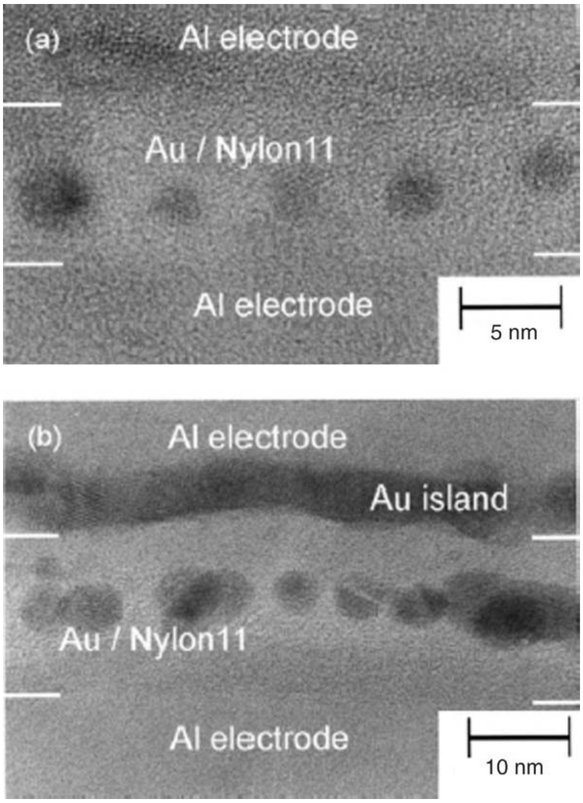

Fig. 16. Cross-sectional transmission electron micrographs of two samples prepared with different thicknesses of nylon 11 and Au. The films are sandwiched between two Al electrodes. Au particles spontaneously align in the middle of the two Al electrodes [226].

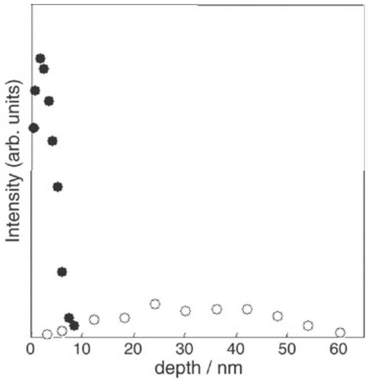

Fig. 17. XPS depth profile of Au after vapor deposition of nominally 21 monolayers of Au on nylon 11. Empty circles: Au cluster diffusion after treatment at 100 °C for 10 min [91].

polar reactive groups like imides, and falls below 1% for poly(tetrafluoroethylene) [233]. Similar results can be obtained when polymer surfaces are functionalized with chemical groups such as carbonyl or amine that can bind metal ions. Dressick et al. showed that X-rays can modify the surface of poly(vinyl benzyl chloride) oxidatively. The thus created carbonyl groups are reductively aminated, and the amine was shown to bind to Pd(II) colloids (clusters containing OH^- and H_2O that are employed as nuclei for electroless deposition). Wagner et al. [231] tried to correlate the condensation energies of various metals (Table 2) with the reactivity of the respective atoms with nylon (amide groups), N in polyethylene and a nitrile-terminated SAM. At least for their system, the correlation is weak. While the condensation energy is surely the driving force to form metal clusters from atoms — whether in the gas phase or on or even inside a polymer — it is proposed to use other relations. Wagner et al. propose to balance the bond breaking energy of chemical groups in the polymer with the bond energy of the metal–heteroatom interaction, and additionally with other newly formed bonds (mainly C–C) in the polymer. As yet, neither the definition of the systems nor the analysis methods are sufficiently developed to gain further insights. Gerenser [234] used oxygen and nitrogen plasmas to create localized chemical defects in polyethylene that appear to bind Ag^+ quite strongly. A more specific approach bases on viologen moieties that are attached to the polymer surface. Au ions can be photochemically reduced to clusters, as shown for a polymer nanosphere substrate [235].

SFM scans of the cluster-covered surfaces after annealing at various temperatures yield a real-space view [236], as does TEM. One should keep in mind that SFM height measurements of hard metal clusters in soft matter are not very reliable. However, when the SFM does not slide the clusters, they can be shown to "sink into" polystyrene 25 K below the glass transition temperature T_g [237]. The employed gold clusters were adsorbed from solution, but they can also be grown by electroless deposition [238], as also possible with silver clusters on polyether urethanes [239]. Large clusters of 10 and 20 nm diameter embed only 3–4 nm below T_g, but nearly completely at higher temperatures. From this — with similar precautions — one might infer a 3–4 nm thick surface layer, whose T_g is about 7 K below the bulk T_g [236].

While SFM is the prime method to investigate the distribution and geometry, SFM can also be used for detection of (partial) embedding and of surface diffusion. Santer and Rühe synthesized polymer brushes on solid supports. The brushes can exhibit phase separation in their surface regions when they consist of mixed or block copolymers. The relatively flat surface of these layers can be changed into a nanoscale pattern with complex lateral structure and height variations up to several nanometers, most easily by treatment with solvents or solvent vapors. Upon repeated treatments, adsorbed silica spheres of 50 nm diameter move on the surface and aggregate (Fig. 14). Mixed and diblock brushes show some differences, for example some "sinking in" was found only for mixed brushes [196]. The most likely mechanism is based on surface forces between the particles and patches of the brush surface, which rise or fall with the solvent treatment — the polymer chains attach and detach when solvent and silica compete for adsorption. Liu et al. [240] investigated thiol-covered 2.5 nm gold clusters on top of a diblock brush. TEM gave indications of lateral movement leading to coalescence, and the X-ray reflectivity showed that the cluster was located in the brush, not in further underlying polymer layers. The lateral movement is based on the mobility of the brush.

Up to now, the systems discussed involved clusters without ligand shell or with easily removable ligands. When gold clusters with thiol ligands are contacted with polystyrene, they simply adsorb in dense layers that are electrically conductive [241]. Systems of this type can be addressed as precursors or first stages in the production of metal overlayers on polymers, e.g. by electroless deposition [242]. Note that complex deposition processes such as electroless deposition can cause complex situations, e.g. large clusters adsorbed on, and smaller clusters located below the surface [243]. A related system of great importance for applications was silver at and in gelatin (photographic films). A classic paper aimed at proving that Ag_4, produced in a size-selected cluster ion beam (see Section 5.2), is the smallest cluster that results in development [244]. While this result is probably not of great direct relevance, it may inspire new ways towards nanoscale control of the closely related process of electroless deposition.

4.7.2.1. Embedding of clusters in polymers. The diffusion in the bulk, mainly observed for noble metals, is of course faster for smaller particles, especially atoms. The diffusion is thermally activated and often follows the Arrhenius law with activation energies around 1 eV (around 100 kJ mol^{-1}) [25]. From the Stokes–Einstein equation

$$\langle x^2 \rangle = \frac{kTt}{3\pi \eta r} \tag{5}$$

the mean square displacement $\langle x^2 \rangle$ becomes orders of magnitude smaller when the temperature falls below T_g, since the viscosity η increases enormously (kT = thermal energy, t = time, r = particle radius). Thus, in a glassy polymer the diffusion is restricted to atoms. However, the mechanism is not simple: a comparison with gas diffusion shows that the preexponential factor multiplied by the root of the mass is of the same order of magnitude (0.1 $cm^2\ s^{-1}\ u^{0.5}$), but the activation energies for gas diffusion cluster around 0.3 eV (around 30 kJ mol^{-1}), not 1 eV. Hence some metal atom–polymer interaction should be present. At high temperatures, the usually very slow self-diffusion of the polymer chains can be faster than the atomic diffusion; the metal atoms may form weak crosslinks.

The atoms or smaller particles can coalesce also in the bulk, and embedded large clusters form. The formation of clusters from atoms can be compared to the scenario on well-defined metal single crystals [67]. However, since the noble metals show little interaction with the polymer surface, Volmer–Weber growth results, which means that the atoms aggregate to clusters rather than to islands — in fact, not only atoms, but also small clusters diffuse on the surface and finally aggregate to larger clusters (Fig. 18). The cluster shape can be near-spherical, and the size distribution quite narrow (+/−10%) [91, 245]. The driving force for cluster formation is obviously the high cohesive (or condensation) energy of metals (Table 2), as compared to metal–polymer interactions (see Section 3).

4.7.2.2. Glass transition of the polymer surface. For noble metals, the atoms and also clusters can easily "sink" or be embedded by the polymer when the surface glass transition temperature is exceeded [246], even if the temperature is still below T_g. Above T_g, even large clusters are embedded. For example, gold clusters below 1.5 nm diameter are embedded in polystyrene up to 6 K below the bulk T_g of 374 K, while 2 nm clusters are only embedded above T_g. The dependence on the molecular weight of the polymer was followed from 3 to 1000 kg mol^{-1}, surface and bulk T_g follow the Fox–Flory relation (decrease of T_g inversely proportional to molecular weight) [245]. The process can be followed by XPS and ISS; while XPS can provide the relative decrease of elemental signals, which is exponential in the embedding depth, ISS can give better access to the depth profile [246]. However, XPS can be combined with depth profiling with an ion beam: now the signal can be interpreted as being solely from the topmost (exposed) surface layer, and very clear results can be obtained [91]. The surface sensitivity of XPS can be much improved at low emission (electron takeoff) angles, which can be used to prove that clusters are embedded in the subsurface region.

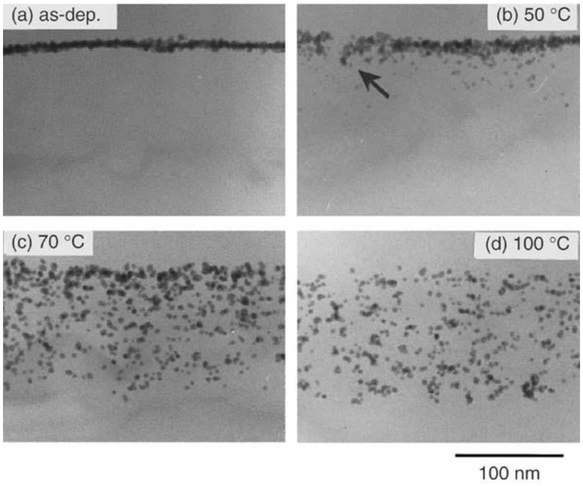

Fig. 18. Cross-sectional TEM images of Au/nylon 11 thin films before and after heat treatment at various temperatures. The thermally activated penetration of Au clusters becomes directly visible (the arrow shows a defect; it does not have much influence on the penetration) [70].

Embedding of clusters in the subsurface region (some nanometers) is usually observed above the surface glass transition temperature. Note that this temperature can be well below T_g, hence the argument made about bulk diffusion does not apply here. The process can be tuned to result in monodisperse distributions. Akamatsu and Deki characterized a gold cluster/nylon system by XPS, high-resolution TEM and optical absorption; the clusters penetrate readily above T_g [91]. The size depends on the initial flux of gold atoms. Subsurface processes are often associated with the interplay between kinetics and thermodynamics, for example between activated penetration of atoms A into a bulk phase B and the exergonic formation of a solution of A in B. However, here one can apply also a purely thermodynamic model, namely the equilibrium between van der Waals forces, which tend to draw the cluster inside the bulk phase, and counteracting entropic forces due to the polymer compression around the cluster [25]. The change of the environment of a cluster translates into a change of its surface energy, and the surface stress can be measured by electron diffraction: the lattice constant of gold clusters increases by about 0.1% when they “sink into” nylon [70].

When the polymer is prepared as a film, one can employ X-ray reflectivity: the oscillations in the plot reflectivity vs. wave vector yield the thickness; with gold nanoclusters (1.8–3.6 nm diameter) beating of the oscillations is observed, whose onset varies with the temperature [69]. Note that the surface T_g can also be found by measuring the fluorescence from embedded dye molecules, based on broadening of spectral features.

4.8. Electronic properties of the system cluster/soft layer/conductive substrate

4.8.1. Single cluster experiments

Many, if not all, physical properties of clusters on soft matter can be measured with a global method — in other words, from a large ensemble of clusters on the soft layer. This is mainly realized by preparing a macroscopic (>1 μm long and wide) sample with a large number of clusters (or even a dense layer), and by subjecting the complete sample to measurements. In this way typical nanoscale properties can also be determined with great precision (see Section 4.8.2). However, one would often prefer to have a local view, especially because even the best chemical control cannot guarantee identical local properties. One important point is of course the size of the cluster, which is mostly not controlled with atomic precision — it is thus desired to correlate the local physical properties with the actually measured size of the measured cluster. Another point concerns the local environment around the cluster: also in this case variations are not only possible, but very likely, given the fact that the quality of soft layers cannot be perfectly controlled. This causes problems especially when some form of coupling to the substrate is investigated, since in this case defects in the layer can mean that the cluster–substrate distance is very variable. Since the local measurements concern almost exclusively electrical properties, the extent of coupling is of utmost importance.

The fact that electrical measurements are much more common than others is due to the problem to localize the probes: imaging on the lateral atomic scale requires an electron beam (TEM or field ion/electron microscopy) or a tunneling contact (STM). Only on a few samples can SFM attain atomic resolution, which is especially hard to obtain when lateral variations in topographic height and surface elasticity are present, as in our case; however, nanometer resolution is well possible. Thus most investigations concentrate on passing a current from an STM or metallized SFM tip through the cluster and the soft layer to a conductive substrate. Such systems show current/voltage characteristics that are directly connected to their size and can be called prime examples for true nanoscale properties, namely Single Electron Transfer (SET). First, the sequential charging of an isolated cluster with electrons is connected to an electrostatic energy

$$E = \frac{e^2}{2C} \tag{6}$$

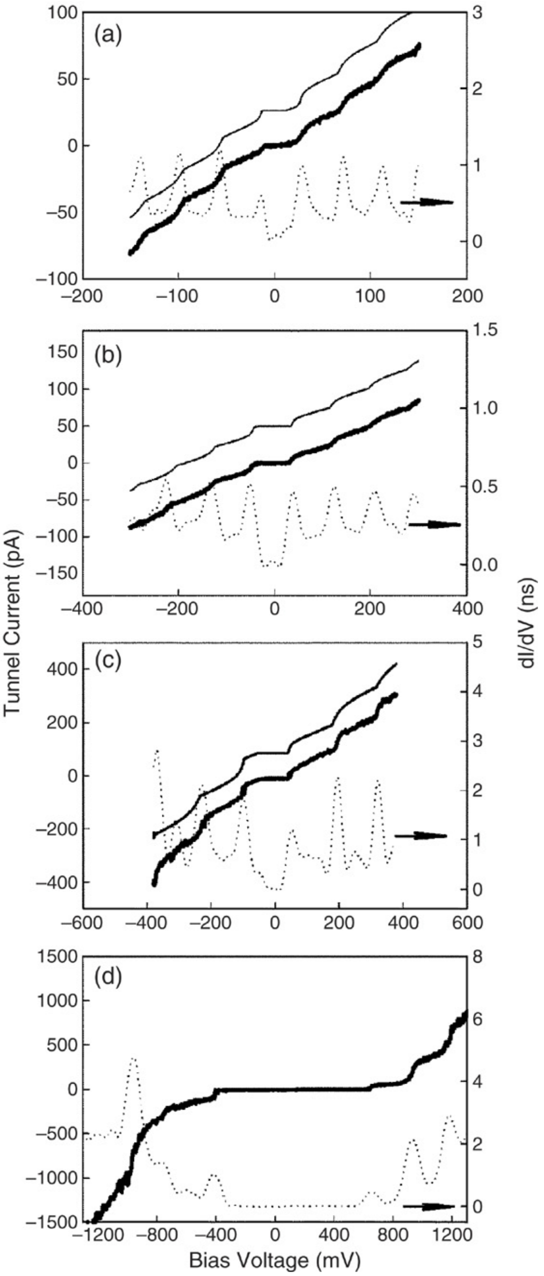

Fig. 19. Local electronic properties of alkanethiol-covered Au clusters on alkanethiol SAMs (on Au substrate), measured by STM. Four typical current–voltage curves I–V (thick solid lines) and the differential conductances $\mathrm{d}I/\mathrm{d}V$ (dotted lines) were taken from different samples with nominal cluster sizes of 15.2 nm, 9.4 nm, 4.6 nm, and 1.8 nm. The set point voltages were all 1.5 V, and the set point currents were 2 nA, but 5 nA for (c). The parameters for fitted I–V curves (thin solid lines) are $C1$ ($C2$), $R1$ ($R2$), and $Q0$: (a) 4.08 (3.95) aF, 69 (1700) MΩ, and 0.15e, (b) 2.23 (1.94) aF, 130 (2960) MΩ, and 0.06e, (c) 0.89 (1.16) aF, 70 (950) MΩ, and 20.21e. The fitting curves are displaced vertically for clarity [248].

(charging of a capacitor of capacitance C with elementary charges e). When it exceeds kT, for example at sufficiently low temperature, or at sufficiently low capacitance, charging with the first electron blocks the transfer of further electrons, the so-called Coulomb blockade [247,248] (Fig. 19). In fact, at 300 K, the charge should be in the attofarad range, which is the capacitance of a metallic sphere of nanometer-range diameter.

The blockade manifests itself by a gap, i.e. a horizontal current–voltage curve, around 0 V. This gap can easily exceed 1 V for clusters with less than 50 atoms [30], e.g. for Au_{38} with a gap of 1.2 eV. For such small clusters, the Coulomb blockade can be interpreted as a HOMO-LUMO gap since a band structure cannot develop. The extreme case, a single atom on a nonconductive layer on a conductive substrate, is better known for rigid layers, e.g. for Au on a bilayer of NaCl on copper: At low temperatures, an STM tip can switch the charge state from 0 to −1 [249].

The potential separating two charging events is $0.5eC_2^{-1}$, the energy separation is $0.5e^2C_2^{-1}$, where C_2 is the capacitance between cluster and substrate (hence across the linker molecules). The required currents vary in steps, the so-called Coulomb staircase. The relative step height is $0.5e^2(C_2kT)^{-1}$ [29], and the absolute step height can be approximated by $0.5e(CR_2)^{-1}$ where C is the overall capacitance [250]. The electrical behavior can be simulated by an equivalent circuit of two serial RC units, one representing the STM–cluster system, the other one the cluster/soft matter/substrate system. The electrical contacts should have tunneling resistances $>h(4e^2)^{-1}$ to suppress quantum fluctuations. Note that Coulomb staircases can also be measured globally, i.e. for an assembly of clusters. This is most convenient in electrochemical systems, where the clusters are dissolved in an electrolyte [30].

However, the metal cluster can also be used simply as a contact pad for one or more molecules in the soft layer. With the conductive substrate as second electrode, the conductivity of a single molecule or a very small ensemble of molecules can be determined. In this case, Coulomb blockade has to be avoided, which is anyway the case when the molecule is conductive — the current–voltage curve around 0 V shows a positive slope. The contacts are in fact essential for proper measurements, and in fact can easily induce huge artifacts when their resistance is too high. To this end, most molecules are provided with two thiol- or sulphur-containing ends to link them to a gold substrate and a gold cluster. An alternative, now developed to excellent performance, is the break junction technique, where the molecule is assembled between two metal tips placed at sub-2 nm distances. The current through alkyl chains follows exponential distance dependence with a prefactor around 0.1 nm^{-1}. High conductivity is usually restricted to conjugated π systems such as carotenes [251].

4.8.1.1. Coulomb blockade by metal clusters. The first proof of Coulomb blockade in clusters on soft matter was obtained with xylene- and benzenedithiol layers on gold. For the xylenedithiol, probably the thiomethyl groups in *para* position on the benzene rings provide sufficient mobility to pack the molecules in a dense SAM. Certainly a loop-like or flat lying attachment of both thiol groups to the substrate can be avoided due to the rigidity of the benzene ring. Size-selected clusters were deposited from the gas phase, obviously bound to the topmost thiol groups. Not surprisingly, clusters on alkanethiol penetrated and/or could be easily moved with the STM tip [252]. With the same system, a Coulomb staircase could be detected at room temperature [5]. The authors also showed that alkane thiols tend to induce surface diffusion and probably penetration, as expected (see Sections 4.7.2 and 5.1). The equivalent circuit for the $I(V)$ curve is given by two RC elements in series; the lower resistance can be interpreted as resistance of the soft layer underneath the cluster. Since the cluster is bound to more than one molecule, an interpretation as molecular resistance requires an estimate of the number of molecules and is not straightforward. However, the values in the $M\Omega$ range are well comparable with values found by other methods.

Another strategy that may indeed give access to single linker molecules is to construct a nonbinding alkane SAM with a small fraction of linkers, e.g. dithiols, or to exchange several passivating ligands on a cluster [148,253]. For example, 1.7 nm gold clusters can be coated with alkane thiols, of which a small fraction can be exchanged to dithiols. However, this method is less reliable than placing the passivated clusters on a dithiol SAM, which results in Coulomb blockade [148]. Au_{55} clusters with a core diameter of 1.4 nm can be coated with sulphonate ligands and assembled in a dense layer on top of a (positively charged) cysteamine layer on gold. STM detected Coulomb staircases at room temperature and at 90 K [254]. Pulsed laser deposition of the clusters — here palladium — allows placing them on top of alkanethiols; Coulomb staircases could be measured at 80 K [255]. Most interesting is the dependence of blockade on cluster size and shape: gold clusters capped with alkane thiols were deposited on alkanethiol SAMs, and scanned by STM at 4 K [248]. Sizes from 15.2 down to 1.8 nm correspond to capacitances from 3.78 down to 0.31 aF, and indeed the blocking was found to vary with the size. However, the spacing of the staircase is not equal for very small sizes (1.8 nm), which should be due to internal energy levels, hence a true quantum effect comes into play. For larger clusters, the staircase steps depend on the STM setpoint, in other words on the top capacitance, as expected from a simple model. At setpoint currents above 15 nA, the measured capacitance differs substantially from the calculated one. This implies compression of the ligand shell by the STM tip. Note that by varying the voltage, an STM tip can pick up a cluster and release it elsewhere.

Shape dependence is inherently present in gold islands of 2–10 nm diameter and single layer height (0.25 nm) deposited on top of thiol SAMs. Most of these clusters penetrate (see Section 5.1); they are smaller on thicker layers, pointing towards surface diffusion of adatoms to form the clusters [256]. Coulomb staircases were found here, too, and the capacitance varied with the SM setpoint. Again, above 10 nA, simple models break down [257]. When the clusters are near-spherical and their diameter is better defined, they can adsorb from solution to form a densely packed layer on top of the thiol/gold substrate, again showing Coulomb staircases [120]. One can also try to correlate Coulomb blockade in a metal cluster with XPS signals of the clusters on top of dithiol layers (see also Section 3.3). For this, gold clusters were deposited on top of dithiol layers on gold, and Coulomb blockade was measured by current–voltage curves. XPS creates holes, which, too, leads to charging of the cluster. This charging shifts the XPS binding energy positively by $e^2(2C)^{-1}$, the same value that corresponds to the Coulomb blocking energy. Hence the blockade as well as XPS can be used to calculate the capacitance — the values do not match completely, but agree reasonably [93].

When palladium clusters are deposited, copper or nickel clusters can be prepared by electroless deposition, or nickel or cobalt can be deposited. In this way, ferromagnetic alloys are used to contact the cluster. At 1.6 K, not only current–voltage curves, but also their dependence on intermediate magnetic fields was tested. A principle magnetoresistive device architecture is now being set up [258].

4.8.1.2. Coulomb blockade by semiconductor clusters.

Coulomb blockade in semiconductor clusters is quite comparable with the corresponding effects in metal clusters. This is not surprising since all that is required is a suitable isolated conductive particle. However, it is advantageous to synthesize semiconductor clusters on the molecular layer, by simple sequential adsorption of aqueous metal cations and reaction with H_2S. The layer can be a thiol with a COOH terminus; CdS particles of 1.2 nm diameter were produced, and STM showed blocking [259]. For PbS, also staircases were obtained; their width depended on the setpoint current [260], as known from metals (see above). Since Langmuir–Blodgett films of acids are well known for their Cd^{2+} binding, they, too, qualify for the synthesis of CdS on top of a molecular layer. In this case, graphite is preferred as conductive and hydrophobic substrate [261]. An ingenious way to address a single semiconductor cluster is the synthesis of embedded CdS and PbS clusters in LB films that were transferred onto a metal STM tip; again, graphite is used as the conductive surface, but no further molecular layers are required to observe Coulomb staircases [210,211]. Conversely, metal clusters can also be bound to soft layers on semiconductors, but this route has not been popular. Lee et al. [262] report a gold cluster on xylenedithiol/GaAs (low temperature grown) with all the usual characteristics. Here an additional motivation is the local fabrication of a metal/semiconductor point contact by chemical means. Finally, the experiments with CdS by Ogawa et al. point towards the following section, switching [125].

4.8.1.3. Nanoscale switches. When the soft matter layer contains a redox-active group, the single electron processes can be switched by tuning the potential, for example the electrochemical potential [29], or the tunneling potential in STM [125] (see Fig. 20). Gittins et al. [263] used dithiols with viologen groups (4, 4′-bipyridinium dication) in the alkane chain. Such groups can easily be reduced to the bipyridyl radical cation, bestowing a much-increased conductivity to the molecules. Inverse decay lengths (from current-tip distance measurements) were determined in presence of electrolyte under polarization of the gold substrate and hence under switching conditions. The current was once more measured by STM on gold clusters on top of the molecules. The observed current jumps are clearly related to the nonconductive state of the molecules (Fig. 21). Note that without the clusters, the molecules are thought to form wires from

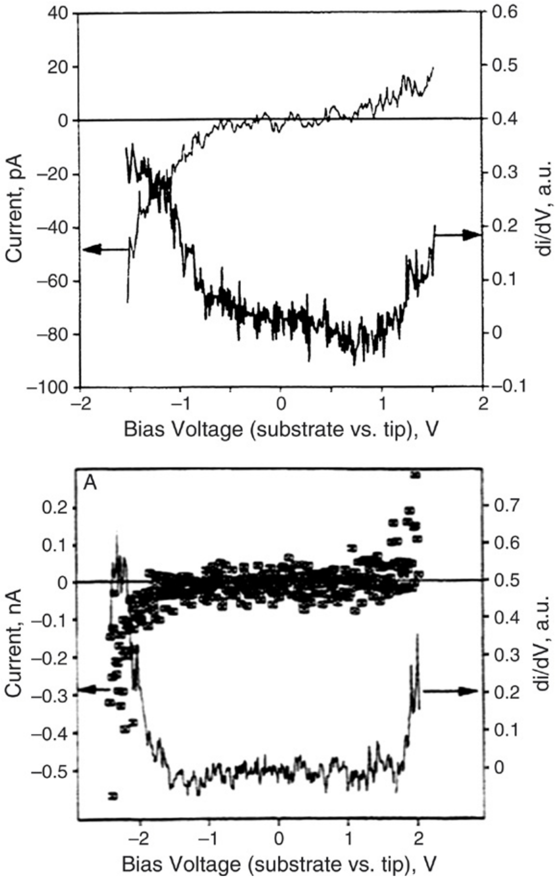

Fig. 20. Top: current and differential conductance as a function of voltage for STM measurements on bulk CdS. The differential conductance dI/dV shows an energy band gap of about 2.3 V. Bottom: current and differential conductance as a function of voltage for a CdS cluster film on an alkanethiol SAMs (on gold substrate). The conditions of gap separation between tip and cluster layer were −2 V, 30 pA [125].

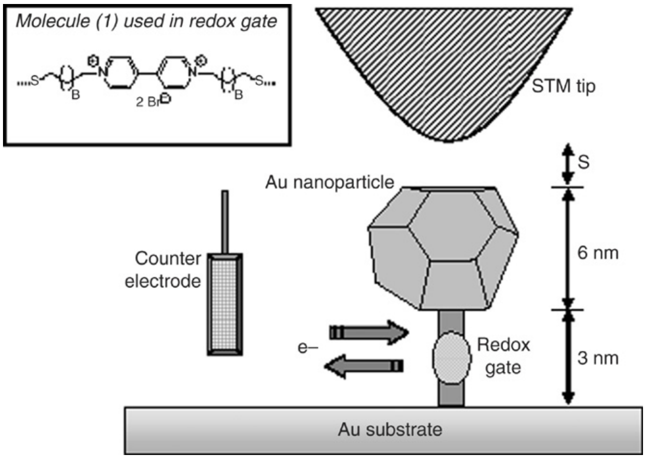

Fig. 21. Schematic representation of a nanoscale switch. ECSTM was used to examine the electrical characteristics of this device. Electrons can be injected into the redox gate by applying a suitable potential between the substrate and the counter electrode. The potential between the tip and the substrate is controlled independently, and s represents the tip–nanoparticle distance. The redox gate consists of up to 60 of the molecules shown in the inset. The counter electrode is immersed in the surrounding electrolyte [263].

the surface to the STM tip. Hence the observed current–voltage steps are most likely not due to staircases, but sequential molecular detachment [264]. One should first form a diluted layer of the molecules in an alkanethiol matrix, and then adsorb gold clusters. Current–voltage and current–distance (tip-sample distance) spectra were recorded.

However, the electronic properties do not have to be tuned by the linker or soft layer: the ligand shell around the cluster can contain either acidic or basic groups, and hence the pH of the solution will tune the charge around the cluster and thus modify its electronic levels. For this, gold clusters were coated with alkane thiols, galvinol (a phenol-containing thiol), and an aminothiol, respectively. The current–voltage characteristics were measured with STM on clusters immobilized on alkanethiol/gold in electrolyte [265]. Changing the pH did not affect Coulomb staircases through the neutral cluster much. Whenever the cluster shell was charged, the whole staircase shifted positively, and the capacitance increased (which it also does for similar monolayers on flat surfaces). Interestingly, the steps in some cases changed to peaks, thus negative differential resistance can be realized. The STM tip can be replaced by a cluster immobilized on the STM tip (a "scanning single electron transfer probe"); now the current–voltage curve depends very strongly on the tunneling distance [250].

Various other effects will be discussed only shortly. For example, the conductivity of single molecules can exhibit stochastic switching or "blinking". This phenomenon is best observed for the system gold cluster/molecule (dithiol)/gold substrate. STM and conductive SFM were able to show the stochastic nature of the conductivity. At least a part of the blinking events is caused by detachment and reattachment of the Au–S bond [266]. More oriented towards device fabrication are studies that employ relatively large islands on top of molecular layers. Langmuir–Blodgett films on platinum can be capped by evaporated titanium islands. Surprisingly, a bistable current–voltage characteristic was found for molecules of various complexity up to rotaxanes. Hence the contacts are likely more involved than the molecules [267]. Other approaches to nanocontacts are based on electromigration, which can produce nm-sized gaps in wires. This approach, too, can be favourably combined with soft layers and clusters. For a similar device, gold clusters of 2–5 nm size on a dithiol were captured in a 5–10 nm gap between two gold electrodes. The special value of this approach is that electrodes with down to 2 nm gaps are produced on a flat surface. At room temperature, Coulomb blockade was found, at 4 K, also a staircase. Here the dependence on a gate voltage (applied to an underlying aluminum electrode) was measured [10]. A device with larger electrode spacing was produced on SiO_2 with a silanethiol monolayer, to which gold clusters were bound. The observed Coulomb blockade was tuned by binding gold-cluster-terminated DNA to the gold clusters. Only when the DNA link was built up properly (proper base-pairing of three substrands), the current was observed, and the staircase depended strongly on the gold cluster size. In this way, an electrical DNA nanosensor was built [268].

4.8.2. *Global experiments*

Local probes have provided us with detailed and fascinating insights on many fields of Surface Science; in the framework of this review, Sections 4.8.1 and 4.3 present work on clusters immobilized mainly on SAMs. However, all research in this direction relies on the chemical fabrication of the respective structure — in other words, many (hopefully) identical cluster–molecule–substrate entities are created in parallel. Obviously, one can also probe all of them in parallel, often with increased sensitivity. The theoretically most appealing measurement would employ a large metal contact on top of the clusters. This is practically very hard to achieve, not only because of the well-known problems of penetration (see Section 5.1), but also because the clusters carry a ligand shell that would have to be opened without disturbing the electronic structure. This problem motivates in turn the use of STM. However, the system can also be probed by analyzing electrochemical currents and by constructing dense cluster layers with macroscopic contacts.

4.8.2.1. Electrochemistry and electronics. Whenever the systems discussed in Section 4.8.1 can be immersed in electrolytes, the substrate can be used as electrode (working electrode). Together with a counter electrode that supplies the current, and a reference electrode for exact determination of the potential, a standard electrochemical cell can be constructed. Three techniques were found to be especially useful: cyclic voltammetry, differential pulse voltammetry, and impedance spectroscopy (all rely on applying a time-dependent potential and on analysis of the current response). It is found that the voltammetric current response, the voltammogram, shows steps, the electrochemical Coulomb staircases, with potential spacings that are well comparable with the STM results. However, now the potential difference depends linearly on the charge state [29,30]. When the clusters are not attached to a substrate, their capacitance features the radius r of the metal (or semiconducting) core, and the thickness d and dielectric constant ε of the ligand shell [30]:

$$C_{\text{cluster}} = 4\pi\varepsilon\varepsilon_0 \frac{r}{\mathrm{d}}(r + d). \qquad (7)$$

Obviously, the electrochemical Coulomb staircase allows determining cluster properties with much greater ease than local probes whenever the clusters exhibit a narrow size distribution. One should note the similarity to the voltammetric response of transition metal complexes with a similar series of steps or peaks, assigned to successive electron transfers. It is clear that especially for small clusters one can try and interpret the data for an (inorganic chemical) cluster compound of low valency. Moreover, one can also think of an applied electrochemical potential as a preparation method of a certain oxidation state of the clusters. One should also note that the choice of electrolyte (solvent and salt) has a huge influence on the measurement — it defines the potential window (below and above it the electrolyte decomposes) and the extent of anion or cation adsorption at the clusters [30].

In passing we note that experiments for dissolved clusters can be carried out without their immobilization. The nature of the working electrodes is here not decisive (gold and platinum are commonly employed). Charge states from −6 to +7 were found on thiol-covered gold clusters [9], and the responses were found to be strongly size-dependent [269]. The other extreme would be a local measurement with the usual global voltammetry with very low (aA) currents. Fan and Bard demonstrated Coulomb staircases between two nanoscale "immobilized clusters" (in the form of two ultramicroelectrodes) in electrolyte [270].

The systems used for electrochemical characterization are nearly identical to those discussed in Section 4.8.1. Once again, dithiols form the most valuable soft matter layers; alternatively, they can be inserted into thiol ligand shells and ensure immobilization of the cluster [271]. When charged groups like viologen (4,4′-bipyridinium dication) are inserted in the dithiol, the process becomes sensitive to the presence of counterions (here anions) [272]. It is interesting that the presence of hydrophobic anions can induce asymmetric currents (currents depend strongly on polarity), hence rectifying behavior was postulated [272]. Pyridyl-terminated thiol SAMs were used to bind sequentially Cu^{2+} and pyridyl-terminated gold clusters [273]. Note that Cu^{2+} here functions as a bridge between the cluster and the SAM. Zn^{2+} can achieve similar results on carboxylate-terminated thiol SAMs and adsorbed clusters that carry carboxylate groups [274]. The question arising now concerns the exact pathway of the transferred electron(s); the path is likely to involve the COO^-—Zn^{2+}–COO^- bond. Another system uses copper instead of zinc; even microcontact printing and nanoshaving patterning of the multilayers was achieved [275]. Diisocyanate SAMs on gold are less known and less ordered than thiols, but they can be well compared to dithiol SAMs. Diisocyanates can bind to platinum clusters, and even multilayers become accessible. Their redox reaction rates decrease when the layers grow thicker [276]. When the clusters have charged ligands, electrostatic assembly becomes another feasible method. Silver clusters with a quarternary ammonium shell can adsorb on a carboxylate thiol SAM on gold, and show quantized charging [277].

4.8.2.2. Electrical properties of large-scale cluster assemblies and metallic overlayers. Clusters assembled on a larger area, say μm^2, are interesting for applications. In this respect, soft matter layers can be problematic since defects are present that can cause electrical contact to the substrate. However, this area of research can become more and more important: whether the electrical properties of the clusters are searched for, or whether the clusters are merely employed as contacts, assemblies on sub-μm scales can be sufficient for nanoelectronics applications.

For example, gold clusters with citrate ligands can be adsorbed at positively charged aminosilanes on aluminum oxide-covered aluminum [278] or on oxidized silicon [110]. In the latter system, the nonlinear current–voltage curve was found to depend on temperature; the activation energy was interpreted as reflecting the charging. When the clusters on aminosilane/aluminum oxide/aluminum are exposed to cysteamine, very large (0.5 mm diameter) gold contact pads can be deposited on top by the "lift off, float on" technique. The current–voltage curves are nonlinear, hence defects play no role, but irradiation can increase the current [278]. For gold clusters and dithiols adsorbed in a layer-by-layer fashion, ohmic behavior was found, and low resistance was achieved after heating that caused coalescence [228]. Well-defined (stoichiometric) clusters have been employed for conductivity measurements only in the case of Au_{55}; impedance spectra of thick layers were recorded [107], and electrostatic forces were determined on Au_{55} and (formally) Pt_{309} monolayers, both on 2-aminoethanethiol on gold. While such a short SAM may allow for interaction between clusters and substrate, distinct differences in between charging gold and platinum clusters were found in capacitance–bias voltage curves, probably resulting from the local density of state on the clusters [279].

Electrical bistability of organic layers could form the basis for new types of memory devices. Aluminum can be deposited sandwiched between two 2-amino-4,5-imidazoledicarbonitrile layers, and two electrical contacts can be formed below and on top of the layers. The middle layer is a complex mixture of oxide and metal clusters, which can be electrically polarized; hysteretic behavior means that charge can be stored. At large potentials, the organic layers are doped, and permanent charge separation was found. The process depends very much on the cluster size, and most likely a metal–insulator transition is responsible [280].

As also discussed elsewhere, a major issue in molecular electronics is to reliably place a SAM between two metallic contacts. In some cases, cluster formation on top of an organic soft layer is the first step towards forming a top contact, so some typical results will be discussed here. As discussed in Section 4.3.2, silane SAMs with phenoxy termini prevent penetration of metal on areas as large as 30 000 μm^2. The high electrical breakdown voltage of the only 2.5 nm thin SAM leads to the construction of a low-voltage organic transistor with the SAM as gate [3]. The Ramanath group investigated layers of tens of nanometers of copper, the most important material for interconnects, on modified silanes, again preventing penetration; in this way, capacitors suitable for the MOS technology were produced [157–159]. Chen et al. [281] developed a procedure to assemble a monolayer of a thiol on a gold contact of less than 50 nm diameter. Defects might be avoided simply by reducing the number of contacted molecules. The second gold contact was evaporated at 77 K to reduce penetration. Large negative differential resistances were detected, and in the case of redox-active chemical groups, the transport was partially blocked. Zhou et al. contacted a biphenylthiol SAM on an area with less than 30 nm diameter. A thin (1 nm) layer of titanium improves the contact to the gold evaporated on top [282]. It is not obvious how the titanium binds (see Section 4.3). Lee et al. [283] were able to build a transistor structure with an underlying aluminum gate, Al_2O_3 insulating layer, and a source and drain contact on top. Keeping the source–drain distance in molecular dimensions is a very difficult task, manageable by lithography and evaporation of contacts at low surface angles. The molecules were dithiols and diisocyanates. In this device, the contact area was only 400 nm^2, again to minimize the influence of defects, but shortcuts were very often present. In some cases, however, switching was attained, based on negative differential resistance. This shows that the testing of electrical nanodevices will be more and more important; noise detection as employed for aluminum-contacted 100 nm thick LB films on silicon [284] may be helpful.

5. Clusters in soft matter — penetration

5.1. Penetration of clusters into soft layers

For most technical applications, and also for most research aims, the penetration of metal atoms or clusters in a soft matter layer is unwanted and has to be suppressed. Nevertheless, penetration is nearly always present when clusters are grown or impinge onto soft matter, and knowledge about the process should help to develop counteracting measures. This section introduces various examples that are typical and also useful for the comparison with on-top growth (without penetration). When metal atoms interact with a metal surface, the thermodynamically stable system comprises the metal in direct contact with the surface, with very little dependence on the presence of organic or other layers on the surface. In other words, the metal–metal interaction is in practically all cases stronger than any metal–organic interactions. The way to such a structure requires that metal atoms, but also clusters and other materials, can diffuse through the soft matter. This process is relatively slow, so very often kinetic rather than thermodynamic arguments apply. In this case, the final configuration is not necessarily a metal/metal interface; rather it is possible that metal atoms or clusters are incorporated deeply inside the soft matter layer. This situation is reminiscent of the matrix isolation technique (here for metals rather than molecules), of metal–monomer co-condensation to produce metal clusters embedded in polymer [285], and also of intermediate stages (e.g. at low temperature) of soft landing as discussed in Section 5.2.

Typical analysis techniques include UPS and XPS, especially XPS at vertical and grazing emission, to probe the electronic properties of the soft matter–substrate interface and of each chemical species. However, ISS and SIMS with carefully calibrated depth profiling turned out to be crucially important. The average distance of penetrating objects from the surface can be determined, but measuring penetration times is equally informative. A good reference is the penetration of metal atoms into polymers — which might be thought of as a soft matter layer of semi-infinite thickness, the border being the surface. Faupel et al. published a review [25] that deals with various aspects of this issue. Some of the results are of great relevance also for thin layers of polymers and even to self-assembling monolayers. First, one should realize that below the glass transition a polymer possesses a high viscosity, very low self-diffusion and essential "freezing" of a semicrystalline or amorphous (random-coil) structure. In our case, the soft matter layer is mainly held below the glass transition. When the structure is semicrystalline, the polymer contains many crystalline regions with high packing density of the chains and thus with a low free volume, resulting in slow diffusion of the penetrating clusters.

A special case is the penetration of clusters into molecular crystals. Diindenoperylene forms very well defined crystalline films with flat terraces and monomolecular steps; the thickness is usually chosen around 10 nm. Evaporation of gold can result in on-top layers, even with (111) texture; but at temperatures above 370 K, gold clusters diffuse into the film. The system was investigated with a combination of X-ray scattering, TEM and ISS [54]. The study and its results should be compared to Section 4.7 that presents similar work on much less defined polymer thin films. A notable difference is that above 430 K the molecules can in turn diffuse through defects on top of the gold layer. UPS shows that the clusters can be charged by accumulating holes on the gold clusters. Visible light creates excitons in the film that can eliminate the charging [286]. From this example it becomes obvious that it is not only desirable to study metals on molecular crystals in view of the usual application of the metal as a top contact, but that the unwanted formation of clusters may open up new research and application fields. Another well-characterized organic layer is PTCDA (a perylene dianhydride). Hirose et al. [287] evaporated a whole range of metals, from highly reactive titanium to nearly inert gold, on top, and followed the penetration by XPS. The penetration depths were found to scale with the first ionization potential; in other words, noble metal atoms do not react and penetrate the layer deeply. Seki et al. [288] confirmed this result for p-sexiphenyl layers; again gold atoms penetrate readily, hence the clusters on top of the layer cannot coalesce as fast as for the very reactive magnesium. Gold atoms also penetrate into electron-transporting fluorinated copper phtalocyanine and alter its properties [289]. However, even the reactive metal lithium can diffuse through organic layers, which can be used for controlled film doping [290].

Surprisingly, the diffusion of metal atoms through polymers is orders of magnitude slower than the diffusion of gases of similar molecular/atomic diameter (see also Section 4.7.2.2). One can argue that the metal atoms form temporary weak crosslinks (no covalent bonds) between polymer chains [25]. In many cases, clusters form at a certain distance (a few nanometers up to tens of nanometers) below the surface, i.e. atoms are trapped by clusters. Alternatively, a preformed cluster can be embedded or "sink in" above the glass transition. The balance between van der Waals forces (cluster–polymer interaction) and entropic forces (polymer compression) imply that these clusters should be located in the subsurface region very close to the surface. This is in fact found; in some cases even below the glass transition temperature [25]. The thickest layers we consider here are made up from long chain alkanoic acids and alkylamine systems, as investigated and reviewed by the Sastry group [19]. Here the penetrating species is an ion from a solution, and it penetrates the acid or amine system, finally binding to a charged group in the system. This simple scheme can be used to assemble more complex structures, too. Depending on the charge of the cluster to be immobilized, the proper terminal group of the chain has to be selected. For example, Pal et al. recorded the embedding of polymer-coated gold/palladium clusters in fatty amine films with SFM [291].

5.1.1. Influence of functional groups on penetration

The relatively fast surface diffusion on top of the polymer (see also Section 4.7) results in cluster formation on top of the polymer. The balance between cluster formation on top of the polymer and penetration has been tested for a range of metals not only on polymers, but also on self-assembling monolayers. For polymers such as polyimides, the metals can be classified in two groups: reactive metals (Ti, Cr, Ce, Al, Ni) and less reactive (noble) ones (Au, Ag, Cu, Pd). The classification even holds for polymers without functionalities such as polyethylene [292]. The reactivities are obviously linked to the reactions with water or oxygen. It is not surprising that some of the reactive metals are frequently employed as adhesion layers between oxides (or hydroxylated surfaces) and metals, and as adhesion layers or diffusion barriers on polymers. They tend to form clusters and even layers on polymer surfaces, new polymer–metal compounds can be detected, and the polymer/metal interface is sharp. Less reactive metals can penetrate atom by atom, in addition to cluster formation.

These results are very much compatible with data on metal evaporation on self-assembling monolayers. Especially end group-modified thiols on gold were investigated, since they are simple to prepare and can be obtained with relatively good crystallinity. A seminal paper by Tarlov [92] and a review by Jung and Czanderna [23] appeared already in the early 1990s, and are still highly recommended for an in-depth introduction. The focus was and is on finding the type of metal and the type of terminal group that result in metal overlayer formation without penetration, while several other parameters such as temperature or metal atom flux are varied. At sufficiently low temperature, metals tend to form clusters on top of the SAMs, irrespective of the chemical nature. Here we concentrate on the high temperature cases where penetration is known to occur, but chemical effects of the end groups CH_3, CN, CH_2OH, and COOH come into play. Titanium was early on recognized as a very reactive metal that forms not only Ti–O, but also Ti–N and even Ti–C bonds with many types of SAMs [293]. Again, less reactive metals such as copper and silver penetrate much faster than reactive ones. The end group of the SAM is decisive: groups without electronegative elements and with low dipole moments, especially alkyl, favor penetration; however, at larger coverages, additional on-top growth is possible [294]. Balzer et al. showed that the most reactive metals like sodium can still penetrate through alkyl SAMs [295]; note that the authors focused on single atoms that they detected with two-photon fluorescence. The considerations appear to hold also for small molecules that can be employed for CVD, for example $Ti(N(CH_3)_2)_4$ penetrates alkyl chains in silane monolayers [296]. When silver is evaporated on LB films, one can record the X-ray reflectivity and determine the penetration depth. Clearly, the same considerations as for SAMs apply also here [201]. Alkyl groups, which allow for penetration, can be contrasted with thiophene end groups [297], and similarly aryl groups can be contrasted with thiolated aryl groups [298]. However, one should also consider the role of defects, which might be responsible for penetration through SAMs with functional end groups (e.g. thiols). Note that in certain cases, e.g. for aryls, the penetration can be stopped by horizontal crosslinking of the SAM [89,299].

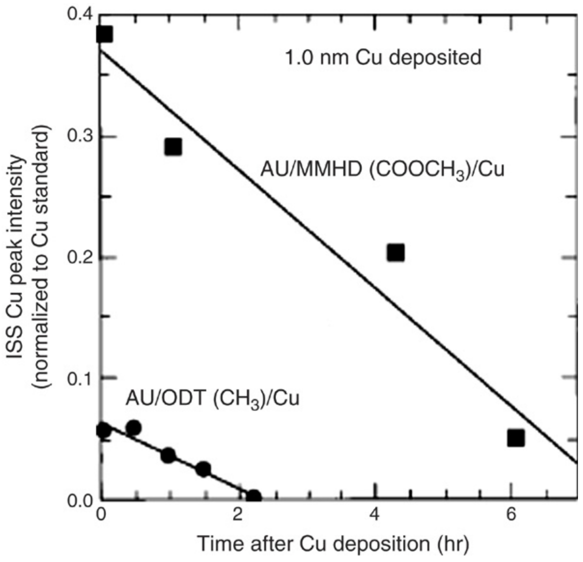

Fig. 22. ISS Cu peak intensity as a function of time after depositing nominally 1.0 nm Cu onto alkane (ODT) and ester-terminated (MMHD) SAMs. The functionalized SAM retains the Cu clusters on its surface [300].

The chemical interaction between metal and SAM might not be strong (no complex formation), but there are clear distinctions between no and weak interactions, e.g. between copper on CH_3- and on $COOCH_3$-terminated SAMs [300] (Fig. 22). An exception with strong interaction is the salt formation for potassium on COOH [301] and aluminum on COOH [302]. Further support for the assumed mechanisms can be achieved by combination of penetration studies with quantum mechanics: The insertion and binding of copper, silver and gold at OCH_3 end groups is impossible or much less favored than for aluminum [303,304], and a weak metal–oxygen bond, without disruption of the SAM, was postulated. These clusters can be visualized with SFM or STM [255]. Long chains obviously inhibit easy penetration, while defects favor penetration. The role of defects is in fact most difficult to ascertain — as already realized by Jung and Czanderna [23] — because a relatively small amount of defects can induce a complete change in behavior of a SAM. This is crucially important for comparison with polymer penetration, since nature and amount of defects are quite well known for polymers — e.g. the free volume of a polymer is the defect structure that opens channels for diffusion. Obvious sources for such defects are substrate defects. Less obvious, but probably of greater relevance, are “transient defects” caused by dynamical changes of a SAM. For example, the chain conformation can fluctuate especially for SAMs of low density, or surface diffusion on the substrate (thiol on gold or thiol-gold on gold) can give access to penetrating species. As mentioned above, crosslinking of the SAM molecules can prevent penetration and in this way highlights the role of transient defects [89,299]. The temperature dependence of the penetration in electrochemical systems points towards the same mechanism [40,76].

After penetration, the final location of the metal is on the soft matter–substrate interface (although probably not always). When the surface is also a metal, the interfacial energy is quite small, islands form below the SAM, and STM can detect their shape [40,76,256,305]. Not surprisingly, clusters on top of SAMs have a high interfacial energy, they "dewet" and form "droplets" on the nanoscale.

5.1.2. Penetration from the solid/liquid interface; electrochemical systems

Thiols on gold substrates are again the most common test samples in electrochemical Surface Science experiments. The additional complexity in such systems arises from the necessity to reduce a metal ion or complex to obtain zero-valent metal. This is possible by applying various negative potentials which themselves can already influence the SAM structure. ECSTM of copper deposition on $C_6H_5CH_2S/Au$ reveals nanoscale dendrites that form by penetration. This mechanism becomes already obvious from voltammograms that show a strong inhibition of underpotential deposition (growth of the first metal-on-metal layer) [306]. Nanoscale silver islands form at the interface between various thiols and gold, even for HS–$(CH_2)_6$–SH [307]. Similarly, copper forms islands below thiol SAMs; shape and kinetics depend much on the alkyl chain length and on temperature [40]. Since the SAM/Cu/Au structure was not oxidized quickly in air, sample transfer to an XPS system followed by analysis at two emission angles became possible. XPS supported the ECSTM conclusions [76].

Alkanethiol layers can exhibit defects, too, either concerning the location of the sulphur or chain disorder; domain boundaries can also be addressed as defects. When immersed in electrolytes, clear indications for defects are changes in voltammetry, especially an increase in capacitance, i.e. a higher current in a cyclic voltammogram (current as a function of sweep voltage). Defects can be caused by increasing temperature, but also by polarization of the electrochemical interface; in addition, they are "natural" for short chain length thiols because the intermolecular interactions (of van der Waals type) are quite weak. Note that the defects are not static (see Section 5.1.1). The electrodeposition of copper becomes faster since copper can more easily penetrate the defective thiol layer. Such effects were investigated by combining three methods: in situ ECSTM and SFG, and ex situ XPS. In this way, a consistent model was developed. Thermodynamically, copper will try to bind to the soft matter–gold interface (and even form an alloy). Angle-resolved XPS showed that copper penetrates the thiol to reach the gold surface, when the surface is polarized sufficiently long (for a $C_{18}H_{37}SH$ SAM this can mean more than 30 min, for $C_6H_{13}SH$ only a few minutes, for bare gold only seconds) [76,77]. The slow kinetics and the existence of small islands can only be explained by penetration through defects. This means that higher temperatures should increase the deposition rate. Indeed the increase is so strong that the growth modes can change from island growth to layer-by-layer [40].

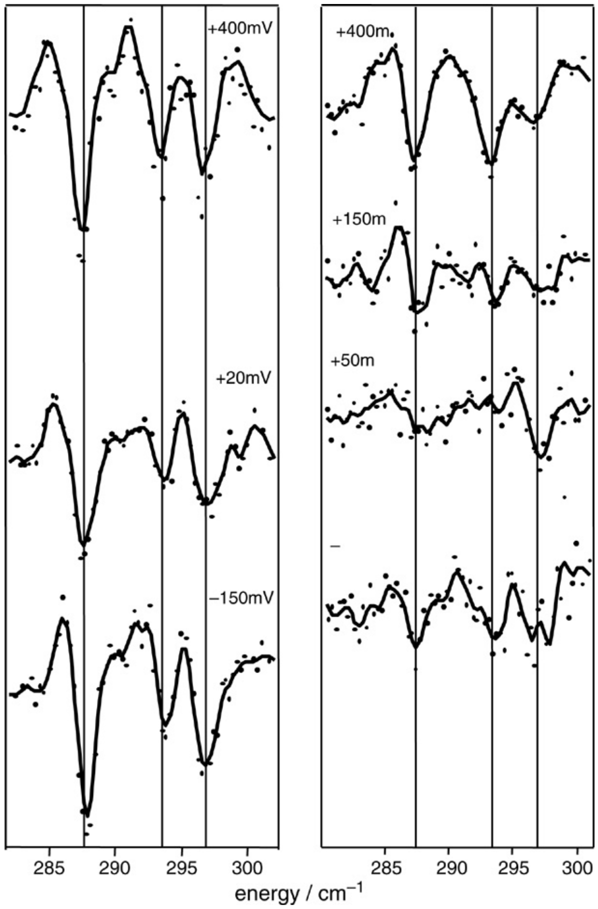

Fig. 23. SFG spectra of a $C_{18}H_{37}SH$ (left) and a $C_6H_{13}SH$ (right) SAM on Au(111) in aqueous 50 mM H_2SO_4 + 1 mM $CuSO_4$ at various electrochemical potentials (versus Cu/Cu^{2+}). While the three typical C–H vibrational resonances of the terminal methyl group (vertical lines as guide for the eye) remain for the long chain, they show drastic intensity changes due to faster penetration of Cu for the short chain: The SAM develops many conformational defects [77].

SFG measurements under identical conditions clarified the nature of the defects: for medium ($C_{12}H_{23}SH$) and long ($C_{18}H_{37}SH$) thiols, the conformation changes very little (some *gauche* defects can develop), even after depositing the maximum amount of copper islands (Fig. 23). The short $C_6H_{13}SH$ shows a mixture of two adsorption geometries already in the absence of copper, and a complete reorientation with deposition of copper (that grows layer-by-layer). This change appears to occur in a slowly moving "front" that is visible in STM even before copper layers appear. The thiol layer apparently "switches" between different geometries once the copper starts to adsorb: the SFG spectral change was neither a function of potential nor of deposition time. A possible scenario is that when the potential decreases, the (solvated) copper ion or atom concentration in the thiol layer increases, i.e. copper penetrates the organic layer, and triggers at a certain concentration a transition to a different structure. A rotation around the S–C bond allows aligning the C–CH_3 axis, which is initially nearly perpendicular, almost parallel to the surface, hence $\nu_{sym}(CH_3)$ becomes very weak, but the tilt of the molecular axis increases only little. Larger changes necessitate "strong activation" such as desorption. Note that spectroscopy and imaging are complementary techniques — each one can only clarify a few aspects, and only the combination of both allows a conclusive characterization of the process (Fig. 23) [77]. The deduced mechanisms are based on transient defects (see Section 5.1.1). The role of larger defects becomes obvious when "mushroom"-type structures result: a channel is opened and completely filled. Since its upper end is always exposed to electrolyte, and since the structure is contacted to the substrate, further deposition ensues, e.g. for Rh on $C_{12}H_{25}SH$ on gold [308].

5.2. *Soft landing of clusters on rare gas layers*

When clusters are deposited on solid or soft surfaces from solution or from the gas phase, they are usually not accelerated towards the surface, hence they impinge on the surface with low kinetic energy. For the gas phase, e.g. for evaporated clusters, the average translational energy is 1.5 kT; for a liquid phase, the energy will be even lower (e.g. stemming from a diffusional jump). An energy around 1 eV or 100 kJ mol^{-1}, which is roughly the amount required to break a chemical bond, will only be reached at extreme temperatures. The situation changes for ion beams that are accelerated towards a sample. Now the energy can be very finely tuned from fractions of 1 eV up to some MeV. The other advantage of ion beams is that ions can be very nicely mass-separated and -selected — clusters with very narrow size distributions become accessible. The challenge is now to produce a sufficient amount to decorate a surface, and to avoid impact energies well above 1 eV per cluster atom, which would likely destroy the cluster. The first problem cannot be resolved easily; the electrical and magnetic filters have to be controlled with great precision, and a certain range of masses should be allowed. The second problem can be solved by careful deceleration, say below 1 eV per atom in the cluster, as recently demonstrated for Au_8 [309]. However, the fine-tuning is a very hard task, given the high (up to kV) range of kinetic energies.

An example of the scenario without deceleration is a molecular beam of silver clusters (2 nm, ca. 300 atoms) with 1500 ms^{-1}, corresponding to 1.3 eV per atom, impinging on a carbon surface. The clusters deform such that they acquire an ellipsoidal shape with an axial ratio of 0.86 (determined from spectral shifts of the plasmon resonance) [310]. Obviously such conditions are also damaging to the substrate, as found by STM for silver cluster deposition on Pt(111) [311]. This can be prevented, and in some cases even the cluster can be prevented from undergoing rearrangement, when the solid substrate is coated with condensed multilayers of rare gas. The role of the gas atoms is twofold: firstly, due to their inertness they will not undergo chemical reactions with the impinging clusters, even when the cluster is composed of very reactive metals such as Fe [312]. Secondly, the cluster's kinetic energy is very well distributed into internal degrees of freedom. This is absolutely required since the (calculated) temperatures of the clusters are thousands of K. Clearly a densely packed single layer of rare gas is insufficient as shown for small Fe clusters, hence several tens of layers are commonly employed [312,313]. In most experiments the sample is then warmed to desorb the rare gas, and it is hoped that the cluster gently descends onto the surface. One should however keep in mind that the thermodynamically stable configuration might be an island rather than a near-spherical cluster (Bromann et al. [311] provide a simple bond-counting argument), and the kinetic barriers can be overcome even at the low temperatures where the rare gas evaporates.

The most popular clusters in soft landing are silver clusters that can be produced by sputtering and laser vaporization. While mainly atoms are created, the formation of large clusters is rare, but the ionization becomes more and more favorable with growing size [65]. Note that the rare gas can either be adsorbed first or be co-condensated with the ions. Low energy electrons may be directed at the sample to neutralize the clusters. Techniques like optical spectroscopy [65,314], X-ray absorption [312] or STM can be employed for the characterization. In passing we note that the optical properties of very small clusters are quite surprising, e.g. blue emission from Au_8, which can be rendered water-soluble by dendrimer ligands [7], or chemiluminescence from Ag_2 and Ag_3 produced during cocondensation of Ag with Ar [315]. These and other properties depend on the cluster structure. As larger examples, Ag_7 and Ag_{19} were produced by sputtering and selected by a quadrupole mass filter. They impinged with up to 1 eV/atom on an argon-covered Pt(111) substrate at 25 K, and STM was performed after warming to 80–90 K to desorb the rare gas (see Fig. 24). The clusters were found to form 2D islands, whose shape (often dendritic) depends on temperature, surface diffusion and cluster flux. Note that the shape in the gas phase is quite different (e.g. a pentagonal bipyramide for Ag_7). In contrast, hard landing with 13.6 eV/atom damaged the substrate locally, pinned the atoms and hindered surface diffusion [311,316]. Ag_{19} was deposited onto Kr at 60 K, and then warmed to 125 K to desorb the Kr. Schaub et al. recorded STM scans and obtained temperature-dependent cluster height distributions. The images can be interpreted based on the adsorption energy of Kr atoms on platinum terraces and steps. After warming, Kr decorates the defect lines (steps) nearly perfectly. In fact, the number of the Kr atoms (12) can be related to the number of metal atoms in the island (19), and even with the number of defects. It is not obvious whether or not the core of the cluster deforms during soft-landing, but the observed island shape makes it very likely. Still such clusters are very small compared to objects usually measured with STM, hence atomic resolution on a cluster was only achieved for Kr atoms [317]. One could thus call the rare gas an "atomic scale visualizer".

Fedrigo et al. carried out a systematic variation of cluster size (2–7 silver atoms), kinetic energy (2.5–0 eV per atom), and rare gas (Ar, Kr, Xe). The clusters were again neutralized with a low energy electron source, most likely after their deposition in the rare gas layer on top of an optical window (see also below, deposition of molecular ions into organic layers). Optical spectra showed that fragmentation increases with increasing rare gas mass. A three-step scenario was deduced: after the impact, the clusters are very quickly decelerated and heat up

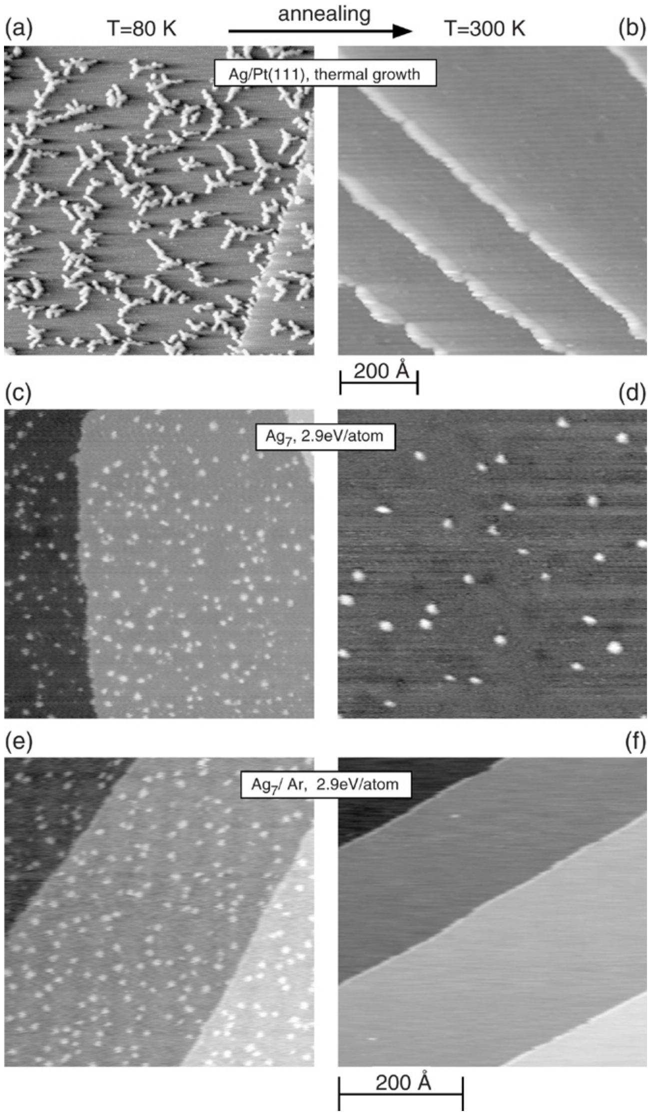

Fig. 24. Top: growth of ramified Ag clusters on Pt(111) at 80 K by evaporation. Middle: deposition of size selected Ag_7 clusters. Heating does not remove all clusters since surface defects have formed. Bottom: Ag_7 deposited onto 10 layers of Ar at 25 K. Heating removes the soft-landed clusters, since no surface defects were created [311].

(i.e. cluster vibrations are excited). The final slow process is cooling embedded in or on the rare gas layers, thereby heating the rare gas layer. Reaggregation has to be taken into account, i.e. fragmentation followed by the reverse process [318]. While the scenario might be different for larger clusters and for other substrates, it is still of great importance for the first interpretation. It appears that any proper interpretation could require simulations (such as molecular modeling). The findings were confirmed with slightly different parameters, and contrasted with XPS data of the silver clusters. The clusters are clearly nonmetallic, but show coalescence to metallic structures upon heating to 500 K [319]. One can also deposit much larger silver clusters with up to 600 000 atoms. Again the rare gas layer helps to induce soft landing, but the clusters change their shape considerably. For example, two-layer high silver islands of hexagonal, hence thermodynamically stable shape, form on Si(111) or on silver-covered Si(111). Arguments well known from homoepitaxial growth can be applied, for example the need to overcome the Schwoebel barrier (diffusion barrier at the steps) in order to spread out the cluster [320]. Repetto et al. recently placed Fe atoms on Xe multilayers to form clusters whose size and shape determines their magnetic properties. In this case, the interaction with the substrate was kept to a minimum, as shown by comparison with the shape and magnetization of non-soft landed clusters [321].

Although there is no theoretical limit to the cluster material to be deposited, the above-mentioned experimental difficulties have as yet not allowed testing many elements. Two groups have investigated small silicon clusters. Honea et al. soft-landed Si clusters with 4, 6 and 7 atoms in a nitrogen matrix, again neutralized with electrons. Raman spectroscopy and ab initio calculations were employed to elucidate the molecular structures [322]. When simple laser ablation is used to produce neutral Si clusters, much larger clusters form, but without size control. A SAM of alkanethiols on Au(111) was exposed to such clusters in the gas phase, and soft landing was postulated. The SAMs were investigated ex situ with STM. The clusters are easily detectable and show a certain height distribution. Various arguments point towards an on-top structure; SFM corroborated the study. Note that SFM showed larger heights than STM; hence we have a case where electronic, not topographical, contrast dominates the STM mechanism. Despite a careful consideration of various possibilities, one might have Si in contact with the gold substrate. Probably the most important result in view of applications is the photoluminescence [323].

The strategy to test further SAMs developed in parallel to the construction of Coulomb blockade devices (see Section 4.8.1): Dithiols were supposed to bind the clusters better. Vandamme et al. deposited gold clusters with a broad size distribution up to 500 atoms with low kinetic energy (0.4 eV per atom) on xylenedithiol/gold. SFM probing was much improved (adhesion reduced) with a hydrophobic tip. In this way, diameters and especially heights of the clusters could be determined quite accurately. The height increases, hence the cluster shape is closer to a spherical structure, compared to hard landing on gold. Again, there are some indications, but no conclusive proof that the clusters indeed reside on top of the SAM [324]. As discussed in Section 4.8, Coulomb blockade measurements can be taken as an indirect proof for the presence of a contact (mainly a metal cluster) on top of a molecular layer. Andres et al. showed this for a cluster beam source with similar properties, up to 500 atoms [5].

Let us now vary not only the soft layer, but also the deposited material: soft landing of organic ions has opened up some new ways in mass spectrometry and in the preparation of ions. For this, ions produced in a mass spectrometer are size selected and deposited with an overall energy of only 10 eV on partially fluorinated thiol SAMs adsorbed on gold. It turns out that the ions reside inside the SAM for many hours, even for samples removed from the vacuum chamber. The resulting system is analyzed by TOF-SIMS [325,326]. Here, the fragmentation ("surface-induced dissociation") can indeed be favorable for the detection, and in this way fluorinated SAMs are advantageous, because they can reduce fast neutralization. A relatively new development is to replace the SAM by a more or less liquid polyol or sugar layer that can preserve the structure of soft-landing proteins (which are electrospray-ionized for acceleration and separation). The proteins retain their biological activity [327]. Two further research trends are loosely related to soft landing: H_3O^+ and Cs^+ ions can be inserted into hydrocarbon films, which are glassy at low temperatures. The mobility of the ions is then of course related to the exact structure and temperature [328]. Vanadium–benzene clusters with up to three metal centers can be ionized, mass-selected and deposited in an Ar matrix. Again, soft landing was attained [329].

6. Clusters on surfaces of large biomolecules

Looking at biomolecules not as complex assemblies of functional groups, but rather as soft matter with a quite well defined surface is probably most familiar to the molecular modeling community. However, the fact that nanocomposites, i.e. inorganic nanoscale compounds immobilized on biomolecules, become attractive, may justify such a new approach. The importance of this topic is that the inorganic structures on biomolecules can help to tackle some of today's most pressing issues such as placing a nanoobject with nanometer precision, and the transition from assembly on surfaces to assembly in three dimensions. Both are required to build new devices on the nanoscale. An important trigger is that macroscopic inorganic materials cannot easily be prepared on the nanoscale, and at the same time cast into special shapes like rods or spheres [330,331]. Biotemplates should be able to circumvent the conventional scaling down of devices as known from microelectronics by employing molecular recognition and self-assembly. Here we are interested in either forming or binding clusters to biomolecules. To simplify matters, let us assume that in a general model a metal ion or cluster binds electrostatically, or by complex formation, or by covalent links to the biomolecule in question. This will highlight the role of certain functional groups on the biomolecule, and in the ideal case — just as for enzymes — their cooperative action.

6.1. Clusters on proteins

Proteins can be viewed simply as polyamide (peptide) structures with side chains; the complexity of the 3D arrangement of the only 20 different functional groups in nature is however nearly infinite. For compatibility with solvated ions or with vacuum conditions, one may choose to concentrate on relatively stable proteins. It turns out that some of the very stable proteins tend to assemble into superstructures. Of special relevance for medicine, but probably also for nanotechnology, are 1D amyloid protein fibers. Because the highly complex functionality of a protein or even oligopeptide cannot be predicted, natural proteins are the prime choice as starting materials. Peptide synthesis with a so-called phage display library can open a way towards combinatorial strategies [332]. In this way, peptides can be tailored to be ideal substrates for biomineralizations of a chosen material. In contrast, one can try to make use of calculation approaches (as yet for peptides) [333].

Biology provides us with various examples for hollow spheres (mainly proteins) that can be filled with clusters; for example so-called heat shock proteins self-assemble into a cage that can be filled with iron oxide clusters [334]. A naturally occurring analogue, ferritin, is not only interesting due to its cage-like shape, it is also a nanoscale antiferromagnet [335]. It can be demineralized to apoferritin, which in turn can be filled with a whole range of binary compounds, even with ferrimagnetic iron oxide [336] and with the technologically relevant CoPt that shows a high intrinsic magnetic moment [337]. The latter example shows that metallization of biotemplates, here at the inner surface of the cage-forming proteins, can yield nanoclusters with a narrow size distribution, which are otherwise hard to synthesize. Moreover, self-assembly into a 2D nanoscale grid was demonstrated, resulting in exactly *the* structure that is needed for ultimate-density magnetic recording media (highly magnetic bits, combined with the absence of magnetic coupling, translate into bit sizes in the 10 nm range and similar bit-to-bit distances). Other 0D objects, too, can be arranged in 2D. Bacterial S layers are very useful because they form very regular and stable grids; they are used as templates for cluster synthesis and arrangement [49,338,339,45,48]. CdS clusters can be synthesized from the respective ions directly on the S layer. These layers are probably the ones that correspond best to SAMs and other thin films (such as LBL films), and their stability is surprisingly high concerning temperature and allowed pH values.

Let us now examine exterior surfaces of biomolecular assemblies, e.g. of microtubuli, which can be coated with FeOOH by a process that corresponds to precipitation (mineralization) on the biomolecule [340], or of peptide nanotubes coated by metal clusters [341,342]. Plant viruses (see the following section) and phages are especially well known as templates for cluster and wire synthesis [59,331, 60–62,332,343,344]. In fact, metal clusters were bound to the tobacco mosaic virus (TMV) as early as 1940 [345]. Inspired from this and other pioneering work on electron microscopy of biological samples, staining methods with metal clusters were developed: gold and platinum clusters [346], and gold cluster-tagged antibodies [347,348] are well established as markers, and even stoichiometric small clusters like Au_{11} can find use in chemistry and biochemistry [349]. However, when the clusters are not preformed, but synthesized on a biomolecule, the first process is binding of the ions, which is at least in general not mechanistically known — the proteins are too complex to allow a good estimate on which group(s) are active. It is still impossible — for chemistry and biochemistry alike — to predict all properties of a nanoscale molecule as complex as a protein. On the other hand, many proteins have not yet been subjected to tests in this direction, so certainly new discoveries will be made.

6.2. Clusters on viruses

Viruses were investigated on the nanoscale already with the first transmission electron microscopes [350]. Virus particles, so-called virions, consist of a nucleic acid strand and a protein cage or tube that is made up from a large number of identical proteins. Hence one could easily compare protein assemblies and viruses concerning their inorganic chemical properties. The proteins can also be glyco- or lipoproteins; they are most commonly arranged in a near spherical (e.g. icosahedral) or helically wound (tubular) exterior shell, the capsid. The simple structure of the virions, too, is very important since it allows us to understand and to explore their chemical behavior. An example is the tobacco mosaic virus (TMV) [350], which is *the* model substance for self-assembly processes, and at the same time *the* model for viruses in general, especially for filamentous plant viruses. Its genome is completely characterized for a range of strains. 2130 protein molecules are helically arranged with 16.3 units building up one turn. The particle length is 300 nm with 18 nm exterior diameter, but linear head-to-tail alignment is frequently found. TMV is quite resilient: it tolerates ethanol, aqueous dimethyl sulphoxide and temperatures up to 90 °C. TMV is not affected by pH values from 3.5 up to about 9 for at least several hours — some virions in a sample remain active even at pH 1.5 — and it retains its infectivity also in dried leaves in cigarettes. In fact, a range of interesting alternatives with nanometer diameter and variable chemical behavior is available for 1D applications, e.g. filamentous viruses, such as potato virus X with its complex surface geometry and chemistry. The M13 phage, well known from the phage display technique, can easily be handled and modified, and has been employed in nanoscale science for some years [332]. Recently, Falkner et al. showed how virions can be used as scaffolds for nanostructures: Pores of cowpea mosaic virions were filled with metal, forming cluster scaffolds [351]. The attractive feature of biochemistry is that mutations can be employed to create an optimal number of reactive groups at preselected sites of a protein or of a protein assembly — like a virion — with nearly atomic precision: gold clusters were attached to genetically engineered thiol groups, placed at exactly defined locations in the capsid of the cowpea mosaic virion [55]. Note that various near-spherical viruses can form ordered and densely packed 2D layers [351,352].

When clusters grow sufficiently fast on a biomolecular surface, they can coalesce. Similar arguments apply also for “biomineralizations”, e.g. of TiO_2 on TMV [343]. A similar scenario operates for the electroless deposition of nickel on TMV (Fig. 25). For this example, one can assume that phosphate attaches to several positively charged pockets on the exterior viral surface. Ni(II) precipitates easily with phosphate, presumably in the form of $Ni_3(PO_4)_2$. Upon contact of the phosphate-covered virions, Ni(II) precipitates in this form on the exterior virion surface. The reduction to metal requires Pd(II), which is reduced to clusters before the nickel deposition process starts (this is the usual electroless deposition scenario). Now, on nickel nuclei, the growth is autocatalytic. The deposition rate increased strongly with temperature; at >85 °C the reaction became uncontrollable. At 25 °C, electroless deposition yields larger clusters of nickel and cobalt exclusively on the exterior viral surface. The produced structure is a nickel tube with a well-defined tubular hole of 18 nm diameter. The coalescence leads to rather large (>10 nm) structures, a problem encountered with all biological rods and tubes, and especially well known for DNA and TMV. Here the attachment is purely mechanical, and for this reason the clusters have to grow fast and coalesce to coat the virion completely. From all these examples it is quite obvious that a Surface Science as for crystalline inorganic surfaces does not (yet) exist for biomolecular surfaces, and that it would be very much based on organic chemistry of the functional groups.

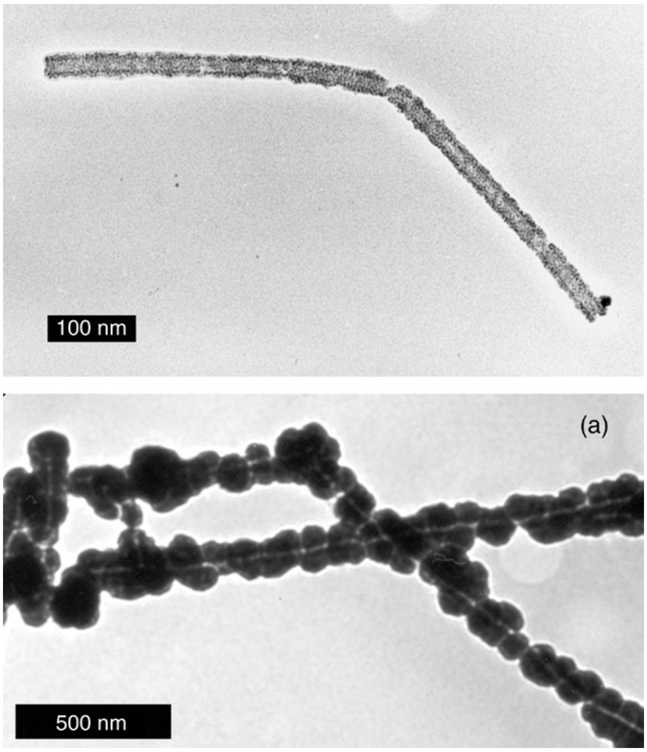

Fig. 25. Tobacco Mosaic Virions linearly assembled. Top: two TMVs coated with a dense layer of palladium clusters. Bottom: similar, but after electroless deposition of nickel (many linearly aggregated TMVs) [61].

6.3. Clusters on other biomolecules

The best-researched biomolecule in Surface Science applications is certainly DNA. The double helix is so small that practically all atoms are accessible; they form the surface, which is not only chemically very heterogeneous, but also curved in a complex way. It is thus not common to employ Surface Science concepts. Nevertheless, the attachment of clusters to chains with defined intercluster distances is possible [353], and metallization of DNA is already so well controlled that it can be used in nanodevices [64]. Other biomolecules play a large role in Langmuir layers: amphiphiles, mainly phospholipids, which form the double layer that makes up membranes in and around cells. These systems have already been covered in Section 2.2.2 in the context of organic analogues of bioamphiphiles. Nature offers many more soft matter surfaces or molecules that form such surfaces, but they are not (yet) exploited for cluster immobilization. With this background, a Surface Science of biomolecules could develop. Finally we note that many systems may not qualify because they are chemically heterogeneous and thus highly complex (e.g. chitin), or because they are difficult to handle, especially on substrates (e.g. sugars).

7. Conclusions and perspectives

Clusters on soft matter cannot form a system that shows simple behavior, the mechanical, chemical and physical differences between these two materials will always induce a certain complexity. Hence it is understandable that no complete theory can be developed; one has to concentrate on singled-out effects. Due to the large variety in the soft, mainly organic matter, these effects can be so well tuned that a range of physical phenomena becomes accessible. Examples comprise optical excitations and their interaction with the soft substrate and with other clusters; penetration of clusters through soft layers, including soft landing of small clusters; single electron charging phenomena (Coulomb blockades and staircases); electrochemical charge transfer, e.g. from a solid substrate through a soft layer to a cluster; metallization of soft layers for nanodevice fabrications. This surprisingly large range becomes possible through a "chemical fine tuning" by the soft layer, especially when it is a self-assembling monolayer of organic molecules, but also through the chemistry of the liquid phase (for soft matter/liquid interfaces).

Organic and biochemistry of cluster immobilization and especially of cluster synthesis are as yet restricted to relatively simple systems, for example electrostatic binding. A big challenge will be to find general concepts for polymer surfaces, and to transfer the results to the complex surfaces of biomolecules, which offer great chemical variability and application potential. Of the many methods of cluster assembly, several can be expected to be applied for mass fabrication of those nanodevices that will contain clusters, although it is not yet obvious whether soft matter will play a major role. Binding prefabricated clusters will be in concurrence to the more complex process of cluster synthesis on or in the soft layer. In this context the importance of analysis methods, especially typical Surface Science techniques, should be stressed. Usually several methods have to be combined to reach clear conclusions.

Acknowledgements

Special thanks go to W.G. Dressick and W. Harbich who shared their experience in the fields of metallization and soft landing.

References

[1] K. Oura, Surface Science — an Introduction, Springer, Berlin, 2003.
[2] M.A. Reed, J.M. Tour, Sci. Am. 282 (2000) 69.
[3] M. Halik, H. Klauk, U. Zschieschang, G. Schmid, C. Dehm, M. Schutz, S. Maisch, F. Effenberger, M. Brunnbauer, F. Stellacci, Nature 431 (2004) 963.
[4] H. Klauk, J. Huang, J. Nichols, T. Jackson, Thin Solid Films 366 (2000) 272.
[5] R. Andres, T. Bein, M. Dorogi, S. Feng, J. Henderson, C. Kubiak, W. Mahoney, R. Osifchin, R. Reifenberger, Science 272 (1996) 1323.
[6] A. Nait-Abdi, J.P. Bucher, P. Rabu, O. Toulemonde, M. Drillon, P. Gerbier, J. Appl. Phys. 95 (2004) 7345.
[7] J. Zheng, C. Zhang, R.M. Dickson, Phys. Rev. Lett. 93 (2004) 077402.
[8] J. Wang, T. Zhu, J.Q. Song, Z.F. Liu, Thin Solid Films 327 (1998) 591.
[9] J. Hicks, D. Miles, R. Murray, J. Am. Chem. Soc. 1243 (2002) 13322.
[10] L.G.M. Olofsson, S.H.M. Persson, A. Morpurgo, C.M. Marcus, D. Golubev, L.K. Gunnarsson, Y. Yao, J. Low Temp. Phys. 118 (2000) 343.
[11] G. Schmid, M. Decker, H. Ernst, H. Fuchs, W. Grünwald, A. Grunwald, H. Hofmann, M. Mayor, W. Rathgeber, U. Simon, D. Wyrwa, Small Dimensions and Material Properties A Definition of Nanotechnology, vol. 35, Europäische Akademie, Bad Neuenahr-Ahrweiler, 2003.
[12] A. Ulman, Characterization of Organic Thin Films, Butterworth-Heinemann, Boston, 1995.
[13] R.A.L. Jones, Soft Condensed Matter, Oxford University Press, New York, 2002.
[14] F. Schreiber, J. Phys.: Condens. Matter. 16 (2004) R881.
[15] F. Schreiber, Prog. Surf. Sci. 65 (2000) 151.
[16] C. Binns, Surf. Sci. Rep. 44 (2001) 1.
[17] K.-H. Meiwes-Broer (Ed.), Metal Clusters at surfaces: Structure, Quantum Properties Physical Chemistry, Springer, Berlin, 2000.
[18] J.H. Fendler, Chem. Mater. 8 (1996) 1616.
[19] M. Sastry, M. Rao, K.N. Ganesh, Acc. Chem. Res. 35 (2002) 847.
[20] J.K. Basu, M.K. Sanyal, Phys. Rep. Rev. 363 (2002) 1.
[21] K. Norgaard, T. Bjornholm, Chem. Commun. (2005) 1812.
[22] M.-C. Daniel, D. Astruc, Chem. Rev. 104 (2004) 293.
[23] D.R. Jung, A.W. Czanderna, Crit. Rev. Solid State Mater. Sci. 19 (1994) 1.
[24] G.C. Herdt, D.R. Jung, A.W. Czanderna, Prog. Surf. Sci. 50 (1995) 103.
[25] F. Faupel, R. Willecke, A. Thran, Mater. Sci. Eng. R 22 (1998) 1.
[26] E. Sacher, Prog. Surf. Sci. 47 (1994) 273.
[27] M. Tirrell, E.E. Parsonage, Polymer Surfaces and Interfaces with Other Materials, in: R.W. Cahn, P. Haasen, E.J. Kramer (Eds.), Materials Science and Technology 12, VCH, Weinheim, 1993, pp. 653–698.
[28] M.J. Hostetler, R.W. Murray, Curr. Opin. Coll. Interface Sci. 2 (1997) 42.
[29] J. Zhang, Q. Chi, T. Albrecht, A.M. Kuznetsov, M. Grubb, A.G. Hansen, H. Wackerbarth, A.C. Welinder, J. Ulstrup, Electrochim. Acta 50 (2005) 3143.
[30] S.W. Chen, J. Electroanal. Chem. 574 (2004) 153.
[31] D. Vuillaume, S. Lenfant, Microelectron. Eng. 70 (2003) 539.
[32] J. Bansmann, S.H. Baker, C. Binns, J.A. Blackman, J.-P. Bucher, J. Dorantes-Dávila, V. Dupuis, L. Favre, D. Kechrakos, A. Kleibert, K.-H. Meiwes-Broer, G.M. Pastor, A. Perez, O. Toulemonde, K.N. Trohidou, J. Tuaillon, Y. Xie, Surf. Sci. Rep. 56 (2005) 189.
[33] W. Harbich, in: K.-H. Meiwes-Broer (Ed.), Metal Clusters at Surfaces: Structure, Quantum Properties Physical Chemistry, Springer, Berlin, 2000, p. 107.
[34] P.A. Dowben, Surf. Sci. Rep. 40 (2000) 151.
[35] M.D. Ward, Curr. Opin. Coll. Interface Sci. 5 (1997) 51.
[36] Y. Gao, K. Koumoto, Cryst. Growth Des. 5 (2005) 1983.
[37] B. Kasemo, Curr. Opin. Solid State Mater. Sci. 3 (1998) 451.
[38] C.M. Niemeyer, Angew. Chem. Int. Edit. 40 (2001) 4128.
[39] P. Damman, S. Coppee, V.M. Geskin, R. Lazzaroni, J. Am. Chem. Soc. 124 (2002) 15166.
[40] O. Cavalleri, H. Kind, A.M. Bittner, K. Kern, Langmuir 14 (1998) 7292.
[41] P.W. Carter, A.C. Hillier, M.D. Ward, J. Am. Chem. Soc. 116 (1994) 944.
[42] K. Kern, G. Comsa, Physisorbed rare gas adlayers, in: R. Vanselow, R. Howe (Eds.), Chemistry and Physics of Solid Surfaces VII, Springer, Heidelberg, 1988, p. 65.
[43] K. Kuhnke, D.M.P. Hoffmann, X.C. Wu, A.M. Bittner, K. Kern, Appl. Phys. Lett. 83 (2003) 3830.
[44] J. Lahann, S. Mitragotri, T.-N. Tran, H. Kaido, J. Sundaram, I.S. Choi, S. Hoffer, G.A. Somorjai, R. Langer, Science 299 (2003) 371.

[45] D.B. Allred, M. Sarikaya, F. Baneyx, D.T. Schwartz, Nano Lett. 5 (2005) 609.
[46] R. Koebnig, K.P. Locher, P.V. Gelder, Mol. Microbiol. 37 (2000) 239.
[47] U.B. Sleytr, M. Sára, D. Pum, B. Schuster, Prog. Surf. Sci. 68 (2001) 231.
[48] U.B. Sleytr, E. Györvary, D. Pum, Prog. Org. Coat. 47 (2003) 279.
[49] S. Dieluweit, D. Pum, U.B. Sleytr, Supramol. Sci. 5 (1998) 15.
[50] K.E. Drexler, Proc. Natl. Acad. Sci. USA 78 (1981) 5275.
[51] E.A. Rietman, Molecular Engineering of Nanosystems, Springer, New York, 2001.
[52] R.J. Composto, R.M. Walters, J. Genzer, Mater. Sci. Eng. R 38 (2002) 107.
[53] J. Schmitt, G. Decher, W.J. Dressick, S.L. Brandow, R.E. Geer, R. Shashidhar, J.M. Calvert, Adv. Mater. 9 (1997) 61.
[54] A.C. Dürr, F. Schreiber, M. Kelsch, H.D. Carstanjen, H. Dosch, O.H. Seeck, J. Appl. Phys. 93 (2003) 5201.
[55] Q. Wang, T. Lin, L. Tang, J.E. Johnson, M.G. Finn, Angew. Chem. Int. Edit. 41 (2002) 459.
[56] F. Fogolari, A. Brigo, H. Molinari, J. Mol. Recognit. 15 (2002) 377.
[57] T. Simonson, Rep. Prog. Phys. 66 (2003) 737.
[58] B. Bagchi, Chem. Rev. 105 (2005) 3197.
[59] T. Douglas, M. Young, Adv. Mater. 11 (1999) 679.
[60] E. Dujardin, C. Peet, G. Stubbs, J.N. Culver, S. Mann, Nano Lett. 3 (2003) 413.
[61] M. Knez, M. Sumser, A.M. Bittner, C. Wege, H. Jeske, T.P. Martin, K. Kern, Adv. Funct. Mater. 14 (2004) 116.
[62] M. Knez, A.M. Bittner, F. Boes, C. Wege, H. Jeske, E. Maiß, K. Kern, Nano Lett. 3 (2003) 1079.
[63] Y. Huang, C.-Y. Chiang, S.K. Lee, Y. Gao, E.L. Hu, J. DeYoreo, A.M. Belcher, Nano Lett. 5 (2005) 1429.
[64] K. Keren, R.S. Berman, E. Buchstab, U. Sivan, E. Braun, Science 302 (2003) 1380.
[65] W. Harbich, Phil. Mag. B 79 (1999) 1307.
[66] M. Paunovic, M. Schlesinger (Eds.), Fundamentals of Electrochemical Deposition, Wiley Interscience, New York, 1998.
[67] H. Brune, Surf. Sci. Rep. 31 (1998) 121.
[68] J. Israelachvili, Intermolecular & Surface Forces, Academic Press, London, 1992.
[69] R. Weber, I. Grotkopp, J. Stettner, M. Tolan, W. Press, Macromolecules 36 (2003) 9100.
[70] K. Akamatsu, S. Deki, J, Coll. Interf. Sci. 214 (1999) 353.
[71] J.A. Lewis, J. Am. Ceram. Soc. 83 (2000) 2341–2359.
[72] A. Gole, C.J. Orendorff, C.J. Murphy, Langmuir 20 (2004) 7117.
[73] J.J. Shyue, Y. Tang, M.R. DeGuire, J. Mater. Chem. 15 (2005) 323.
[74] S.-H. Park, J.-H. Im, J.-W. Im, B.-H. Chun, J.-H. Kim, Microchem. J. 63 (1999) 71.
[75] D. Kolb, Angew. Chem. Int. Edit. 40 (2001) 1162.
[76] O. Cavalleri, A.M. Bittner, H. Kind, K. Kern, T. Greber, Z. Phys. Chem. 208 (1999) 107.
[77] M. Epple, A.M. Bittner, K. Kuhnke, K. Kern, W.-Q. Zheng, A. Tadjeddine, Langmuir 18 (2002) 773.
[78] J.A. Larsson, M. Nolan, J.C. Greer, J. Phys. Chem. B 106 (2002) 5931.
[79] A.M. Bittner, M. Epple, K. Kuhnke, R. Houriet, A. Heusler, H. Vogel, A.P. Seitsonen, K. Kern, J. Electroanal. Chem. 550–551 (2003) 113.
[80] M. Knez, M.P. Sumser, A.M. Bittner, C. Wege, H. Jeske, D.M.P. Hoffmann, K. Kuhnke, K. Kern, Langmuir 20 (2004) 441.
[81] M.A. Hines, J.A. Todd, P. Guyot-Sionnest, Langmuir 11 (1995) 493.
[82] M.R. Anderson, M.N. Evaniak, M. Zhang, Langmuir 12 (1996) 2327.
[83] M. Esplandiu, H. Hagenstrom, D. Kolb, Langmuir 17 (2001) 828.
[84] M. Zolk, F. Eisert, J. Pipper, S. Herrwerth, W. Eck, M. Buck, M. Grunze, Langmuir 16 (2000) 5849.
[85] L.M. Liz-Marzán, Mater. Today 7 (2004) 26.
[86] E. Hutter, J.H. Fendler, Adv. Mater. 16 (2004) 1685.
[87] J.E. Huheey, Inorganic Chemistry: Principles of Structure and Reactivity, Harper &Row, New York, 1983.
[88] H. Kind, A.M. Bittner, O. Cavalleri, K. Kern, T. Greber, J. Phys. Chem. B 102 (1998) 7582.
[89] Y. Tai, A. Shaporenko, M. Grunze, M. Zharnikov, J. Phys. Chem. B 109 (2005) 19411.
[90] G. Bar, S. Rubin, R.W. Cutts, T.N. Taylor, T.A. Zawodzinski, Langmuir 12 (1996) 1172.
[91] K. Akamatsu, S. Deki, J. Mater. Chem. 7 (1997) 1773.
[92] M.J. Tarlov, Langmuir 8 (1992) 80.
[93] T. Ohgi, H.-Y. Sheng, Z.-C. Dong, H. Nejoh, D. Fujita, Appl. Phys. Lett. 79 (2001) 2453.
[94] A. Samokhvalov, R.W. Gurney, M. Lahav, S. Cohen, H. Cohen, R. Naaman, J. Phys. Chem. B 107 (2003) 4245.
[95] D.Q. Li, L.W. Moore, B.I. Swanson, Langmuir 10 (1994) 1177.
[96] M. Abe, T. Kondo, K. Uosaki, Y. Sasaki, J. Electroanal. Chem. 473 (1999) 93.
[97] M. Abe, T. Michi, A. Sato, T. Kondo, W. Zhou, S. Ye, K. Uosaki, Y. Sasaki, Angew. Chem. Int. Edit. 42 (2003) 2912.
[98] J.I. Henderson, S. Feng, G.M. Ferrence, T. Bein, C.P. Kubiak, Inorg. Chim. Acta 242 (1996) 115.
[99] G.M. Ferrence, J.I. Henderson, D.G. Kurth, D.A. Morgenstern, T. Bein, C.P. Kubiak, Langmuir 12 (1996) 3075.
[100] A. Cornia, A.C. Fabretti, M. Pacchioni, L. Zobbi, D. Bonacchi, A. Caneschi, D. Gatteschi, R. Biagi, U.D. Pennino, V.D. Renzi, L. Gurevich, H.S.J.V.d. Zant, Angew. Chem. Int. Edit. 42 (2003) 1645.
[101] J.S. Steckel, N.S. Persky, C.R. Martinez, C.L. Barnes, E.A. Fry, J. Kulkarni, J.D. Burgess, R.B. Pacheco, S.L. Stoll, Nano Lett. 4 (2004) 399.
[102] S. Liu, D. Volkmer, D.G. Kurth, J. Cluster Sci. 14 (2003) 405.
[103] L. Cheng, L. Niu, J. Gong, S. Dong, Chem. Mater. 11 (1999) 1465.
[104] S. Liu, R. Maoz, G. Schmid, J. Sagiv, Nano Lett. 2 (2002) 1055.
[105] O. Vidoni, S. Neumeier, N. Bardou, J. Pelouard, G. Schmid, J. Cluster Sci. 14 (2003) 325.
[106] G. Schmid, E. Emmrich, J.-P. Majoral, A.M. Caminade, Small 1 (2005) 73.
[107] V. Torma, G. Schmid, U. Simon, Chem. Phys. Chem. 2 (2001) 321.
[108] N. Fishelson, I. Shkrob, O. Lev, J. Gun, A.D. Modestov, Langmuir 17 (2001) 403.
[109] R. Maoz, S.R. Cohen, J. Sagiv, Adv. Mater. 11 (1999) 55.
[110] G. Schmid, U. Simon, Chem. Commun. (2005) 697.
[111] S. Peschel, G. Schmid, Angew. Chem. Int. Edit. 34 (1995) 1442.
[112] E.S. Soldatov, V.V. Kislov, S.P. Gubin, M. Artemyev, D. Kisiel, A.N. Sergeev-Cherenkov, S.A. Pavlov, A.S. Trifonov, G.B. Khomutov, Microelectron. Eng. 81 (2005) 400.
[113] C. Zeng, B. Wang, B. Li, H. Wang, J.G. Hou, Appl. Phys. Lett. 79 (2001) 1685.
[114] S. Rauschenbach, F. Stadler, E. Lunedei, N. Malinowski, S. Koltsov, G. Costantini, K. Kern, Small 2 (2006) 540.
[115] J.V. Barth, Surf. Sci. Rep. 40 (2000) 75.
[116] C. Winter, U. Weckenmann, R.A. Fischer, J. Käshammer, V. Scheumann, S. Mittler, Chemical Vapor Depos. 6 (2000) 199.
[117] J. Käshammer, P. Wohlfart, J. Weiß, C. Winter, R. Fischer, S. Mittler-Neher, Opt. Mater. 9 (1998) 406.
[118] U. Weckenmann, S. Mittler, S. Krämer, A.K.A. Aliganga, R.A. Fischer, Chem. Mater. 16 (2004) 621.
[119] N.G. Semaltianos, J.-L. Pastol, P. Doppelt, Surf. Sci. 562 (2004) 157.
[120] H. Osman, J. Schmidt, K. Svensson, R.E. Palmer, Y. Shigeta, J.P. Wilcoxon, Chem. Phys. Lett. 330 (2000) 1.
[121] Z. Peng, X. Qu, S. Dong, Langmuir 20 (2004) 5.
[122] M. Aslam, N.K. Chaki, J. Sharma, K. Vijayamohanan, Curr. Appl. Phys. 3 (2003) 115.
[123] M. Aslam, I.S. Mulla, K. Vijayamohanan, Langmuir 17 (2001) 7487.
[124] V.L. Colvin, A.N. Goldstein, A.P. Alivisatos, J. Am. Chem. Soc. 114 (1992) 5221.
[125] S. Ogawa, F.-R.F. Fan, A.J. Bard, J. Phys. Chem. 99 (1995) 11182.
[126] S. Ogawa, K Hu, F.-R.F. Fan, A.J. Bard, J. Phys. Chem. B 101 (1997) 5707.
[127] V. Ivanova, T. Baunach, D.M. Kolb, Electrochim. Acta 50 (2005) 4283.
[128] T. Baunach, V. Ivanova, D.M. Kolb, H.-G. Boyen, P. Ziemann, M. Büttner, P. Oelhafen, Adv. Mater. 16 (2004) 2024.

[129] K. Stolarczyk, R. Bilewicz, A. Skwierawska, J.F. Biernat, J. Incl. Phenom. Macro. Chem. 49 (2004) 173.

[130] M. Huang, Y. Shen, W. Cheng, Y. Shao, X. Sun, B. Liu, S. Dong, Anal. Chim. Acta 535 (2005) 15.

[131] D.-H. Woo, S.-J. Choi, D.-H. Han, H. Kang, S.-M. Park, Phys. Chem. Chem. Phys. 3 (2001) 3382.

[132] G.O. Mallory, J.B. Hajdu (Eds.), Electroless Plating: Fundamentals And Applications, American Electroplaters and Surface Finishers Society, Orlando, 1990.

[133] D.I. Ma, L. Shirey, D. McCarthy, A. Thompson, S.B. Qadri, W.J. Dressick, M.-S. Chen, J.M. Calvert, R. Kapur, S.L. Brandow, Chem. Mater. 14 (2002) 4586.

[134] M. Knez, M. Sumser, A.M. Bittner, C. Wege, H. Jeske, S. Kooi, M. Burghard, K. Kern, J. Electroanal. Chem. 522 (2002) 70.

[135] X.C. Wu, A.M. Bittner, K. Kern, Langmuir 18 (2002) 4984.

[136] A.M. Bittner, X.C. Wu, K. Kern, Adv. Funct. Mater. 12 (2002) 432.

[137] D. Li, J. Li, Surf. Sci. 522 (2003) 105.

[138] Q. Guo, X. Sun, Y. Chen, R.E. Palmer, Surf. Sci. 497 (2002) 269.

[139] C.M. Whelan, J. Ghijsen, J.-J. Pireaux, K. Maex, J. Electroanal. Chem. 464–465 (2004) 388.

[140] Y. Sakotsubo, T. Ohgi, D. Fujita, Y. Ootuka, Appl. Surf. Sci. 241 (2005) 33.

[141] K. Stolarczyk, B. Palys, R. Bilewicz, J. Electroanal. Chem. 564 (2004) 93.

[142] U.-W. Grummt, M. Geissler, T. Schmitz-Huebsch, Chem. Phys. Lett. 263 (1996) 581.

[143] C.T. Mortimer, Rev. Inorg. Chem. 6 (1984) 233.

[144] T. Sagara, N. Kato, N. Nakashima, J. Phys. Chem. B 106 (2002) 1205.

[145] T. Zhu, X. Fu, T. Mu, J. Wang, Z. Liu, Langmuir 15 (1999) 5197.

[146] A. Gole, S.R. Sainkar, M. Sastry, Chem. Mater. 12 (2000) 1234.

[147] J.J. Lee, S.J. Lee, K. Kim, Molec. Crystals Liquid Crystals 424 (2004) 1.

[148] L.E. Harrell, T.P. Bigioni, W.G. Cullen, R.L. Whetten, P.N. First, J. Vac. Sci. Technol. B 17 (1999) 2411.

[149] Y. Men, K. Kubo, M. Kurihara, H. Nishihara, Phys. Chem. Chem. Phys. 3 (2001) 3427.

[150] F. Sbrana, M.T. Parodi, D. Ricci, E. DiZitti, Mater. Sci. Eng. C 22 (2002) 187.

[151] F. Balzer, H.-G. Rubahn, Nanotechnology 12 (2001) 105.

[152] E.W.L. Chan, L. Yu, Langmuir 18 (2002) 311.

[153] M. Wanunu, R. Popovitz-Biro, H. Cohen, A. Vaskevich, I. Rubinstein, J. Am. Chem. Soc. 127 (2005) 9207.

[154] R. Zirbs, F. Kienberger, P. Hinterdorfer, W.H. Binder, Langmuir 21 (2005) 8414.

[155] G. Meshulam, N. Rosenberg, A. Caster, L. Burstein, M. Gozin, S. Richter, Small 1 (2005) 848.

[156] D. Qin, Y. Xia, B. Xu, H. Yang, C. Zhu, G.M. Whitesides, Adv. Mater. 11 (1999) 1433.

[157] G. Ramanath, G. Cui, P.G. Ganesan, X. Guo, A.V. Ellis, M. Stukowski, K. Vijayamohanan, P. Doppelt, M. Lane, Appl. Phys. Lett. 83 (2003) 383.

[158] P.G. Ganesan, A.P. Singh, G. Ramanath, Appl. Phys. Lett. 85 (2004) 579.

[159] A. Krishnamoorthy, K. Chanda, S.P. Murarka, G. Ramanath, J.G. Ryan, Appl. Phys.Lett. 78 (2001) 2467.

[160] I. Doron-Mor, Z. Barkay, N. Filip-Granit, A. Vaskevich, I. Rubinstein, Chem. Mater. 16 (2004) 3476.

[161] M. Chen, S.L. Brandow, T.L. Schull, D.B. Chrisey, W.J. Dressick, Adv. Funct. Mater. 15 (2005) 1364.

[162] S. Kolliopoulou, P. Dimitrakis, P. Normand, H.-L. Zhang, N. Cant, S.D. Evans, S. Paul, C. Pearson, A. Molloy, M.C. Petty, D. Tsoukalas, Microelectronic Eng. 73–74 (2004) 725.

[163] K.C. Grabar, P.C. Smith, M.D. Musick, J.A. Davis, D.G. Walter, M.A. Jackson, A.P. Guthrie, M.J. Natan, J. Am. Chem. Soc. 118 (1996) 1148.

[164] W. Cheng, S. Dong, E. Wang, Chem. Mater. 15 (2003) 2495.

[165] J.-Y. Tseng, M.-H. Lin, L.-K. Chau, Coll. Surf. A 182 (2001) 239.

[166] S.-S. Bae, D.K. Lim, J.-I. Park, J. Cheon, I.C. Jeon, S. Kim, Appl. Phys. A: Mater. Sci. Process. 80 (2005) 1305.

[167] K. Bandyopadhyay, V. Patil, K. Vijayamohanan, M. Sastry, Langmuir 13 (1997) 5244.

[168] R.M. Crooks, M. Zhao, L. Sun, V. Chechik, L.K. Yeung, Acc. Chem. Res. 34 (2001) 181.

[169] J.A. Harnisch, A.D. Pris, M.D. Porter, J. Am. Chem. Soc. 123 (2001) 5829.

[170] R. Zanella, E.V. Basiuk, P. Santiago, V.A. Basiuk, E. Mireles, I. Puente-Lee, J.M. Saniger, J. Phys. Chem. B 109 (2005) 16290.

[171] T. Sainsbury, J. Stolarczyk, D. Fitzmaurice, J. Phys. Chem. B 109 (2005) 16310.

[172] X.C. Wu, A.M. Bittner, K. Kern, J. Phys. Chem. B 109 (2004) 230.

[173] T. Nakanishi, B. Ohtani, K. Uosaki, J. Phys. Chem. B 102 (1998) 1571.

[174] P. Jiang, Z.-F. Liu, S.-M. Cai, Langmuir 18 (2002) 4495.

[175] T. Tsuruoka, K. Akamatsu, H. Nawafune, Langmuir 20 (2004) 11169.

[176] A. Shavel, N. Gaponik, A. Eychmüller, Chem. Phys. Chem. 6 (2005) 449.

[177] T. Franzl, D.S. Koktysh, T.A. Klar, A.L. Rogach, J. Feldmann, N. Gaponik, Appl. Phys. Lett. 84 (2004) 2904.

[178] A.S. Susha, F. Caruso, A.L. Rogach, G.B. Sukhorukov, A. Kornowski, H. Möhwald, M. Giersig, A. Eychmüller, H. Weller, Coll. Surf. A 163 (2000) 39.

[179] A. Shavel, N. Gaponik, A. Eychmüller, Eur. J. Inorg. Chem. 2005 (2005) 3613.

[180] Z. Tang, Y. Wang, N.A. Kotov, Langmuir 18 (2002) 7035.

[181] E. Granot, F. Patolsky, I. Willner, J. Phys. Chem. B 108 (2004) 5875.

[182] R. Rizza, D. Fitzmaurice, S. Hearne, G. Hughes, G. Spoto, E. Ciliberto, H. Kerp, R. Schropp, Chem. Mater. 9 (1997) 2969.

[183] C.-C. Chen, J.-J. Lin, Adv. Mater. 13 (2001) 136.

[184] V. Patil, M. Sastry, J. Chem. Soc. Faraday Trans. 93 (1997) 4347.

[185] S. Mandal, C. Damle, S.R. Sainkar, M. Sastry, J. Nanosci. Nanotechno. 1 (2001) 281.

[186] S.S. Shankar, S. Chatterjee, M. Sastry, Phys. Chem. Comm. 6 (2003) 36.

[187] S.S. Shankar, D. Rautaray, R. Pasricha, N.R. Pavaskar, A.B. Mandale, M. Sastry, J. Mater. Chem. 13 (2003) 1108.

[188] C. Winter, J. Käshammer, S. Mittler-Neher, R. Fischer, Opt. Mater. 9 (1998) 352.

[189] S.D. Bader, Rev. Modern. Phys. 78 (2006) 1.

[190] D. Rautaray, K. Sinha, S. Sainkar, R. Pasricha, N. Pavaskar, M. Sastry, J. Am. Ceram. Soc. 88 (2005) 24.

[191] J. Aizenberg, A.J. Black, G.M. Whitesides, Nature 398 (1999) 495.

[192] T.P. Niesen, J. Bill, F. Aldinger, Chem. Mater. 13 (2001) 1552.

[193] M. Tominaga, A. Ohira, Y. Yamaguchi, M. Kunitake, J. Electroanal. Chem. 566 (2004) 323.

[194] M.A. Correa-Duarte, M. Giersig, N.A. Kotov, L.M. Liz-Marzan, Langmuir 14 (1998) 6430.

[195] Y. Masuda, W.S. Seo, K. Koumoto, Thin Solid Films 382 (2001) 183.

[196] S. Santer, J. Rühe, Polymer 45 (2004) 8279.

[197] L.F. Chi, S. Rakers, M. Hartig, M. Gleiche, H. Fuchs, G. Schmid, Coll. Surf. A 171 (2000) 241.

[198] M. Burghard, G. Philipp, S. Roth, K.v. Klitzing, G. Schmid, Opt. Mater. 9 (1998) 401.

[199] S.J. Huang, G. Tsutsui, H. Sakaue, S. Shingubara, T. Takahagi, J. Vac. Sci. Technol. B 19 (2001) 2045.

[200] J.-I. Park, W.-R. Lee, S.-S. Bae, Y.J. Kim, K.-H. Yoo, J. Cheon, S. Kim, J. Phys. Chem. B 109 (2005) 13119.

[201] G. Reiter, C. Bubeck, M. Stamm, Langmuir 8 (1992) 1881.

[202] K.M. Mayya, N. Jain, A. Gole, D. Langevin, M. Sastry, J. Coll. Interf. Sci. 270 (2004) 133.

[203] S. Paul, C. Pearson, A. Molloy, M.A. Cousins, M. Green, S. Kolliopoulou, P. Dimitrakis, P. Normand, D. Tsoukalas, M.C. Petty, Nano Lett. 2 (2003) 533.

[204] D.J. Elliot, D.N. Furlong, F. Grieser, Coll. Surf. A 155 (1999) 101.

[205] Y.N. Savin, S.V. Vitushkina, Phys. Status Solidi B 241 (2004) 1026.

[206] L. Konopny, M. Berfeld, R. Popovitz-Biro, I. Weissbuch, L. Leiserowitz, M. Lahav, Adv. Mater. 13 (2001) 580.

[207] J. Holman, S. Ye, D.J. Neivandt, P.B. Davies, J. Am. Chem. Soc. 126 (2004) 14322.

[208] G.K. Zhavnerko, V.E. Agabekov, M.O. Gallyamov, I.V. Yaminsky, A.L. Rogach, Coll. Surf. A 202 (2002) 233.

[209] T. Torimoto, N. Tsumura, H. Nakamura, S. Kuwabata, T. Sakata, H. Mori, H. Yoneyama, Electrochim. Acta 45 (2000) 3269.

[210] P. Facci, V. Erokhin, S. Carrara, C. Nicolini, Proc. Natl. Acad. Sci. USA 93 (1996) 10556.

[211] V. Erokhin, P. Facci, S. Carrara, C. Nicolini, Biosensor Bioelectronics 12 (1997) 601.

[212] M. Clemente-León, H. Soyer, E. Coronado, C. Mingotaud, C.J. Gómez-García, P. Delhaès, Angew. Chem. Int. Edit. 37 (1998) 2842.

[213] S.A. Iakovenko, A.S. Trifonov, M. Giersig, A. Mamedov, D.K. Nagesha, V.V. Hanin, E.C. Soldatov, N.A. Kotov, Adv. Mater. 11 (1999) 388.

[214] D.K. Lee, Y.S. Kang, Coll. Surf. A 257–258 (2005) 237.

[215] D. Lee, R.E. Cohen, M.F. Rubner, Langmuir 21 (2005) 9651.

[216] W.J. Dressick, C.S. Dulcey, S.L. Brandow, H. Witschi, P.F. Neeley, J. Vac. Sci. Technol. A 17 (1999) 1432.

[217] C. Lesser, M. Gao, S. Kirstein, Mater. Sci. Eng. C 8–9 (1999) 159.

[218] S. Ghannoum, Y. Xin, J. Jaber, L.I. Halaoui, Langmuir 19 (2003) 4804.

[219] I. Lee, P.T. Hammond, M.F. Rubner, Chem. Mater. 15 (2003) 4583.

[220] T.C. Wang, M.F. Rubner, R.E. Cohen, Chem. Mater. 15 (2003) 299.

[221] P.G. Ganesan, J. Gamba, A. Ellis, R.S. Kane, G. Ramanath, Appl. Phys. Lett. 83 (2003) 3302.

[222] W. Song, M. Okamura, T. Kondo, K. Uosaki, Phys. Chem. Chem. Phys. 5 (2003) 5279.

[223] S.L. Ren, S.L. Yang, Y.P. Zhao, Langmuir 20 (2004) 3601.

[224] H. Tanaka, M. Mitsuishi, T. Miyashita, Langmuir 19 (2003) 3103.

[225] J.P. Spatz, V.Z.H. Chan, S. Mossmer, F.M. Kamm, A. Plettl, P. Ziemann, M. Möller, Adv. Mater. 14 (2002) 1827.

[226] Y. Inoue, M. Fujii, M. Inata, S. Hayashi, K. Yamamoto, K. Akamatsu, S. Deki, Thin Solid Films 372 (2000) 169.

[227] M. Charbonnier, Y. Goepfert, M. Romand, D. Leonard, J. Adhes. 80 (2004) 1103.

[228] L. Supriya, R.O. Claus, J. Phys. Chem. B 109 (2005) 3715.

[229] W.H. Yu, E.T. Kang, K.G. Neoh, Ind. Eng. Chem. Res. 43 (2004) 5194.

[230] Y. Chen, E.T. Kang, K.G. Neoh, W. Huang, Langmuir 17 (2001) 7425.

[231] A. Wagner, G. Wolfe, D. Fairbrother, Appl. Surf. Sci. 219 (2003) 317.

[232] V. Zaporojtchenko, J. Zekonyte, A. Biswas, F. Faupel, Surf. Sci. 532–535 (2003) 300.

[233] V. Zaporojtchenko, K. Behnke, A. Thran, T. Strunskus, F. Faupel, Appl. Surf. Sci. 144–145 (1999) 355.

[234] L.J. Gerenser, J. Vac. Sci. Technol. A 6 (1988) 2897.

[235] L. Cen, K.G. Neoh, E.T. Kang, Adv. Mater. 17 (2005) 1656.

[236] J.H. Teichroeb, J.A. Forrest, Phys. Rev. Lett. 91 (2003) 016104.

[237] V.M. Rudoy, O.V. Dement'eva, I.V. Yaminskii, V.M. Sukhov, M.E. Kartseva, V.A. Ogarev, Colloid J. 64 (2002) 746.

[238] O.V. Dement'eva, M.E. Kartseva, A.V. Bol'shakova, O.F. Vereshchagina, V.A. Ogarev, M.A. Kalinina, V.M. Rudoy, Colloid J. 67 (2005) 123.

[239] J.E. Gray, P.R. Norton, K. Griffiths, Thin Solid Films 484 (2005) 196.

[240] Z. Liu, K. Pappacena, J. Cerise, J. Kim, C.J. Durning, B. O'Shaughnessy, R. Levicky, Nano Lett. 2 (2002) 219.

[241] H. Shiigi, Y. Yamamoto, H. Yakabe, S. Tokonami, T. Nagaoka, Chem. Commun. (2003) 1038.

[242] W.K. Ng, L. Wu, P.M. Moran, Appl. Phys. Lett. 81 (2002) 3097.

[243] Y. Li, Q. Lu, X. Qian, Z. Zhu, J. Yin, Appl. Surf. Sci. 233 (2004) 299.

[244] P. Fayet, F. Granzer, G. Hegenbart, E. Moisar, B. Pischel, L. Wöste, Phys. Rev. Lett. 55 (1985) 3002–3004.

[245] J. Erichsen, J. Kanzow, U. Schürmann, K. Dolgner, K. Günther-Schade, T. Strunskus, V. Zaporojtchenko, F. Faupel, Macromolecules 37 (2004) 1831.

[246] N. Marin, Y. Serruys, Nucl. Instrum. Methods Phys. Res. B 105 (1995) 175.

[247] D. Anselmetti, T. Richmond, A. Baratoff, G. Borer, M. Dreier, M. Bernasconi, H.-J. Güntherodt, Europhys. Lett. 25 (1994) 297.

[248] B. Wang, H.Q. Wang, H.X. Li, C.G. Zeng, J.G. Hou, X.D. Xiao, Phys. Rev. B 63 (2001) 035403.

[249] J. Repp, G. Meyer, F.E. Olsson, M. Persson, Science 305 (2004) 493.

[250] W.P. McConnell, J.P. Novak, L.C. Brousseau, R.R. Fuierer, R.C. Tenent, D.L. Feldheim, J. Phys. Chem. B 104 (2000) 8925.

[251] G.K. Ramachandran, J.K. Tomfohr, J. Li, O.F. Sankey, X. Zarate, A. Primak, Y. Terazono, T.A. Moore, A.L. Moore, D. Gust, L.A. Nagahara, S.M. Lindsay, J. Phys. Chem. B 107 (2003) 6162.

[252] M. Dorogi, J. Gomez, R. Osifchin, R.P. Andres, R. Reifenberger, Phys. Rev. B 52 (1995) 9071–9077.

[253] G. Yang, L. Tan, Y. Yang, S. Chen, G.-Y. Liu, Surf. Sci. 589 (2005) 129.

[254] L.F. Chi, M. Hartig, T. Drechsler, T. Schwaack, C Seidel, H. Fuchs, G. Schmid, Appl. Phys. A 66 (1998) S187.

[255] N. Oncel, A.-S. Hallback, H.J.W. Zandvliet, E.A. Speets, B.J. Ravoo, D.N. Reinhoudt, B. Poelsema, J. Chem. Phys. 123 (2005) 044703.

[256] B. Wang, X. Xiao, P. Sheng, J. Vac. Sci. Technol. B 18 (2000) 2351.

[257] J. Hou, B. Wang, J. Yang, X. Wang, H. Wang, Q. Zhu, X. Xiao, Phys. Rev. Lett. 86 (2001) 5321.

[258] Y.A. Ovchenkov, H. Geisler, J.M. Burst, S.N. Thornburg, C.A. Ventrice, C. Zhang, Y. Losovyj, L. Rosa, P.A. Dowben, B. Doudin, Chem. Phys. Lett. 381 (2003) 7.

[259] P. Jiang, Z.-F. Liu, S.-M. Cai, Surf. Sci. 486 (2001) L507.

[260] P. Jiang, Z.-F. Liu, S.-M. Cai, J. Appl. Phys. 90 (2001) 2039.

[261] G. Hemakanthi, A. Dhathathreyan, Proc. Indian Acad. Sci. (Chem. Sci.) 114 (2002) 487.

[262] T. Lee, J. Liu, D. Janes, V. Kolagunta, J. Dicke, R. Andres, J. Lauterbach, M. Melloch, D. McInturff, J. Woodall, R. Reifenberger, Appl. Phys. Lett. 74 (1999) 2869.

[263] D. Gittins, D. Bethell, D. Schiffrin, R. Nichols, Nature 408 (2000) 67.

[264] W. Haiss, R.J. Nichols, S.J. Higgins, D. Bethell, H. Höbenreich, D.J. Schiffrin, Faraday Discuss. 125 (2004) 179.

[265] L.C. Brousseau, Q. Zhao, D.A. Shultz, D.L. Feldheim, J. Am. Chem. Soc. 120 (1998) 7645.

[266] G.K. Ramachandran, T.J. Hopson, A.M. Rawlett, L.A. Nagahara, A. Primak, S.M. Lindsay, Science 300 (2003) 1413.

[267] D.R. Stewart, D.A.A. Ohlberg, P.A. Beck, Y. Chen, R.S. Williams, J.O. Jeppesen, K.A. Nielsen, J.F. Stoddart, Nano Lett. 4 (2004) 133.

[268] C.-C. Chen, C.-Y. Tsai, F.-H. Ko, C.-C. Pun, H.-L. Chen, P.-H. Chen, Japan. J. Appl. Phys. 43 (2004) 3843.

[269] S. Chen, R. Ingram, M. Hostetler, J. Jeremy, R.W.M. Pietron, T. Gregory Schaaff, J.T. Khoury, M.M. Alvarez, R.L. Whetten, Science 280 (1998) 2098.

[270] F.-R.F. Fan, A.J. Bard, Science 277 (1997) 1791.

[271] S. Chen, R.W. Murray, J. Phys. Chem. B 103 (1999) 9996.

[272] S. Chen, F. Deng, Langmuir 18 (2002) 8942.

[273] S. Chen, R. Pei, T. Zhao, D.J. Dyer, J. Phys. Chem. B. 106 (2002) 1903.

[274] J.F. Hicks, F.P. Zamborini, R.W. Murray, J. Phys. Chem. B 106 (2002) 7751.

[275] F.P. Zamborini, L.E. Smart, M.C. Leopold, R.W. Murray, Anal. Chim. Acta 496 (2003) 3.

[276] S.L. Horswell, I.A. O'Neil, D.J. Schiffrin, J. Phys. Chem. B 107 (2003) 4844.

[277] W. Cheng, S. Dong, E. Wang, Electrochem. Commun. 4 (2002) 412.

[278] Y. Jin, N. Friedman, J. Am. Chem. Soc. 127 (2005) 11902.

[279] F. Müller, A.-D. Müller, G. Schmid, Phys. Rev. B 63 (2001) 205403.

[280] L. Ma, S. Pyo, J. Ouyang, Q. Xu, Y. Yang, Appl. Phys. Lett. 82 (2003) 1419.

[281] J. Chen, M.A. Reed, A.M. Rawlett, J.M. Tour, Science 286 (1999) 1550.

[282] C. Zhou, M.R. Deshpande, M.A. Reed, L. Jones II, J.M. Tour, Appl. Phys. Lett. 71 (1997) 611.

[283] J. Lee, G. Lientschnig, F. Wiertz, M. Struijk, R.A.J. Janssen, R. Egberink, D.N. Reinhoudt, P. Hadley, C. Dekker, Nano Lett. (2003) 113.

[284] S. Malik, A.K. Ray, S. Bruce, Semicond. Sci. Technol. 20 (2005) 453.

[285] G.B. Sergeev, T.I. Shabatina, Surf. Sci. 500 (2002) 628.

[286] N. Koch, A.C. Dürr, J. Ghijsen, R.L. Johnson, J.-J. Pireaux, J. Schwartz, F. Schreiber, H. Dosch, A. Kahn, Thin Solid Films 441 (2003) 145.

[287] Y. Hirose, A. Kahn, V. Aristov, P. Soukiassian, V. Bulovic, S.R. Forrest, Phys. Rev. B 54 (1996) 13748–13758.

[288] K. Seki, N. Hayashi, H. Oji, E. Ito, Y. Ouchi, H. Ishii, Thin Solid Films 393 (2001) 298.

[289] C. Shen, A. Kahn, J. Appl. Phys. 90 (2001) 4549.

[290] G. Parthasarathy, C. Shen, A. Kahn, S.R. Forrest, J. Appl. Phys. 89 (2001) 4986.

[291] U. Pal, J.F.S. Ramirez, R.S. Gonzalez, J.R. Diaz-Estrada, Appl. Phys. A 80 (2005) 477.

[292] A. Ringenbach, Y. Jugnet, T.M. Duc, J. Adhes. Sci. Technol. 9 (1995) 1209.

[293] K. Konstadinidis, P. Zhang, R.L. Opila, D.L. Allara, Surf. Sci. 338 (1995) 300.

[294] A. Hooper, G. Fisher, K. Konstadinidis, D. Jung, H. Nguyen, R. Opila, R. Collins, N. Winograd, D. Allara, J. Am. Chem. Soc. 121 (1999) 8052.

[295] F. Balzer, K. Bammel, H.-G. Rubahn, J. Chem. Phys. 98 (1993) 7625.

[296] A. Killampalli, P. Ma, J. Engstrom, J. Am. Chem. Soc. 127 (2005) 6300.

[297] H. Ahn, J. Whitten, J. Phys. Chem. B 107 (2003) 6565.

[298] B. de Boer, M.M. Frank, Y.J. Chabal, W. Jiang, E. Garfunkel, Z. Bao, Langmuir 20 (2004) 1539.

[299] Y. Tai, A. Shaporenko, H. Noda, M. Grunze, M. Zharnikov, Adv. Mater. 17 (2005) 1745.

[300] G.C. Herdt, A.W. Czanderna, J. Vac. Sci. Technol. A 15 (1997) 513.

[301] Z. Zhu, B. Haynie, N. Winograd, Appl. Surf. Sci. 231 (2004) 318.

[302] G.L. Fisher, A.E. Hooper, R.L. Opila, D.L. Allara, N. Winograd, J. Phys. Chem. B 104 (2000) 3267.

[303] A.V. Walker, T.B. Tighe, O.M. Cabarcos, M.D. Reinard, B.C. Haynie, S. Uppili, N. Winograd, D.L. Allara, J. Am. Chem. Soc. 126 (2004) 3954.

[304] A.V. Walker, T.B. Tighe, M.D. Reinard, B.C. Haynie, D.L. Allara, N. Winograd, Chem. Phys. Lett. 369 (2003) 615.

[305] T. Ohgi, D. Fujita, W. Deng, Z.-C. Dong, H. Nejoh, Surf. Sci. 493 (2001) 453.

[306] T. Baunach, D.M. Kolb, Anal. Bioanal. Chem. 373 (2002) 743.

[307] H. Hagenstrom, M.J. Esplandiu, D.M. Kolb, Langmuir 17 (2001) 839.

[308] S. Langerock, H. Ménard, P. Rowntree, L. Heerman, Langmuir 21 (2005) 5124.

[309] B. Yoon, H. Häkkinen, U. Landman, A.S. Wörz, J.-M. Antonietti, S. Abbet, K. Judai, U. Heiz, Science 307 (2005) 403.

[310] H. Hövel, A. Hilger, I. Nusch, U. Kreibig, Z. Phys. D 42 (1997) 203.

[311] K. Bromann, H. Brune, C. Félix, W. Harbich, R. Monot, J. Buttet, K. Kern, Surf. Sci. 377–379 (1997) 1051.

[312] J.T. Lau, W. Wurth, H.-U. Ehrke, A. Achleitner, Low Temp. Phys. 29 (2003) 223.

[313] T. Irawan, D. Boecker, F. Ghaleh, C. Yin, B.V. Issendorff, H. Hövel, Appl. Phys. A 82 (2006) 81.

[314] I. Rabin, W. Schulze, G. Ertl, C. Felix, C. Sieber, W. Harbich, J. Buttet, Chem. Phys. Lett. 320 (2000) 59.

[315] W. Schulze, I. Rabin, G. Ertl, Chemphyschem 5 (2004) 403.

[316] K. Bromann, C. Félix, H. Brune, W. Harbich, R. Monot, J. Buttet, K. Kern, Science 274 (1996) 956.

[317] R. Schaub, H. Jödicke, F. Brunet, R. Monot, J. Buttet, W. Harbich, Phys. Rev. Lett. 86 (2001) 3590–3593.

[318] S. Fedrigo, W. Harbich, J. Buttet, Phys. Rev. B 58 (1998) 7428.

[319] J.N. O'Shea, J. Schnadt, S. Andersson, L. Patthey, S. Rost, A. Giertz, B. Brena, J.-O. Forsell, A. Sandell, O. Björneholm, P.A. Brühwiler, N. Mårtensson, J. Chem. Phys. 113 (2000) 9233.

[320] S.J. Chey, L. Huang, J.H. Weaver, Surf. Sci. 419 (1998) L100.

[321] D. Repetto, J. Honolka, S. Rusponi, H. Brune, A. Enders, K. Kern, Appl. Phys. A 82 (2006) 109–112.

[322] E.C. Honea, A. Ogura, C.A. Murray, K. Raghavachari, W.O. Sprenger, M.F. Jarrold, W.L. Brown, Nature 366 (1993) 42.

[323] K. Hata, S. Yoshida, M. Fujita, S. Yasuda, T. Makimura, K. Murakami, H. Shigekawa, J. Phys. Chem. B 105 (2001) 10842.

[324] N. Vandamme, J. Snauwaert, E. Janssens, E. Vandeweert, P. Lievens, C.V. Haesendonck, J. Electroanal. Chem. 558 (2004) 57.

[325] S.A. Miller, H. Luo, J. Pachuta, R.G. Cooks, Science 275 (1997) 1447.

[326] H. Luo, S.A. Miller, R.G. Cooks, S.J. Pachuta, Int. J. Mass Spectrom. Ion Phys. 174 (1998) 193.

[327] B. Gologan, J.R. Green, J. Alvarez, J. Laskin, R.G. Cooks, Phys. Chem. Chem. Phys. 7 (2005) 1490.

[328] R.C. Bell, H. Wang, M.J. Iedema, J.P. Cowin, J. Am. Chem. Soc. 125 (2003) 5176.

[329] K. Judai, K. Sera, S. Amatsutsumi, K. Yagi, T. Yasuike, S. Yabushita, A. Nakajima, K. Kaya, Chem. Phys. Lett. 334 (2001) 277.

[330] A.M. Bittner, Naturwissenschaften 92 (2005) 51.

[331] T. Douglas, M. Young, Nature 393 (1998) 152.

[332] C.E. Flynn, S.-W. Lee, B.R. Peelle, A.M. Belcher, Acta Mater. 51 (2003) 5867.

[333] A. Reiter, J. Adams, H. Zhao, J. Am. Chem. Soc. 116 (1994) 7827.

[334] M.L. Flenniken, D.A. Willits, S. Brumfield, M.J. Young, T. Douglas, Nano Lett. 3 (2003) 1573.

[335] M.T. Klem, M. Young, T. Douglas, Mater. Today 8 (2005) 28.

[336] S. Mann (Ed.), Biomimetic Materials Chemistry, VCH, New York, 1996.

[337] E. Mayes, A. Bewick, D. Gleeson, J. Hoinville, R. Jones, O. Kasyutich, A. Nartowski, B. Warne, J. Wiggins, K.K.W. Wong, IEEE Trans. Magn. 39 (2003) 624.

[338] M. Mertig, R. Wahl, M. Lehmann, P. Simon, W. Pompe, Eur. Phys. J. D 16 (2001) 317.

[339] W. Shenton, D. Pum, U.B. Sleytr, S. Mann, Nature 389 (1997) 585.

[340] A.K. Boal, T.J. Headley, R.G. Tissot, B.C. Bunker, Adv. Funct. Mater. 14 (2004) 19.

[341] R. Djalali, Y.-F. Chen, H. Matsui, J. Am. Chem. Soc. 125 (2003) 5873.

[342] I.A. Banerjee, L. Yu, H. Matsui, Proc. Natl. Acad. Sci. USA 100 (2003) 14678.

[343] S. Fujikawa, T. Kunitake, Langmuir 19 (2003) 6545.

[344] C. Mao, C.E. Flynn, A. Hayhurst, R. Sweeney, J. Qi, G. Georgiou, B. Iverson, A.M. Belcher, Proc. Natl. Acad. Sci. USA 100 (2003) 6946.

[345] G.A. Kausche, Biol. Zbl. 60 (1940) 179.

[346] R.D. Powell, C.M.R. Halsey, W. Liu, V.N. Joshi, J.F. Hainfeld, J. Struct. Biol. 127 (1999) 177.

[347] M.H.V.v. Regenmortel, Phil. Trans. R. Soc. Lond. B 354 (1999) 559.

[348] M. Bendahmane, M. Koo, E. Karrer, R.N. Beachy, J. Mol. Biol. 290 (1999) 9.

[349] G.H. Woehrle, J.E. Hutchison, Inorg. Chem. 44 (2005) 6149.

[350] G.A. Kausche, E. Pfankuch, H. Ruska, Naturwissenschaften 27 (1939) 292.

[351] J.C. Falkner, M.E. Turner, J.K. Bosworth, T.J. Trentler, J.E. Johnson, T. Lin, V.L. Colvin, J. Am. Chem. Soc. 127 (2005) 5274.

[352] Y.G. Kuznetsov, A.J. Malkin, R.W. Lucas, M. Plomp, A. McPherson, J. Gen. Virol. 82 (2001) 2025.

[353] G.H. Woehrle, M.G. Warner, J.E. Hutchison, Langmuir 20 (2004) 5982.